

Pre/W/46
2002 114 880

16 Feb 2002 To be submitted to JGR-Atmospheres

The 1998-2000 SHADOZ (Southern Hemisphere ADditional OZonesondes) Tropical Ozone Climatology. 2. Stratospheric and Tropospheric Ozone Variability and the Zonal Wave-One

Anne M. Thompson, Jacquelyn C. Witte (SSAI)
NASA/Goddard, Atmospheric Chemistry & Dynamics Branch
Samuel J. Oltmans
NOAA/Climate Monitoring and Diagnostics Laboratory
Francis J. Schmidlin
NASA/Wallops Flight Facility
Jennifer A. Logan
Harvard University
Masatomo Fujiwara
Radio Science Center for Space and Atmosphere (RASC)/Kyoto
University
Volker W. J. H. Kirchhoff
INPE/ Laboratorio Ozonia
Françoise Posny
Université de la Réunion
Gert J. R. Coetzee
South African Weather Bureau
Bruno Hoegger
Swiss Aerological Observatory
Shuji Kawakami and Toshihiro Ogawa
NASDA/Earth Observations Research Center

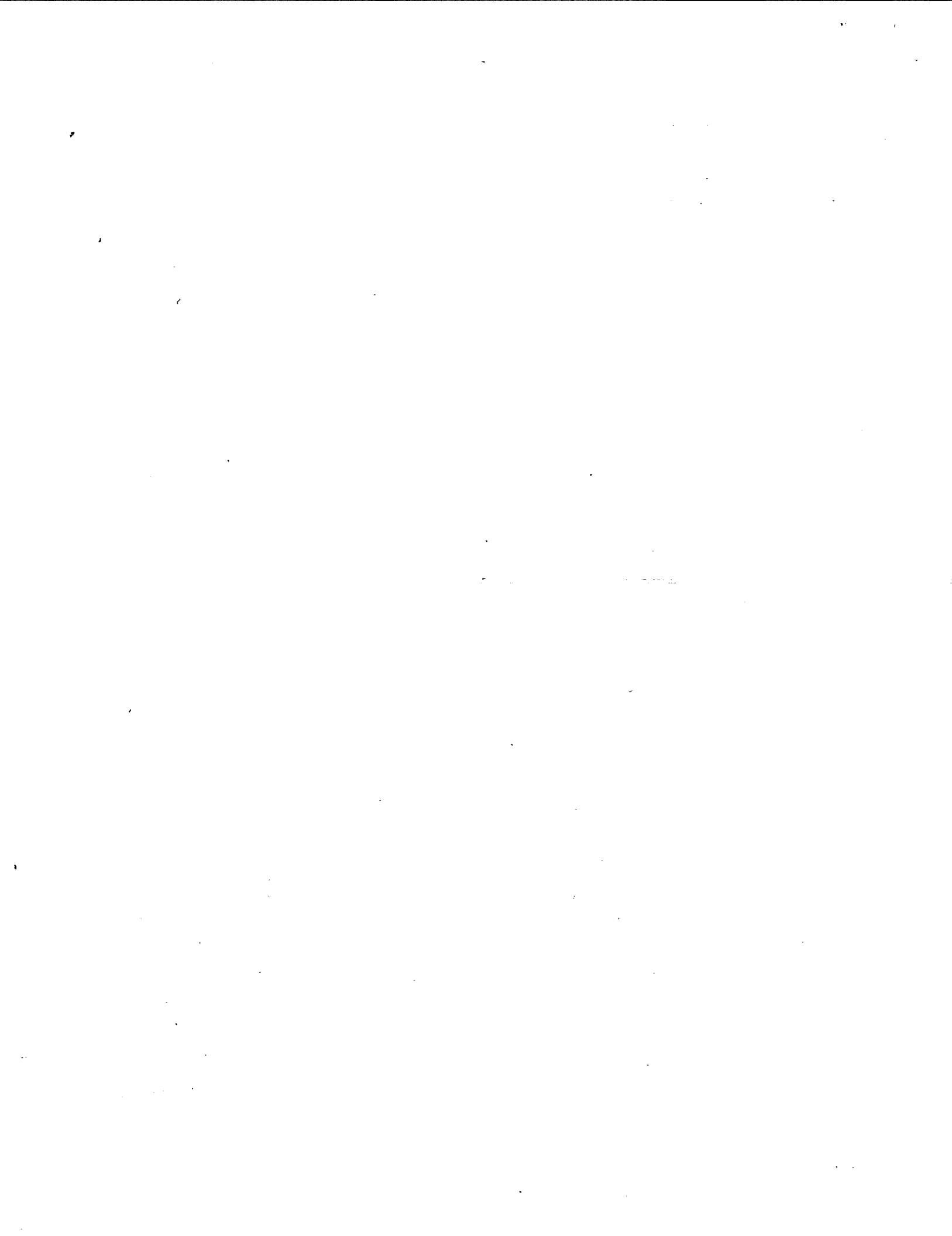
Keywords/Index Terms: 3309 - Climatology (Meteorology & Dynamics); Regions - 9305, 9325, 9340, 9355/Africa - Atlantic - Indian Ocean - Pacific Ocean; 1640 - Remote Sensing - Global Change; 0365- Tropospheric Composition

Free Words - Ozone, Ozonesondes, Satellite Ozone, Tropical Climatology, Wave-one, Biomass burning

Running Head: Thompson et al.: 1998-2000 SHADOZ Tropical Ozone: Wave-One

Corresponding Author:

Anne M. Thompson, NASA-Goddard Space Flight Center, Lab. for Atmospheres
Greenbelt, Maryland 20771 USA; contact: thompson@gator1.gsfc.nasa.gov



Popular Summary

for Paper submitted to JGR-Atmospheres, Feb 02

“The 1998-2000 SHADOZ (Southern Hemisphere Additional OZonesondes) Tropical Ozone Climatology. 2. Stratospheric and tropospheric ozone variability and the zonal wave-one”

Anne M Thompson and Jacquelyn C Witte [SSAI], NASA/GSFC/Code 916, Greenbelt, MD 20771
Samuel J Oltmans (NOAA/CMDL, Boulder, CO 80303)
Francis J Schmidlin at NASA/GSFC/Wallops Flight Facility, Wallops Is., VA 23337
Jennifer A Logan, Dept Earth and Planetary Sciences, Harvard Univ., Cambridge MA
G J R Coetzee (South African Weather Bureau; Pretoria, SA)
Bruno Hoegger (Meteo-Suisse - Aerological Station - Payerne, Switzerland)
V W J H Kirchhoff (INPE - Institute for Space Sciences, São Jose dos Campos, Brazil)
Toshihiro Ogawa & Shuji Kawakami (NASDA, Earth Observations Res. Center, Tokyo, Japan)
Françoise Posny (Université de La Réunion, Saint-Denis, Réunion, France)
Masatomo Fujiwara, Kyoto University, Japan

This is the second “reference” or “archival” paper for the SHADOZ (Southern Hemisphere Additional Ozonesondes) network and is a follow-on to the recently accepted paper with similar first part of title. The latter paper compared SHADOZ total ozone with satellite and ground-based instruments and showed that the equatorial wave-one in total ozone is in the troposphere. The current paper presents details of the wave-one structure and the first overview of tropospheric ozone variability over the southern Atlantic, Pacific and Indian Ocean basins. The principal new result is that signals of climate effects, convection and offsets between biomass burning seasonality and tropospheric ozone maxima suggest that dynamical factors are perhaps more important than pollution in determining the tropical distribution of tropospheric ozone. The SHADOZ data at (http://code916.gsfc.nasa.gov/Data_services/shadoz) are setting records in website visits and are the first time that the zonal view of tropical ozone structure has been recorded - thanks to the distribution of the 10 sites that make up this validation network.

***The 1998-2000 SHADOZ (Southern Hemisphere ADditional
OZonesondes) Tropical Ozone Climatology. 2. Stratospheric and
Tropospheric Ozone Variability and the Zonal Wave-One.***

SHADOZ Team Author List

c/o Anne M. Thompson, NASA-Goddard Space Flight Center, Lab. for Atmospheres
Greenbelt, Maryland 20771 USA; contact: thompson@gator1.gsfc.nasa.gov

ABSTRACT

The first view of stratospheric and tropospheric ozone variability in the southern hemisphere tropics is provided by a 3-year, 10-site record of ozone soundings from the Southern Hemisphere ADditional OZonesondes (SHADOZ) network: http://code916.gsfc.nasa.gov/Data_services/shadoz. Observations covering 1998-2000 were made over Ascension Island; Nairobi, Kenya; Irene, South Africa; Réunion Island; Watukosek, Java; Fiji; Tahiti; American Samoa; San Cristóbal, Galapagos; Natal, Brazil. Total, stratospheric and tropospheric column ozone amounts usually peak between August and November and are lowest in the first half of the year. Other features are a persistent zonal wave-one pattern in total (and tropospheric) column ozone and signatures of the Quasi-Biennial Oscillation (QBO) in stratospheric ozone. The wave-one pattern refers to a greater concentration of free tropospheric ozone over the Atlantic than the Pacific and appears to be associated with tropical general circulation and seasonal pollution from biomass burning. Tropospheric ozone column varies by a factor of three at most SHADOZ sites. Tropospheric ozone over the Indian and Pacific Ocean displays influences of the waning 1997-1998 Indian Ocean Dipole and El-Niño, seasonal convection and pollution transport from Africa. Tropospheric ozone over the Atlantic Basin reflects regional subsidence and recirculation as well as pollution sources. With boundary layer ozone usually < 30 ppbv at SHADOZ stations, errors in buv satellite algorithms for these locations are expected to be 2-3% in total column.

1. Introduction.

Tropical ozone is an active player in atmospheric chemistry and dynamics. Ozone profile data are remarkably rich in information about atmospheric transport. In the upper troposphere, ozone is a greenhouse gas that plays a key role in radiative forcing and potential climate change [Hansen *et al.*, 2002]. Thus, ozone profile data are needed to determine whether or not ozone is increasing or decreasing [WMO/SPARC, 1998]. Tracer studies, i.e., measurements of ozone with aerosols, CO, H₂O, or with trajectories, allow determination of the "age" and origins of air parcels.

Ozone profile observations are typically made in three ways. (1) Field campaigns with *in-situ* measurements from aircraft, ground-based and similar platforms capture ozone in certain regions and under various conditions. Intensive campaigns are required to quantify processes, but give a limited regional view and only a snapshot in time. Examples of campaigns that have studied tropical ozone under various conditions are listed in Table 1.

(2) Satellite observations represent one extreme from campaign sampling by offering global coverage. There are a number of stratospheric ozone profiling satellite instruments. Tropospheric ozone in the tropics is now tracked in near-real time (<metosrv2.umd.edu/~tropo>), allowing us to follow, for example, trans-boundary pollution from biomass fires [Thompson *et al.*, 2001]. The drawback to satellite measurements is that, at present, only column amounts can be retrieved in the troposphere. Gradients and layers that give evidence of transport [Newell *et al.*, 1999] and other processes must be deduced indirectly.

(3) Regular balloon-borne ozone sensors complement campaigns (costly and limited in time and space) and satellites (continuous but limited in vertical resolution). A network of regular ozonesonde launches records large-scale variability, stratosphere-troposphere exchange (STE), pollution layers, convective transport, seasonal and interannual variations, along with vertical structure that manifests multiple processes.

Unfortunately, ozonesonde launches in the tropics have been highly sporadic, with a dozen or so stations operating intermittently since the mid-1980's. Accordingly, it has been difficult to evaluate ozone structure and variability from observations, especially in the troposphere. With the 1998 initiation of the SHADOZ (Southern Hemisphere Additional Ozonesondes) project, a systematic effort was made to collect regular ozone profile data at stations distributed throughout the southern hemisphere tropics and subtropics (sites listed in Table 2). As an augmentation of launches at operational stations, SHADOZ built on campaign efforts and infrastructure at nine sites. A tenth station joined SHADOZ in late 1998 (Irene, South Africa) and an eleventh in late 1999 (Paramaribo, Surinam, 5N, 55W). The Malindi station, at a Kenyan coastal location, joined in 2001. Since 1998, SHADOZ has provided more than 1300 ozone soundings from these tropical and subtropical sites. The SHADOZ data reside at: <http://code916.gsfc.nasa.gov/Data_services/shadoz>.

The first overview of SHADOZ [Thompson *et al.*, 2002; hereafter referred to as THOM1] covered station operations and techniques, evaluated sonde precision and accuracy, and compared column ozone from the sondes with satellite data. The present paper uses approximately 1100 SHADOZ sondes from 1998-2000 to characterize seasonality and variability in ozone. Specific questions addressed include:

- What is the seasonal and interannual variability in total, stratospheric, and tropospheric ozone columns amounts (Sections 3, 5)? What is the seasonality in lower, middle and upper tropospheric ozone layers (Sections 5, 6)?
- What is the structure of the wave-one pattern in tropical tropospheric ozone that SHADOZ stations display when data are viewed zonally (Section 4)? How

- is the wave related to tropical dynamics?
- Can mechanisms controlling tropospheric ozone in SHADOZ be deduced from week-to-week variability in profiles, in seasonal patterns, trajectories, correlations with simultaneous relative humidity soundings, and other indicators of sources or processes? Is there a signature of the waning El-Niño over Indian Ocean and Pacific stations (Section 5)?
- How does the profile climatology from SHADOZ compare to that typically used in satellite ozone retrievals (Section 6)?

2. SHADOZ Network and Data

2.1 Measurements of Ozone, Temperature, Relative Humidity

Ozone measurements at SHADOZ sites (Table 2) are made with balloon-borne ECC (electrochemical concentration cell) ozonesondes coupled with a standard radiosonde and a sensor for relative humidity [Komhyr, 1986; Komhyr *et al.*, 1995]. At Watukosek, Java, prior to conversion to ECC sondes in August 1999, MEISEI sondes were used [Komala *et al.*, 1996; Fujiwara *et al.*, 2000; Kobayashi and Toyama, 1966]. Radiosondes produced by three manufacturers are used at SHADOZ stations; seven use the Vaisala manufactured sonde. Temperature is measured accurately with all radiosondes, to within 0.5°C. Humidity is measured with less accuracy; we use only data to -60C. The nominal sampling schedule at SHADOZ stations is once-per-week, usually but not always, mid-week. Details of ozone, humidity and temperature instrumentation for each SHADOZ station are given in the Appendix of THOM1.

Because each sonde launched is essentially a new instrument, estimates of precision and accuracy in total ozone from typical sondes are required. Sonde precision, defined as the reproducibility of the total integrated ozone column, is 5% [THOM1]. Sonde precision and accuracy in the troposphere is estimated at 2-3% [Johnson *et al.*, 2002]. Accuracy of integrated total ozone from the sondes, determined through comparison with rigorously calibrated ground-based total ozone instruments [R. Evans, personal communication, 2000] at five SHADOZ stations is 2-5% [THOM1]. The TOMS total ozone column, determined from a mid-day satellite overpass (Level 2, version 7 data from the Earth-Probe TOMS instrument), is 2-4% higher than the ground-based total ozone at these stations [THOM1], suggesting a high-ozone bias in the TOMS observation. Over all ten stations examined in this paper and in THOM1, mean sonde total ozone differences with the column determined from TOMS satellite overpasses range from 2-11%, when total ozone is computed with an above-balloon burst extrapolation from SBUV (see next section). Only some of the differences are explained by the satellite algorithm.

Closer examination of sonde-TOMS and sonde-Dobson offsets in total ozone suggests station-to-station biases among SHADOZ stations [THOM1] due to differences in sonde technique [Johnson *et al.*, 2002]. Data processing, sensor solution and hardware vary, even though the same basic instrument is used at all sites. The relationship of individual station offsets to technical details are not entirely clear. There are no significant differences in total stratospheric column ozone amount among stations, nor in the integrated column amount in the lower stratosphere [THOM1]. The various sonde techniques used at SHADOZ stations were evaluated through comparison with test chamber results that simulated tropical ozone profiles (JOSIE-2000, Juelich Ozonesonde Intercomparison Experiment; H. Smit, personal communication, 2000; <www.fz-juelich.de/icg/icg2/forschung/Josie>]. The implications of these tests for SHADOZ data are currently being analyzed.

2.2 Data Selection and Treatment

The 1998-2000 data used in this study are taken from the SHADOZ website code916.gsfc.nasa.gov/Data_services/shadoz and are also available from the World Ozone and Ultraviolet Data Center (WOUDC) in Toronto <http://woudc.ec.gc.ca>. Coordinates for each SHADOZ station are summarized in Table 2, along with those for two campaign datasets that reside in the archive. Aerosols99 data were taken between 30N and 30S from the *R/V Ronald H Brown* oceanographic vessel as described in *Thompson et al.*, [2000]. The INDOEX data were taken in January-March 1999 from the Kaashidhoo Observatory at Male in the Maldives Islands.

Total ozone in each SHADOZ data record (as used here) is based on integration to 7 hPa or balloon burst (whichever is higher), with extrapolation to 1 hPa based on the SBUV satellite climatology of *McPeters et al.* [1997]. No normalization is made to total ozone from another instrument, ie satellite or a co-located ground-based total ozone sensor. The difference between total ozone computed with an SBUV (solar back-scatter- ultraviolet) extrapolation may be up to 8% lower than using a constant-mixing-ratio approach [*McPeters et al.*, 1997; *Johnson et al.*, 2002; THOM1].

Tropospheric ozone is determined by integration to a "chemical tropopause," which is defined as the point at which extrapolation of the lower stratospheric ozone mixing ratio reaches 100 ppbv ozone. This is within 10-15 hPa of the temperature-based tropopause (supplied by NCEP analyses, for example) except at Irene where the temperature sometimes shows a double tropopause. Stratospheric ozone column amounts are determined by integration from the chemical tropopause to balloon burst with extrapolation as described above. Tropospheric ozone from the sondes compares well with the corresponding TOMS-based column tropospheric ozone [*Thompson and Hudson*, 1999] - to within 6-7 DU, better than the total ozone-sonde comparison at most stations. This suggests that disagreements between total ozone determined from sondes and from satellite or ground-based instruments arise from the stratospheric as well as tropospheric part of the sonde profile. In the following sections, analyses are based on features at individual stations and/or seasonal averages for which station-to-station biases in ozone amounts have no impact.

3. Seasonal Dependence of Total and Stratospheric Ozone. Mean Vertical Profiles

3.1. Total and Stratospheric Ozone. Quasi-biennial Oscillation.

Figure 1 shows total ozone at eight SHADOZ sites in separate panels for 1998, 1999, 2000; Figure 2 shows stratospheric ozone at the same sites. Previous studies of ozone at some of these stations [*Logan and Kirchoff*, 1986; *Olson et al.*, 1996; *Thompson et al.*, 1996a,b; *Oltmans et al.*, 1998, 2000; *Taupin et al.*, 1999; *Logan*, 1999a,b; *Fujiwara et al.*, 2000] show that a typical pattern is a period of highest total (and highest stratospheric) ozone in the August through November period. For the sites operational in the early-mid 1990's (all except Nairobi and San Cristóbal), the same pattern occurred during 1998-2000. Some of the seasonal difference in stratospheric ozone is due to a lower tropopause in the latter part of the year (Figure 3). The tropopause is normally between 16 and 18 km except for the two most southerly sites (Réunion, Irene) where the tropopause sometimes falls below 14 km. At Réunion, intrusions have been noted in soundings and other observations. Stratospheric ozone may approach 2-3 km of the surface [*Randriambelo et al.*, 1999; *Chane-Ming et al.*, 2000].

Interannual variability in total column ozone over the equator is dominated by the quasi-biennial oscillation (QBO), [e.g., *Bowman et al.*, 1989; *Hollandsworth et al.*, 1995; *Thompson et al.*, 1996b]. The QBO is a downward propagating oscillation between easterly and westerly wind regimes in the equatorial stratosphere, with a period of about 28 months

[Reed et al., 1961; Baldwin, 2001]. The 1998-2000 SHADOZ data cover a complete cycle of the QBO [Logan et al., 2002]. The winds above ~30 hPa are easterly in the first half of 1998, and the westerly shear zone descends from near 10 hPa in mid-1998 to ~35 hPa by the end of 1998. The westerlies continue during 1999 at 20 hPa, and the next easterly shear zone descends through 10 hPa at the middle of 1999. The winds become westerly at 10 hPa in December 2000. The descending westerly shear zone in mid-late 1998 leads to a large increase in the stratospheric column that is evident in the sondes over most stations (Figure 2) and the TOMS overpass data (Fig. 7 in THOM1). There is a gap in some sonde records prior to September 1998 (e.g. Nairobi and San Cristóbal; Figure 4A,B) but the sonde data clearly mimic the TOMS variations. The SHADOZ data for Nairobi, Ascension (not shown) and San Cristóbal are the first in-situ data to document the change in shape of the equatorial ozone profile from 17 to 34 km [Logan et al., 2002]. During 1998, the QBO signal reinforces the seasonal cycle, leading to an increase in ozone from August to November. Ozone partial pressures at Nairobi exceed 15 mPa at 26 km (6-7 ppmv mixing ratio in Figure 4A) from September 1998 until May 1999.

Analyses of column and SAGE (Stratospheric Aerosols and Gases Experiment) profile data have shown that the QBO in ozone is strongest over the equator [Bowman et al., 1989; Hollandsworth et al., 1995; Zawodny and McCormick, 1991; Hasebe, 1994; Randel and Wu, 1996]. The column ozone variations within 10 degrees of the equator are approximately in phase with the equatorial winds near 30 hPa, whereas the extratropical variations are of opposite phase, with the phase change near 10-15 degrees of the equator. The QBO signal is not readily apparent in the stratospheric column data for Samoa, Fiji and Tahiti (14-18S; Figure 4) because of the change in phase, although there is a QBO signal at the same altitudes as at Nairobi and San Cristóbal. A full analysis of the QBO in the SHADOZ data is given in Logan et al. [2002].

3.2 Seasonal Mean Profiles.

Figure 5 shows seasonal mean ozone profiles for 6 sites. Tahiti, not shown, is nearly identical to the Samoa profiles. Watukosek is not illustrated because the instrument change in August 1999 may have affected statistics. Refer to Fujiwara et al. [2000] for Watukosek ozone seasonality in the 1993-1998 record. The seasonal means for all sites show that the September-October-November (SON) ozone profiles are greater than for March-April-May (MAM) throughout the entire profile. Seasonal mean differences for total ozone range from 9-30 DU (Table 3), depending on site. Except for San Cristóbal and Nairobi (Figure 5), the typical stratospheric seasonal column difference is 11-20 DU (Table 3). Less than 5 DU of this difference is due to the tropopause being lower in SON than in MAM. The variability of tropospheric ozone within MAM and SON profiles is examined in Section 6.

4. The Zonal Wave-One in Tropospheric Ozone.

4.1 Summary of Column-integrated Ozone. Wave-one.

A number of studies have attempted to determine whether the equatorial wave-one pattern in total ozone seen in satellite data [Shiotani, 1992] is in the troposphere, the stratosphere or both. Satellite data are inconclusive because they are at poorest precision in the region (70-100 hPa) where the stratospheric wave is expected. Although sondes resolve the vertical structure with the required resolution, prior to SHADOZ, a complete zonal view was lacking due to temporal and spatial gaps. There is a wave-one pattern visible in the tropospheric ozone data when the 1998-2000 SHADOZ data are considered longitudinally. The statistics in Table 3 suggest a "tropospheric wave-one." Tropospheric ozone column amounts at Natal, Ascension, Nairobi (and Réunion) are usually higher than at Watukosek, Fiji, Samoa and Tahiti. A wave-one is also apparent when TOMS total ozone at these stations

(and Dobson where applicable) are contrasted [THOM1]. Table 5 in THOM1 shows total, stratospheric and tropospheric ozone averaged over the sets of four stations and estimates the magnitude of the wave obtained by subtracting the two quantities. Even given fairly high standard deviations, total ozone and tropospheric ozone show 10-15 DU wave-one amplitudes at all times of year. Stratospheric ozone shows no statistically significant wave (Figures 12-14 in THOM1). In particular, lower stratospheric ozone is uniform at all SHADOZ stations except Irene, which is higher because of its frequent mid-latitude character.

4.2 Structure of the Tropospheric Ozone Wave-one and Zonal Relative Humidity.

The wave-one in tropospheric ozone is evident when seasonally averaged profile data are displayed zonally (Figures 6A,B). Longitudinal cross-sections in DJF and JJA (not shown) confirm that the wave persists throughout the year. Between 40W (just west of Natal) and ~60E, enriched mid-tropospheric ozone gives rise to the wave-one. Regions in brown (> 80 ppbv) appear at lower altitude over the Atlantic, Africa and the western Indian Ocean than over the Pacific and eastern Indian Ocean. This tendency is prominent in SON when ozone subsidence maximizes over the Atlantic [Krishnamurti et al., 1996]. Free tropospheric ozone mixing ratios > 60 ppbv over the Atlantic have been observed with aircraft, balloon and shipboard soundings [Smit et al., 1989; Browell et al., 1996; Weller et al., 1996; Thompson et al., 1996a; 2000]. In addition to subsidence, transported ozone and ozone precursors that form ozone during advection and recirculation enrich lower-mid-tropospheric ozone in SON (Figure 6B). A significant amount of ozone may form from NO created by lightning [Moxim and Levy, 2000; Martin et al., 2002]. Note that ozone near the surface is much lower than in the mid-troposphere (20-30 ppbv except for Watukosek in SON). This is because SHADOZ sites are remote from regions polluted in ozone and rich with ozone precursors. During SAFARI-2000 in September 2000, for example, surface ozone at Lusaka, Zambia, in the heart of active fire regions in Africa, was 55-95 ppbv.

In MAM (Figure 6A) the tropopause is higher than 16 km (steep ozone gradients, crowded contours) over all stations, whereas the SON appears to be 1-3 km lower (Figure 6B). The ozone distribution in Figure 6 (and water vapor, shown for SON in Figure 7) reflects large-scale tropical circulation. The SHADOZ record began as the intense 1997 El-Niño-Southern Oscillation (ENSO) was winding down and returning to normal conditions. Figure 8 illustrates these typical patterns of large-scale transport and convection. The regions of intense convection are mostly oceanic (remote from sources) so the local effect on ozone tends to be reduction of the ozone column as ozone-rich air in the mid-to-upper troposphere is displaced by ozone-poor air from the surface. In MAM, ozone averaging < 20 ppbv extends from the surface to 3 km over the western Pacific (Fiji-Samoa-Tahiti). In the same region an ozone minimum (20 ppbv contour) also extends from 8-13 km (Figure 6A). The convective character of this region has been pointed out by Folkins et al. [1999; 2000]; see Pickering et al. [2001] for a case study of convective impact on ozone near Fiji in early 1999.

In SON (Figure 6B), the upper-tropospheric convective signature in ozone is most prominent over Watukosek. There is also higher ozone and lower water vapor (Figure 7) near the surface, presumably from aged pollution [Fujiwara et al., 2000; Thompson et al., 2001], but low ozone at 9-14 km. Over the central Pacific, surface ozone concentrations in SON are higher than in MAM, but still appear as regional minima, mixed throughout the lower troposphere and with some impact at 10-12 km. Upper tropospheric descent over the western Indian Ocean to Atlantic (40W-70E, Figure 7) is more apparent in ozone for SON than MAM, as indicated by location of the 70-80 ppbv contours. This is mirrored in the relative humidity distribution, for which the green contours for relative humidity are thinner and lower in the atmosphere than they are in MAM (not shown). Note the extension of low relative humidity (purple-violet) to < 5 km over Réunion.

5. Tropospheric Ozone Variability in the SHADOZ (1998-2000) Period.

Tropospheric ozone data from the 1998-2000 SHADOZ record are used to address the following:

- What is the general seasonal and interannual variability seen in tropospheric ozone among SHADOZ sites? Are there signatures of the waning ENSO in the early SHADOZ record? (Section 5.1)
- Can episodes of convection, pollution transport and upper tropospheric or lower stratospheric ozone exchange be observed when individual sondes are viewed as a time-vs-altitude series during 1998-2000 (Section 5.2)
- What appear to be general influences on tropospheric ozone at SHADOZ stations, e.g. origins of free tropospheric air, biomass burning? (Section 5.3)

5.1 General Seasonal and Station Variability. ENSO.

Figure 9, depicting tropospheric segments (column-integrated amounts below tropopause), shows that in general, there is more tropospheric ozone between June and November than at other times of year. Depending on the station and the year, minimum ozone occurs between January and May. All the Pacific stations (top panel) resemble one another in seasonality and magnitude. A number of soundings with 10-DU column or less appear, especially in early 1999 during the PEM-Tropics-B field campaign [Oltmans *et al.*, 2001]. Tropospheric ozone column amounts and variability at Watukosek (Figure 9, lowest panel) are generally similar to the Pacific stations.

On average, as Section 4 showed, tropospheric ozone during 1998-2000 reflected normal or "unperturbed" tropical circulation. However, the SHADOZ record started during the latter stages of the 1997-1998 ENSO. Modified convection patterns associated with the ENSO tend to perturb total column ozone amounts, a phenomenon that was first reported by Shiotani [1992]. Ozone over the central and eastern Pacific decreases as convection brings low ozone from the surface up through the troposphere. Low ENSO-induced tropospheric ozone column amounts in the eastern Pacific during the 1980's were described by Kim and Newchurch [1996], Ziemke *et al.* [1998], and Thompson and Hudson [1999].

Signatures of 1990's ENSO events were detected in Watukosek sondes [Fujiwara *et al.*, 1999] and observed over the maritime continent in TOMS tropospheric ozone [Chandra *et al.*, 1998]. During the 1997 ENSO, increased subsidence over the maritime continent led to large forest fires in Indonesia [Wooster *et al.*, 1999]. Smoke and tropospheric ozone pollution spread rapidly to other countries in the southeastern Asian region [Thompson *et al.*, 2001], with the ozone plume extending westward as far as southern India. Ozone pollution from Indonesian fires was also detected in soundings launched in Malaysia [Yonemura *et al.*, 2001]. This pollution ozone maximized in October 1997 and was superimposed on a regional ozone increase that was touched off by rapid subsidence at the ENSO onset in March 1997 [Thompson *et al.*, 2001]. In March 1997, tropospheric ozone column depth from Africa to the maritime continent increased more than 20 DU. In addition to the strong ENSO, there occurred a remarkable warming of the Indian Ocean, which began in late 1997 and peaked during March-May 1998. The Indian Ocean Dipole [Saji *et al.*, 1999; Webster *et al.*, 1999] refers to anomalies in sea-surface temperature in the eastern and western Indian Ocean associated with wind and precipitation anomalies. Although initiated by physical processes distinct from the El Niño, in 1997 the Indian Ocean Dipole coincided with the ENSO, reinforcing the subsidence and drought that occurred over the eastern Indian Ocean (80-100E) in mid-1997 [Latif, 1999]. The Dipole effect peaked in October-November 1997 and reversed sign when the ENSO switched to the La Niña phase in 1998. At this point, there was a return to normal tropospheric ozone column depth over the Indonesian maritime continent [Thompson *et al.*, 2001]. Elevated ozone at the transition was detected over Fiji (Figure 9, top

panel) and Watukosek soundings (Figure 9, bottom panel). Tropospheric ozone at Fiji in early 1998 is much higher than for the same period in 1999 and 2000. Although the Watukosek soundings (25-28 DU in early 1998) are much less than the 55 DU recorded in October 1997, these values are greater than normal (compare January-March 1999, 2000; see Komala *et al.*, 1996). There was a secondary fire outbreak over Indonesia in February-March 1998 [Figure 1 in Thompson *et al.*, 2001].

In the second panel of Figure 9, Natal and Ascension appear similar to one another although the data record is somewhat sparse in 1998. These stations, along with Réunion, have the highest tropospheric ozone column values and the greatest sonde-to-sonde variability. Indeed, only two stations (San Cristóbal, Nairobi) display less than a factor of 3 difference in tropospheric column among individual soundings within a calendar year. Where coincident data are available from all SHADOZ sites, Ascension tends to be highest in tropospheric ozone (Figure 9, middle panel). An exception occurred in April 1999 when a column amount of ~20 DU was recorded at Ascension and Natal. Very low tropospheric ozone during the wet season at Natal (10 DU) was reported by Kirchhoff *et al.*, [1990] during the ABLE-2B campaign in April-May 1987. Early 1998 tropospheric ozone total at Ascension is much lower than for the same period in 1999 and 2000 (note soundings < 30 DU). Usually, tropospheric ozone at Ascension is never as low as the minimum at other SHADOZ stations. Except for April-May, soundings with > 40 DU of tropospheric ozone have been recorded in every month at Ascension. This occurred also during the 1990-1992 TRACE-A observing period [Thompson *et al.*, 1996a ; Olson *et al.*, 1996]. Ascension ozone increases begin in June, when the southern hemisphere biomass burning begins, and ozone peaks between September and November. Aircraft sampling in the south tropical Atlantic during TRACE-A [Browell *et al.*, 1996] showed ozone and aerosol pollution from fires was frequently concentrated in two layers, one below 5 km and one between 8 and 12 km. As the southern hemisphere dry season progresses, ozone from African fires is enriched by ozone from South American burning and lightning. An ozone buildup from these sources causes south tropical Atlantic ozone to maximize in September-November, several months after the peak of southern African burning (see Figure 13, below). This mechanism is supported by observations of lightning NO and ozone during TRACE-A [Pickering *et al.*, 1996; Smyth *et al.*, 1996; Thompson *et al.*, 1997].

At Réunion (Figure 9, lowest panel), there appear to be two ozone maxima, one in April-June, possibly from central African burning in the early part of the dry season. Pollution in SON from more southerly Africa and Madagascar biomass fires has been well-studied [Baldy *et al.*, 1996; Taupin *et al.*, 1999 and references therein]. Fiji (Figure 9, top) also displays two periods of elevated ozone in 1999 and 2000. The influence of African fires is usually greatest in Fiji after August [Oltmans *et al.*, 2001]. At Fiji there occurs some of the lowest upper troposphere (UT) ozone seen in the SHADOZ record. Fiji's proximity to the SPCZ (South Pacific Convergence Zone) brings unpolluted marine air to the upper troposphere. Nairobi's tropospheric ozone column (Figure 9, bottom) is relatively low for a site near sources. One reason is that high terrain removes ozone equivalent to 3-5 DU. Another reason is frequent isolation from ozone resulting from African biomass fires. In Section 5.3, it will be seen that air parcels reaching the free troposphere over Nairobi are often from marine areas. Although there is considerable variability in individual profiles at Nairobi (Section 6), the tropospheric column amount usually changes little over the course of the year.

5.2 Interannual and Seasonal Variability in Time-vs-Altitude Curtains

Week-to-week variability over 1998-2000 at six SHADOZ sites (Ascension, Natal, Nairobi, Réunion, Fiji, Samoa) is depicted in time-altitude "curtain" plots (Figure 10). Sonde coverage at Irene, Watukosek and San Cristóbal is more scattered than the stations

shown. Tahiti (also not shown) is similar to Samoa.

In early 1999 at Natal, Ascension, and Nairobi, in addition to clean marine air (purple), layers of ozone > 50 ppbv are found at 4-10 km in a number of soundings. An oceanographic cruise ("Aerosols99," time-vs-altitude ozone in Figure 11) in late January-early February 1999 showed that the high ozone at Natal, Ascension and the south Atlantic may originate from several sources. Ozone soundings were taken by shipboard launches between Norfolk (US) to South Africa with one launch within 10 km of Ascension. Convective redistribution of clean marine air took place north of the ITCZ (Intertropical Convergence Zone) during the cruise (Figure 11; profiles in Figures 3 in *Thompson et al.* [2000]). During the Aerosols99 cruise, pollution traceable to west African biomass burning was redistributed by convection at the ITCZ, detraining north and south of the convective zone to mix northern and southern hemisphere air. The alternation of clean and polluted conditions in middle and upper troposphere over Ascension, Natal (and Nairobi; Figures 10A-C) in January-March 1999 might result from a variable ITCZ location during this period. *Fortuin et al.*, unpublished work, 2001, report a similar phenomenon at Surinam, which was mostly north of the ITCZ, in early 2000.

Integrated tropospheric ozone in the tropical Atlantic [*Thompson et al.*, 2000] measured during the Aerosols99 cruise data within 10 degrees of the equator (at 33-14W) averaged 39 ± 4.2 DU, similar to Natal and Ascension tropospheric ozone amounts during the same time (Figure 5-1). TOMS tropospheric ozone (Figure 3A in *Thompson et al.*, 2000) showed that the values measured by the sondes were typical of the entire south tropical Atlantic in January 1999 and were ~ 4 DU greater than ozone over the tropical north Atlantic. When tropospheric ozone is higher in the non-burning southern hemisphere than in the actively burning northern hemisphere, a tropical Atlantic "ozone paradox" is said to occur.

It is likely that not all the mid-troposphere high ozone observed at Natal, Ascension and Nairobi in early 1999 was due to pollution. During the Aerosols99 cruise, many of the high ozone layers sampled in the mid-troposphere between 5-15S (cf 5-12 km features at Ascension, Natal and Nairobi) were accompanied by low water vapor (Figure 3 in *Thompson et al.*, 2000). Subsidence of aged upper tropospheric air was inferred although it is possible that some of the ozone was photochemically formed from NO produced by lightning. The high ozone at Ascension between 5 and 12 km in early 1999 suggests upper troposphere descent, as did the Aerosols99 cruise sondes (Figure 11). The first soundings at Natal in 1998 are similar. Early 1999 soundings at Nairobi resemble those at Natal and Ascension.

Ozone over Nairobi and Réunion (Figures 10C,D) in March-April-May is more variable and, on average, greater in free tropospheric mixing ratio, than over Natal or Ascension. The reason for this enhanced mid-tropospheric ozone (pronounced in 1999, less clear in 2000, when Nairobi has a data gap) probably includes biomass burning from northern and central Africa. Although biomass burning over equatorial Africa peaks in December-January-February (north of the equator) and June-July-August (JJA, south of the equator), there is always enough fire activity over central Africa to affect Nairobi and Réunion. (Source characteristics for these two stations are similar; Section 5.3.3). After JJA, the greatest concentration of fires moves southward. In SON, when fire density is greatest in Mozambique, Swaziland and South Africa [*Justice et al.*, 1996], ozone pollution at Nairobi is more sporadic than in MAM (Figure 10C). SON burning in southern Africa and Madagascar affects Réunion [*Baldy et al.*, 1996; *Taupin et al.*, 1999] as does subsidence from the upper troposphere [*Randriambelo et al.*, 1999]. Réunion has a lower chemical tropopause than the other SHADOZ stations (except for more southerly Irene) throughout the year, and upper tropospheric descent (yellow color) is most pronounced between August and November.

Southern hemisphere biomass burning in SON makes a clear contribution to lower and mid-tropospheric ozone at Natal and Ascension (note green-yellow in Figures 10A,B in

Days 240-330). This was documented in SAFARI-92/TRACE-A sondes and with aircraft data over Africa and the Atlantic basin [Browell *et al.*, 1996; Olson *et al.*, 1996; Thompson *et al.*, 1996a]. Subsidence and recirculation of stratified air parcels over the south tropical Atlantic lead to greater column ozone over the ocean than over the adjacent continents (see Kim *et al.*, 1996, for a typical map). The upper troposphere at Natal and Ascension in SON is suggestive of these influences along with convective redistribution of ozone from biomass burning and ozone from lightning NO. The lightning contribution is difficult to quantify [Martin *et al.*, 2002], but episodic connections to high ozone layers have been made during aircraft sampling [Pickering *et al.*, 1996; Thompson *et al.*, 1997].

The pollution observed at Nairobi could originate from African burning or from India. Aircraft and shipboard soundings during INDOEX [Lelieveld *et al.*, 2001] and the Kaashidhoo ozonesondes archived in SHADOZ (Figure 12) showed the Indian Ocean west of India to be very polluted in early 1999. The Kaashidhoo sondes captured ozone pollution layers hundreds-thousands of km downwind from source regions. High ozone levels are attributed to mostly Indian sources, pyrogenic, vehicular and industrial [Dickerson *et al.*, 2002]. At other times, low ozone at higher altitudes suggests marine convection and less continental influence.

5.3 Processes Affecting Tropospheric Ozone

Ozone time-series (Figures 9 and 10) point to multiple influences on ozone, eg convection, biomass burning, stratosphere-troposphere exchange (STE), lightning, large-scale circulation (Walker, Hadley). Here we consider specifically the influences of biomass burning, convection, and source locations for free tropospheric ozone measured in the SHADOZ soundings.

5.3.1 Biomass burning

In the discussion in Sec 5.1 reference was made to the influence of biomass burning on tropospheric ozone. It is true that layers of elevated tropospheric ozone, particularly between the mixed layer and 300-400 hPa, are frequently traceable to biomass fires. In general, tropospheric ozone column amounts are greatest during the southern hemisphere dry (burning) season. Figure 13 (dashed line) displays the seasonality of biomass burning as half-monthly averaged TOMS aerosol index (a proxy for biomass burning) for four regions covered by SHADOZ stations: south tropical Atlantic, central Pacific, eastern Pacific, Indonesian maritime continent. The satellite data are based on the Nimbus 7 record (1979-1992; Herman *et al.*, 1997) which precedes the SHADOZ observing period. However, including the Earth-Probe record (1996-present) in the statistics does not alter the seasonal cycle. Also shown is TOMS tropospheric ozone column (solid line, from Nimbus 7 statistics) and tropospheric ozone from the SHADOZ sondes taken within each region. All the sonde values are indicated as stars with the full range shaded.

The satellite seasonality is a good representation of the features suggested by the SHADOZ sondes over the Atlantic and central Pacific (Figures 13A,B). The satellite ozone agrees well with the seasonal cycle displayed by SHADOZ sondes over the eastern Pacific and Indonesian regions, at San Cristóbal and Watukosek, respectively, but overestimates the magnitude. Both sondes and satellite ozone, however, do not correlate simply with the biomass burning signal, suggesting that dynamical factors play a role. Figures 10A, B show signs of higher ozone mixing ratio in the upper troposphere, indicating greater subsidence (or stratospheric influence) over Ascension and Natal between August and October. The persistence of subsidence in this region is one reason that a wave-one pattern is seen in the troposphere throughout the year (Section 4). Seasonal offsets are particularly pronounced over the Atlantic where they were noted during the TRACE-A period [Thompson *et al.* 1996a,b; Olson *et al.*, 1996] and the Aerosols99 cruise [Thompson *et al.*, 2000; 2001]. A

couple of recent model analyses suggest that lightning enriches south Atlantic ozone in the early wet season (September-October) and may cause the south Atlantic ozone maximum to extend into November [Moxim and Levy, 2000; Martin et al., 2000].

5.3.2 Convective Influences

Convective influences appear as low ozone, < 20 ppbv (purple color in the middle and upper troposphere in Figure 10) are summarized for as follows:

Ascension (Figure 10A) has the least convective influence of SHADOZ sites.

Natal: Low ozone (as purple, Figure 10B) and upper troposphere or lower stratospheric influence occur often between 5 and 17 km. The DJF convective influence can last until May. Kirchhoff et al. [1990] reported convective influence and very low ozone (integrated tropospheric ozone, 10 DU) from sondes launched at Natal during the ABLE-2B campaign (Amazon Boundary Layer Expt, March-May 1987). This occurs from December 1998 through May 1999 even though north central African burning may add higher-ozone layers between 3 and 12 km. Wet season convection influences ozone up to 15 km at Natal.

Nairobi (Figure 10C) has the greatest convective influence in early 1998, similar to Réunion, although the latter has fewer sondes for comparison. After 1998 there is little convection at Nairobi until early 2000.

Réunion. Although the general characteristics seen at Nairobi hold at Réunion (Figure 10D), this station is the most variable (diverse) with mid-late 1998 heavy in stratospheric influence and some convective influence in 2000.

Fiji and Samoa (Figures 10 E,F) show heavy convective influence, especially in the first 100 days of each year. At these stations (WatuKosek, not shown, is similar) convective influence reaches 15 km routinely.

5.3.3 Mid-Troposphere Trajectory Origins

The NASA/Goddard kinematic trajectory model [Schoeberl and Newman, 1995] is used to examine source regions for mid-tropospheric ozone. Figure 14 shows the origin points of 5-day back trajectories that were initialized for each launch date at 500 hPa. Pressures at the end points corresponded to 325-450 hPa and the latitude-longitude of the origin after 5 days is marked with a diamond. How does the trajectory climatology (TC) for each point correspond to the picture deduced from the altitude-vs-time curtains and the UT mixing ratios? Ascension and Natal (Figure 14A,B) air parcel origins resemble one another. The two stations are not far apart, within 2 latitude degrees of one another, and are fairly similar with respect to the ITCZ. Most origin points for Ascension and Natal cluster within a region 30W-10E, 2S-10N. Ascension origins are displaced farther east and south, over Africa and the eastern Atlantic, where tropospheric ozone is on average at its highest tropical value [Thompson and Hudson, 1999; see maps at <metosrv2.umd.edu/~tropo>]. The TC for Natal has origins farther north and more central Atlantic, ie closer to the ITCZ. This is consistent with Natal showing more signs of convection, ie mid-tropospheric ozone with surface ozone mixing ratios (< 40 ppbv).

The Nairobi cluster of origin points (Figure 14C) is confined to 30-80E, a region that may be influenced by pollution from Africa [Gatebe et al., 1999] or India [Lelieveld et al., 2001]. Nairobi origins are approximately half polluted and half clean, as the individual profiles show (below in Figure 16). Réunion, not surprising because it is most subtropical of the sites under discussion, shows diffuse trajectory origins corresponding to greater wind speeds, ie farthest away - across the Atlantic and even to eastern South America (Figure 14D). However, the greatest clustering of Réunion origins is over Africa, the eastern Indian Ocean and Madagascar. These locations are subject to stratospheric and biomass burning influences [Taupin et al., 1999; Randriambelo et al., 2000]. Central Indian Ocean origins for Réunion occur frequently in December through March; these correspond to the lowest UT

ozone in 1999 and 2000. The Réunion (Figure 14D) origins penetrate Africa more deeply (ie to the west) than trajectories from Nairobi, which is more representative of an equatorial location and therefore subject to lighter winds and regional influences.

To put Fiji TC (Figure 14E) into context, it helps to look at the TC for Watukosek (Figure 14F), San Cristóbal (Figure 14G). Watukosek origins do not coincide with those from Réunion or Nairobi (sites to the east) nor with San Cristóbal to the east. Fiji has air parcel origins within Réunion range and some overlap with Watukosek in the eastern Indian Ocean and over Australia. Fiji origins (and Samoa origins, not shown) are heavily marine, ie over the western Pacific in the vicinity of the SPCZ [Pickering *et al.*, 2001]. That is why low ozone marine air penetrates to the mid-troposphere so frequently (cf Figure 10E). Most origins for air parcels reaching San Cristóbal (Figure 14G) are over equatorial South America.

5.3.4 Ancillary Data: TTO Biomass Burning, Convection Indicators

Figure 15A, B shows aerosol index from E-P/TOMS based on 9-day averages over a 10x10-degree box centered at five SHADOZ stations. Natal and Ascension are generally similar in Aerosol Index (AI, proxy for biomass burning) and TRMM (Tropical Rainfall Measuring Mission) precipitation fields (Adler ref) with two exceptions. First, in early 1999, more precipitation is recorded at Natal (and it is assumed, convection). This contrast is expected to manifest itself as lower mid- and upper tropospheric ozone at Natal than Ascension and is borne out in the altitude-vs-time curtains (Figure 10A,B). The second difference is in the Aerosol Index (AI, the proxy for biomass burning and/or dust), which is greater at Ascension. The two stations track each other fairly well but Ascension is closer to the African sources that affect both (Figure 15A) and picks up AI increases a few weeks ahead of Natal and AI is of greater magnitude. Late 1999-early 2000 where AI is high, both stations show high ozone in the mid-troposphere.

Nairobi and Réunion (Figure 15B) began 1998 under the transition from El-Niño to La Niña, with the heaviest precipitation recorded during the 1998-2000 period. The precipitation is linked with greater convection. Tropospheric ozone from the sondes (Figure 9, lowest frame) is very low. See the mid-tropospheric low ozone (purple) in the Nairobi sonde (Figure 10C). In 1999 and 2000 Réunion and Nairobi were much drier. The increased ozone could be a result of increased subsidence and/or biomass burning sources of ozone. The smoke aerosol (AI) at Nairobi and Réunion is not in phase. Nairobi is not consistently downwind of fire sources (Figure 14C) and AI varies within 0.15 of 0.35 most of 1998-1999. There are 2-3 maxima in AI the course of a year, possibly as the ITCZ migrates north and south of Nairobi. Réunion, on the other hand, is more regular in AI (Figure 15A), probably because it is usually downwind of south central African and Madagascar burning. Fires are most active between 12S and 25S Sept-December; this is followed by a switch to DJF burning in central Africa. At Fiji, the AI is similar in timing and in magnitude to Réunion.

6. Tropospheric Ozone Profile Variability and Satellite Climatology

A primary motivation for SHADOZ is to better characterize the variability of tropospheric ozone in the tropics while improving the tropical ozone profile climatology used in satellite retrievals based on the BUV measurement. Here we discuss:

- Individual and mean profiles for MAM and SON periods. Six stations capture variability within the SHADOZ data and illustrate seasonal contrasts and differences among stations (Section 6.1).
- Histograms of mean ozone mixing ratios in the lower (0-5 km), middle (5-10 km) and upper (10-15 km) troposphere (Section 6.2).
- Seasonal mean profiles compared to the tropical profile used in the TOMS v. 7 algorithm (Section 6.3).

6.1 Seasonal Ozone Profiles.

Individual and mean tropospheric profiles for MAM and SON for six stations appear in Figure 16. The MAM-SON differences in mean integrated tropospheric ozone column for Ascension, Natal, Reunion and Fiji are 10-15 DU [Table 3]. The following are the most prominent features:

1) Ascension and Natal profiles (Figure 16 A,B) are similar in shape to one another. As has been noted previously [Olson *et al.*, 1996; Thompson *et al.*, 1996a] the column amount over Ascension exceeds that over Natal on average in MAM and SON. Surface ozone is greater at Ascension than Natal. During MAM, surface mixing ratios average 12 ppbv at Natal and 18 ppbv at Ascension. During SON, surface mixing ratios average ~15 ppbv at Natal and 30 ppbv at Ascension. Between 3 and 15 km, the Ascension mean is greater than for Natal, with the former showing a local maximum (bulge). Between 5-10 km, Ascension is more variable than Natal. Ascension shows a number of profiles with ozone at > 90 ppbv (a value in only one Natal sounding). In SON, variability is comparable at the two stations. Both show a local maximum around 5 km and have soundings with layers > 100 ppbv. These high levels of ozone typify the south Atlantic basin in SON where photochemically produced ozone from biomass burning and lightning [Thompson *et al.*, 1996a; Moxim and Levy, 2000] recirculates in the tropical anticyclone [Garstang *et al.*, 1996] and mixes with subsiding ozone from the upper troposphere [Krishnamurti *et al.*, 1996].

2) Some of the same influences operating over the Atlantic affect ozone at Réunion (Figure 16C). A bulge during SON appears between 5 and 10 km (but not in MAM); the mean ozone mixing ratio at 5-10 km increases from 45 ppbv (MAM) to ~70 ppbv in SON. In contrast to Ascension, variability at Réunion is less in MAM - note tightness of the mixing ratio distribution.

3) At Fiji (Figure 16D), there is a strong seasonal contrast throughout the troposphere. In the upper troposphere above 14 km, ozone layers varying from 10-150 ppbv occurred in SON. There is greater clustering about the MAM mean profile (see histograms below). At 13 km in MAM there is a local ozone mixing ratio minimum of ~15 ppbv, and between 5-10 km a tight clustering ~ 30 ppbv. These patterns are similar to ozone distributions over Samoa and Watukosek during MAM (not shown); all three stations show a slight bulge in the 3-7 km range. In SON, transport from African biomass fires leads to high ozone layers (> 60 ppbv) over Fiji [Newell *et al.*, 1999; Oltmans *et al.*, 2001]. The mean ozone between 5-10 km at Fiji is 50% greater in SON than in MAM. SON high-ozone layers are also found over Samoa, Tahiti and Watukosek, but magnitude and frequency are less than over Fiji. There is high ozone in many layers over Fiji above 9-10 km in SON, but not at Samoa or Watukosek. Impacts of ozone from lightning NO over Fiji might be stronger [Hauglaine *et al.*, 2001; Pickering *et al.*, 2001].

4) Figures 16E,F represent two stations (Nairobi and Irene) with the least seasonal difference between mean ozone profiles. Nairobi profiles are highly variable during both seasons whereas Irene changes very little. The Nairobi minimum is ~20 ppbv from the surface to 15 km. Between 8-15 km, layers with 115 ppbv sometimes occur, suggestive of pollution or a stratospheric source. In SON the ozone concentrations reach 120 ppbv. The local maximum (bulge) is at higher altitude (9-10 km) in SON than in MAM, where the ozone bulge occurs at 7-8 km. The Irene MAM ozone profile (not based on many profiles) resembles the Nairobi mean without the middle tropospheric bulge. Both stations average 20-25 ppbv near the surface. At Irene (Figure 16F) there are some very low (below detection limit) ozone layers just above the surface in MAM and SON. The greatest difference between Nairobi and Irene is that the mean profiles in MAM and SON are similar in the latter case and not in the former.

6.2 Seasonal Variability (Histograms) in Layers.

Figures 17 and 18, with histograms of layer-averaged mixing ratio at five stations (Ascension, Natal, Réunion, Fiji, Samoa), depict quantitatively some of the variability among stations and seasons described above. This can be seen in the Atlantic (Natal and Ascension) sondes. All-sonde histograms (not shown) are similar for Natal and Ascension at 0-5 km, with a broad peak at 25-50 ppbv. Seasonally, however, there are contrasts in the 0-5 km layer at both sites. For MAM at Ascension (Figures 17A, 18A) there is a 30-35 ppbv peak, but SON mixing ratios are all > 40 ppbv with one peak at 35 ppbv and a cluster at ~60 ppbv. At Natal, the 0-5 km mixing ratios have almost no overlap in their seasonality. All MAM soundings are < 40 ppbv; SON averages 40-50 ppbv.

As for 0-5 km, the Natal distribution at 5-10 km is nearly uniform within a 30-60 ppbv range, whereas Ascension values are at 40-80 ppbv, with a peak around 50 ppbv. Seasonally, Natal at 5-10 km (Figures 17B, 18B) has two distinct distributions with little overlap whereas at Ascension, there is considerable seasonal overlap at 50-60 ppbv. Either pollution reaches Ascension at both seasons or a non-chemical mechanism contributes to the relatively high ozone mixing ratio at all times. At 10-15 km, in MAM, there are a number of Natal soundings with mean ozone < 25 ppbv, indicative of convective influence. Mean mixing ratios at 10-15 km with 45-90+ ppbv occur during SON. At 10-15 km at Ascension, there is more seasonal overlap although the skew toward higher values is clearly SON. There are no means < 25 ppbv at Ascension.

Réunion (Figures 17C, 18C) and Fiji (Figures 17D, 18D) sondes represent distinct populations. For 0-5 km, the most probable Fiji concentration, combining the two seasons shown, is 10-15 ppbv. The corresponding Réunion peak is 25-35 ppbv. At 5-10 km, where the greatest long-range transport is expected, a number of Fiji soundings fall between 50-75 ppbv where Réunion ozone peaks. However, Réunion has a number of soundings at > 80 ppbv, a SON occurrence that has been linked to African pyrogenic sources [Baldy *et al.*, 1996; Thompson *et al.*, 1996a; Randriambelo *et al.*, 1999; Taupin *et al.*, 2000]. At Réunion, there is only one sounding at < 30 ppbv at 5-10 km at either season. Fiji has a cluster of values at < 20 ppbv (all but one in MAM), ie, clean air reaches Fiji frequently (Figure 14E). At 10-15 km, the Fiji and Réunion distributions are markedly distinct: 40-100 ppbv at Réunion compared to 10-50 ppbv at Fiji. The low ozone values at Fiji are a marker for convective transport from the boundary-layer [Folkins *et al.*, 2002; Oltmans *et al.*, 2001]. Of four stations shown, Réunion has the broadest 10-15 km distribution of mixing ratio values (20-120 ppbv). A stratospheric contribution to the higher values has been described [Baray *et al.*, 2000; Randriambelo *et al.*, 1999; Taupin *et al.*, 2000], although these may be most significant in austral winter (not shown). The highest values occur in SON and the lowest in MAM, but a number of 60-80 ppbv values occur at both seasons at 10-15 km at Réunion. Samoa (Figures 17E, 18E) also display a very low ozone distribution at 0-5 km (like Fiji); the mid-upper tropospheric ozone values are lower than Fiji (see also Figures 10E,F).

6.3 Comparison of SHADOZ Mean Ozone Profiles with TOMS Climatology.

Tropical profiles currently used in the TOMS algorithm use several values of total ozone with stratospheric variations but almost no difference in the troposphere. For example, a standard profile based on 225 DU total ozone assumes a tropospheric ozone column amount (1000 to 100 hPa) of 29.8 DU; the 275 DU profile is 31.0 DU. Both profiles are 14.6 DU from the surface to 500 hPa. However, the SHADOZ climatology shows that individual tropospheric column ozone amounts are 10-50 DU (Figure 9) with seasonally averaged extremes of 16 DU (Samoa in MAM; Table 3) and 43 DU (Ascension in SON). The standard profile for a TOMS tropical ozone column of 250 DU (tropospheric section only), obtained by averaging the 225 and 275 DU profiles, is the black line in each panel of Figure

19. The MAM and SON means are indicated in blue and red, respectively (1-sigma standard deviation in shaded gray). Some of the mean profiles agree with the standard profile very well, e.g. Ascension (MAM), Fiji (SON). Samoa has the overall poorest agreement.

The most serious divergence from the standard profile is below 500 hPa. This is the point at which the retrieval efficiency drops off rapidly over low-reflectivity (0.1-0.3) surfaces [Klenk *et al.*, 1982]. For the satellite at nadir, the efficiency with which ozone is measured at 1000 hPa is only 25% when the reflectivity is 0.1 [Figure 2 in Hudson *et al.*, 1995]. Because all the SHADOZ stations are relatively remote from ozone sources (relatively small discrepancy with the standard unpolluted profile at 1000-800 hPa), the mean profiles at the sites with greatest pollution (Ascension, Natal, Réunion) do not give large errors. Note that at 500-800 hPa, one-third of the ozone profiles lie outside the shaded range and the many of the distributions in Figure 17 and 18 are not clustered about the mean. For example, Figure 18B shows that during SON, the mean mixing ratio for Ascension in the 0-5 km layer is 50 ppbv; this represents an average between two peaks centered at 40 ppbv and 60 ppbv. The latter value is about a factor of 1.5 greater than the standard profile.

Table 4 summarizes the mean column amount for the MAM and SON profiles to 100 hPa and 500 hPa. If it is assumed that the satellite retrieval down to 500 hPa is accurate, then, the average potential error is estimated as the difference between the seasonal mean column amounts and the climatology when the latter is greater than actual. In other words,

Table 4. Column integrated ozone for TOMS standard profile and seasonal means from SHADOZ (1998-2000) data, as in Figure 19.

Station	Surf to 100 hPa, MAM	Surf to 100 hPa, SON	Surf to 500 hPa, MAM	Surf to 500, SON
TOMS, 225 DU	29.8 DU	29.8 DU	14.6	14.6
Ascension	30.7	42.7	13.0	18.6
Natal	24.2	40.3	10.5	17.0
Réunion	28.2	42.3	10.8	16.0
Fiji	15.9	28.4	7.7	11.3
Samoa	15.2	22.3	6.7	9.1

at Samoa, in MAM, the mean overestimate is 8.0 DU. This is ~50% of the tropospheric column or 2.8% of a total 225 DU ozone column. For stations for which the actual ozone exceeds climatology, 65% is assumed to be an estimate of retrieval efficiency for the difference. At Ascension in SON, for example, $(42.7 - 29.8 \text{ DU}) \times 0.65 = 8.5 \text{ DU}$ would be added to 29.8 DU (38.3 DU) in the measurement. This is ~10% lower than actual tropospheric ozone and represents a 2% error in the total column.

7. Summary

Over 1100 soundings over the southern hemisphere tropics and sub-tropics give an overview of tropical ozone during the 1998-2000 period. Time-series of individual ozone profiles, column-integrated ozone (total, stratospheric, tropospheric), and seasonally averaged profiles show:

-> Normal southern hemisphere patterns - higher ozone throughout the column

during the second half of the year compared to the first half. Stratospheric column ozone is typically 10-20 DU higher in September-October-November than in March-April-May.

-> Stratospheric ozone shows variations with phase shifts of the QBO.

-> The zonal wave-one pattern seen in satellite total ozone (referring to 10-15 DU more ozone over the Atlantic-African-western Indian Ocean region than over the eastern Indian Ocean-western Pacific) appears in tropospheric ozone throughout the year. The magnitude of the wave is greatest in SON, when downwelling from the upper troposphere concentrates ozone over the Atlantic, where it is further enhanced by ozone transported and recirculated from African burning regions and from lightning-produced NO.

-> Tropospheric ozone varies up to a factor of three in column amount over the course of the year at all but two SHADOZ sites. Very clean and polluted conditions prevail, with varying frequency at different SHADOZ stations. The most persistent pollution is found at Réunion, Natal, Ascension, and Fiji, sites where biomass burning impacts (predominantly from Africa) occur several months each year.

-> Dynamic signals apparent in individual soundings include the varying ITCZ, regional convective influence (strongest over Indonesia and the central Pacific), and the ENSO-La Niña transition in 1998-1999. Ozone profiles across the ITCZ during the trans-Atlantic Aerosols99 cruise resembled 1999 Ascension and Natal soundings.

-> Tropospheric ozone seasonal behavior based on a 14-year satellite (TOMS) record is in generally good agreement with the SHADOZ sondes. However, the satellite overestimates tropospheric ozone at Fiji and Watukosek. The timing of ozone and biomass burning seasonal cycles does not match at most SHADOZ sites. The inference is that dynamics controls much of the ozone distribution, similar to evidence from the "ozone paradox" [Thompson *et al.*, 2000].

-> A comparison between SHADOZ data and ozone profiles used in buv satellite retrievals shows the limitations of the latter with respect to tropospheric ozone variability. Errors are relatively low at SHADOZ stations because the boundary layer is unpolluted.

The SHADOZ data show complex interactions between tropospheric ozone and dynamics, with the latter possibly dominating over the influences of fires and lightning. More definitive quantification of ozone sources requires further observations and models.

Acknowledgments. SHADOZ is supported by NASA's Atmospheric Chemistry Modeling and Analysis Program (ACMAP) and the TOMS project. Individual SHADOZ sites are supported by in-country agencies and universities, including NOAA, NASDA (National Space Development Agency of Japan), LAPAN (Lembaga Penerangan Bangan Dan Antariksa Nasional, the National Institute of Aeronautics and Space Agency of Indonesia), INPE (Instituto dos Nacional de Pesquisas Espaciais, the National Space Agency of Brazil), the South African Weather Service (in the Dept. of Tourism and the Environment), the Swiss Meteorological Agency, the Kenyan Meteorological Department, the University of the South Pacific (Suva, Fiji), CNRS and the University of Réunion Island (France).

References.

- Andreae, M. O., P. Artaxo, H. Fischer H *et al.*, Transport of biomass burning smoke to the upper troposphere by deep convection in the equatorial region, *Geophys. Res. Lett.*, *28*, 951-954, 2001.
- Baldwin, M., Rev. *Geophys.* In press, 2001.
- Baldy, S., G. Ancellet, M. Bessafi, A. Badr, and D. L. S. Luk, Field observations of the vertical distribution of tropospheric ozone at the island of Reunion (southern tropics), *J. Geophys. Res.*, *101*, 23835-23849, 1996.
- Baray, J.-L., V. Daniel, G. Ancellet, and B. Legras, Planetary-scale tropopause folds in the southern subtropics, *Geophys. Res. Lett.*, *27*, 353-356, 2000.
- Bhartia, P.K., R.D. McPeters, C.L. Mateer, L.E. Flynn, and C. Wellemeyer, Algorithm for the estimation of vertical ozone profiles from the backscattered ultraviolet technique, *J. Geophys. Res.*, *101*,

18793-18806, 1996.

- Bowman, K. Global patterns of the quasi-biennial oscillation in total ozone, *J. Atmos. Sci.*, **46**, 3328-3342, 1989.
- Browell E. V. et al., Ozone and aerosol distributions and air mass characteristics over the South Atlantic basin during the burning season, *J. Geophys. Res.*, **101**, 24043-24068, 1996.
- Chandra, S., J. R. Ziemke, W. Min and W. G. Read, Effects of 1997-1998 El Nino on tropospheric ozone and water vapor, *Geophys. Res. Lett.*, **25**, 3867-3870, 1998.
- Chane-Ming, F., F. Molinaro, J. Leveau, P. Keckhut, A. Hauchecorne, and S. Godin, Vertical short-scale structures in the upper tropospheric-lower stratospheric temperature and ozone at La Réunion Island, *J. Geophys. Res.*, **105**, 26857-26866, 2000.
- Dickerson, R. R., M. O. Andreae, T. Campos, O. L. Mayol-Bracero, C. Neuseuss, and D. G. Streets, Analysis of black carbon and carbon monoxide observed over the Indian Ocean: Implications for emissions and photochemistry, *J. Geophys. Res.*, in press, 2002.
- Folkens, I., M. Loewenstein, J. Podolske, S. J. Oltmans, and M. Proffitt, A 14 km mixing barrier in the tropics: Evidence from ozonesondes and aircraft measurements, *J. Geophys. Res.*, **104**, 22095-22102, 1999.
- Folkens, I., S. J. Oltmans, and A. M. Thompson, Tropical convective outflow and near-surface equivalent potential temperatures, *Geophys. Res. Lett.*, **27**, 2549-2552, 2000.
- Folkens, I., C. Braun, A. M. Thompson, and J. C. Witte, Tropical ozone as an indicator of deep convective outflow, *J. Geophys. Res.*, in press, 2002.
- Fujiwara, M., K. Kita, and T. Ogawa, Stratosphere-Troposphere exchange of ozone associated with the equatorial Kelvin wave as observed with ozonesondes and rawinsondes, *J. Geophys. Res.*, **103**, 19173-19182, 1998.
- Fujiwara, M., K. Kita, S. Kawakami, T. Ogawa, N. Komala, S. Saraspriya and A. Suropto, Tropospheric ozone enhancements during the Indonesian forest fire event in 1994 and 1997 as revealed by ground-based observations, *Geophys. Res. Lett.*, **26**, 2417-2420, 1999.
- Fujiwara, M., K. Kita, T. Ogawa, S. Kawakami, T. Sano, N. Komala, S. Saraspriya, and A. Suropto, Seasonal variation of the tropospheric ozone in Indonesia revealed by 5-year ground based observations, *J. Geophys. Res.*, **105**, 1879-1888, 2000.
- Fujiwara, M., and M. Takahashi, Role of the equatorial Kelvin wave in stratosphere-troposphere exchange in a general circulation model., *J. Geophys. Res.*, **106**, 22763-22780, 2001.
- Fujiwara, M., F. Hasebe, M. Shiotani, N. Nishi, H. Vömel, and S. J. Oltmans, Water vapor control at the tropopause by equatorial Kelvin waves observed over the Galapagos, *Geophys. Res. Lett.*, **28**, 3143-3146, 2001.
- Garstang, M., P. D. Tyson, R. Swap, M. Edwards, P. Källberg, and J. A. Lindesay, Horizontal and vertical transport of air over southern Africa, *J. Geophys. Res.*, **101**, 23721-23736, 1996.
- Hansen, J. E., M. Sato, I. Nazarenko, R. Ruedy, A. Lacis, D. Koch, I. Tegen, T. Hall, D. Shindell, P. Stone, T. Novakov, L. Thomason, R. Wang, Y. Wang, D. Jacob, S. Hollandsworth, L. Bishop, J. Logan, A. Thompson, R. Stolarski, J. Lean, R. Willson, S. Levitus, J. Antonov, N. Rayner, D. Parker, and J. Christy, Climate forcings in GISS SI2000 simulations, *J. Geophys. Res.*, in press, 2002.
- Hasebe, F., Quasi-biennial oscillations of ozone and diabatic circulation in the equatorial stratosphere, *J. Atmos. Sci.*, **51**, 729-745, 1994.
- Hauglataine, D., et al., On the role of lightning NO_x in the formation of tropospheric ozone plumes: A global model perspective, *J. Atmos. Chem.*, **38**, 277-294, 2001.
- Herman, J. R., P. K. Bhartia, O. Torres, C. Hsu, C. Seftor, and E. Celarier, *J. Geophys. Res.*, **102**, 16,911-16,927, 1997.
- Hollandsworth, S. M., R. D. McPeters, L. E. Flynn, W. Planet, A. J. Miller, and S. Chandra, Ozone trends deduced from combined Nimbus 7 SBUV and NOAA 11 BUV/2 data, *Geophys. Res. Lett.*, **22**, 905-908, 1995.
- Hudson, R. D., J. Kim, and A. M. Thompson, On the derivation of tropospheric column ozone from radiances measured by the Total Ozone Mapping Spectrometer, *J. Geophys. Res.*, **100**, 11138-11145, 1995.
- Johnson, B. J., S. J. Oltmans, H. Vömel, T. Deshler, C. Kroger and H. G. J. Smit, ECC ozonesonde pump efficiency measurements and sensitivity tests of buffered and unbuffered sensor solutions, *J.*

- Geophys. Res.*, in press, 2002.
- Kim, J-H., and M. J. Newchurch, Climatology and trends of tropospheric ozone over the eastern Pacific Ocean: The influences of biomass burning and tropospheric dynamics, *Geophys. Res. Lett.*, **23**, 3723-3726, 1996.
- Kim, J-H., R. D. Hudson and A. M. Thompson, A new method of deriving time-averaged tropospheric column ozone over the tropics using total ozone mapping spectrometer (TOMS) radiances: Intercomparison and analysis using TRACE-A data, *J. Geophys. Res.*, **101**, 24317-24330, 1996.
- Kirchhoff, V. W. J. H., E. V. Browell, and G. L. Gregory, Ozone measurements in the troposphere of an Amazonian rainforest environment, *J. Geophys. Res.*, **93**, 15850-15860, 1988.
- Kirchhoff// 1990.
- Kirchhoff, V. W. J. H., R. A. Barnes, and A. L. Torres, Ozone climatology at Natal, Brazil, from in-situ ozonesonde data, *J. Geophys. Res.*, **96**, 10899-10909, 1991.
- Kirchhoff, V. W. J. H., J. R. Alves, F. R. da Silva and J. Fishman, Observations of ozone concentrations in the Brazilian cerrado during the TRACE-A field expedition, *J. Geophys. Res.*, **101**, 24029-24042, 1996.
- Klenk, K. F., P. K. Bhartia, A. J. Fleig, V. G. Kaveeshwar, R. D. McPeters and P. M. Smith, Total ozone determination from the Baskscattered Ultraviolet (BUV) experiment, *J. Appl. Meteor.*, **21**, 1672-1684, 1982.
- Kley, D., P. J. Crutzen, H. G. J. Smit, H. Vömel, S. J. Oltmans, H. Grassl, and V. Ramanathan, Observations of near-zero ozone concentrations over the convective Pacific: Effects on air chemistry, *Science*, **274**, 230-233, 1996.
- Kobayashi, J. and Y. Toyama, On various methods of measuring the vertical distribution of atmospheric ozone (III) carbon-iodine type chemical ozonesonde, *Papers in Meteorology and Geophysics*, **17**, 113-126, 1966.
- Kornala, N., S. Saraspriya, K. Kita, and T. Ogawa, Tropospheric ozone behavior observed in Indonesia, *Atmos. Environ.* **30**, 1851-1856, 1996.
- Komhyr, W. D., S. J. Oltmans, P. R. Franchois, W.F.J. Evans, and W. A. Matthews, The latitudinal distribution of ozone to 35 Km altitude from ECC ozonesonde observations, 1985-1987, *Ozone in the Atmosphere*, ed. R. D. Bojkov and P. Fabian, Proceedings of Quadrennial Ozone Symposium 1988 and Tropospheric Ozone Workshop, 147-150, 1989.
- Komhyr, W. D., Operations Handbook - Ozone measurements to 40 km altitude with model 4A-ECC-ozone sondes, NOAA Techn. Memorandum ERL-ARL-149, 1986.
- Komhyr, W. D., R. A. Barnes, G. B. Brothers, J. A. Lathrop, and D. P. Opperman, Electrochemical concentration cell ozonesonde performance during STOIC, *J. Geophys. Res.*, **100**, 9231-9244, 1995.
- Krishnamurti, T. N., M. C. Sinha, M. Kanamitsu, D. Oosterhof, H. Fuelberg, R. Chatfield, D. J. Jacob, and J. Logan, Passive tracer transports relevant to the TRACE-A experiment, *J. Geophys. Res.*, **101**, 23889-23908, 1996.
- Latif M., D. Dommenges, M. Dima and A. Groetzner, The role of Indian Ocean sea surface temperature in forcing east African climate anomalies *J. Climate*, **12**, 3497-3504, 1999.
- Lelieveld, J., et. al., The Indian Ocean Experiment: Widespread air pollution from South and Southeast Asia, *Science*, **291**, 1031-1036, 2001.
- Logan, J. A., An analysis of ozonesonde data for the troposphere: Recommendations for testing 3-D models and development of a gridded climatology for tropospheric ozone, *J. Geophys. Res.*, **104**, 16115-16149, 1999a.
- Logan, J. A., An analysis of ozonesonde data for the lower stratosphere, *J. Geophys. Res.*, **104**, 16151-16170, 1999b.
- Logan, J. A. and V. W. J. H. Kirchhoff, Seasonal-variations of Tropospheric Ozone at Natal, Brazil, *J. Geophys. Res.*, **91**, 7875-7881, 1986.
- Logan, J. A., D. B. A. Jones, I. A. Megretaskaia, S. J. Oltmans, W. J. Randel, W. Kimani, and F. J. Schmidlin, The quasi-biennial oscillation in tropical ozone as revealed by ozonesonde data, *J. Geophys. Res.*, *submitted*, 2002.
- Martin, R. V., D. J. Jacob, J. A. Logan, and J. M. Ziemke, R. Washington, Detection of a lightning influence on tropical tropospheric ozone, *Geophys. Res. Lett.*, **27**, 1639-1642, 2000.

- Martin, R. V., et al., Global model analysis of TOMS and in-situ observations of tropical tropospheric ozone, *J. Geophys. Res.*, submitted, 2002.
- McPeters et al., A satellite-derived ozone climatology for balloonsonde estimation of total column ozone, *J. Geophys. Res.*, *102*, 8875-8885, 1997.
- Moxim W. J. and H. Levy, A model analysis of the tropical South Atlantic Ocean tropospheric ozone maximum: The interaction of transport and chemistry, *J. Geophys. Res.*, *27*, 2229-2232, 2000.
- Newell R. E., V. Thouret, J. Y. N. Cho, P. Stoller, A. Marengo, and H. G. Smit, Ubiquity of quasi-horizontal layers in the troposphere, *Nature*, *398*, 316-319, 1999.
- Olson, J. R., J. Fishman, V. W. J. H. Kirchhoff, D. Nganga, and B. Cros, An analysis of the distribution of O₃ over the southern Atlantic region, *J. Geophys. Res.*, *101*, 24083-24094, 1996.
- Oltmans, S. J. et al., Ozone in the Pacific tropical troposphere from ozonesonde observations, *J. Geophys. Res.*, *106*, 32503-32526, 2001.
- Pickering, K. E., A. M. Thompson, W. K. Tao, and T. L. Kucsera, Upper tropospheric ozone production following mesoscale convection during STEP EMEX, *J. Geophys. Res.*, *98*, 8737-8749, 1993.
- Pickering, K. E., et al., Convective transport of biomass burning emissions over Brazil during TRACE A, *J. Geophys. Res.*, *101*, 23993-24012, 1996.
- Pickering, K. E., A. M. Thompson, H. C. Kim, A. J. DeCaria, L. Pfister, T. L. Kucsera, J. C. Witte, M. Avery, D. R. Blake, J. H. Crawford, B. G. Heikes, G. W. Sachse, S. T. Sandholm, R. W. Talbot, Trace gas transport and scavenging in PEM-Tropics-B SPCZ convection, *J. Geophys. Res.*, *106*, 32591-32608, 2001.
- Randel, W. J., and F. Wu. Isolation of the ozone QBO in SAGE II data by singular-value decomposition, *J. Atmos. Sci.*, *53*, 2546-2559, 1996.
- Randriambelo, T., J-L. Baray, and S. Baldy, Effect of biomass burning, convective venting, and transport on tropospheric ozone over the Indian Ocean: Reunion Island field observations, *J. Geophys. Res.*, *105*, 11813-11832, 2000.
- Reed, R. J., A tentative model of the 26-month oscillation in tropical latitudes, *Q. J. R. Meteorolog. Soc.*, *90*, 441-446, 1964.
- Saji, N. H., B. N. Goswami, P. N. Vinayachandran, and T. Yamagata, A dipole mode in the tropical Indian Ocean, *Nature*, *401*, 360-363, 1999.
- Schoeberl, M. R. and P. A. Newman, A multiple-level trajectory analysis of vortex filaments, *J. Geophys. Res.*, *100*, 25801-25815, 1995.
- Shiotani, M. Annual, quasi-biennial and El Nino-Southern Oscillation (ENSO) time-scale variations in Equatorial total ozone, *J. Geophys. Res.*, *97*, 7625-7634, 1992.
- Smit, H., D. Kley, S. McKeen, A. Volz, and S. Gilge, The latitudinal and vertical distribution of tropospheric ozone over the Atlantic Ocean in the southern and northern hemispheres, in *Ozone in the Atmosphere*, ed. R. D. Bojkov and P. Fabian, 419-422, 1989.
- Smyth, S., et al., Comparison of free tropospheric western Pacific air mass classification schemes for the PEM-West A experiment, *J. Geophys. Res.*, *101*, 1743-1762, 1996.
- Taupin, F. G., M. Bessafi, S. Baldy, and P. J. Bremaud, Tropospheric ozone above the southwestern Indian Ocean is strongly linked to dynamical conditions prevailing in the tropics, *J. Geophys. Res.*, *104*, 8057-8066, 1999.
- Thompson, A. M. and R. D. Hudson, Tropical tropospheric ozone (TTO) Maps from Nimbus 7 and Earth-Probe TOMS by the modified-residual method: Evaluation with sondes, ENSO signals and trends from Atlantic regional time series, *J. Geophys. Res.*, *104*, 26961-26975, 1999.
- Thompson, A. M., K. E. Pickering, D. P. McNamara, M. R. Schoeberl, R. D. Hudson, J. H. Kim, E. V. Browell, V. W. J. H. Kirchhoff, and D. Nganga, Where did tropospheric ozone over southern Africa and the tropical Atlantic come from in October 1992? Insights from TOMS, GTE/TRACE-A and SAFARI-92, *J. Geophys. Res.*, *101*, 24251-24278, 1996a.
- Thompson, A. M., et al., Ozone over southern Africa during SAFARI-92/TRACE A, *J. Geophys. Res.*, *101*, 23793-23807, 1996b.
- Thompson, A. M., W.-K. Tao, K. E. Pickering, J. R. Scala, and J. Simpson, Tropical deep convection and ozone formation, *Bull. Amer. Met. Soc.*, *78*, 1,043-1,054, 1997.
- Thompson, A. M., B. G. Doddridge, J. C. Witte, R. D. Hudson, W. T. Luke, J. E. Johnson, B. J. Johnson, S. J. Oltmans, and R. Weller, A tropical Atlantic ozone paradox: Shipboard and satellite views of a

- tropospheric ozone maximum and wave-one in January-February 1999, *Geophys. Res. Lett.*, **27**, 3317-3320, 2000.
- Thompson, A. M., J. C. Witte, R. D. Hudson, H. Guo, J. R. Herman, and M. Fujiwara, Tropical tropospheric ozone and biomass burning, *Science*, **291**, 2128-2132, 2001.
- Thompson, A. M. et al., The 1998-2000 SHADOZ (Southern Hemisphere ADDitional Ozonesondes) tropical ozone climatology. 1. Comparison with TOMS and ground-based measurements, *J. Geophys. Res.*, in press. 2002..
- Webster, J. W., A. M. Moore, J. P. Loschnigg, and R. R. Leben, Coupled ocean-atmosphere dynamics in the Indian Ocean during 1997-98, *Nature*, **401**, 356-360, 1999.
- Weller, R., R. Lillischkis, O. Schrems, R. Neuber, and S. Wessel, Vertical ozone distribution in the marine atmosphere over the central Atlantic Ocean (56°S-50°N), *J. Geophys. Res.*, **101**, 1387-1399, 1996.
- WMO (World Meteorological Organization), SPARC/IOC/GAW Assessment of Trends in the Vertical Distribution of Ozone, ed. By N. Harris, R. Hudson and C. Phillips, SPARC Report No. 1, WMO Global Ozone Research and Monitoring Project, Report No. 43, Geneva, 1998.
- Wooster, M. J., P. Ceccato, and S. P. Flasse, Indonesian fires observed using AVHRR, *Int. J. Remote Sens.*, **19**, 383-386, 1998.
- Yonemura, S., H. Tsuruta, S. Sudo, L. C. Peng, L. S. Fook, Z. B. Johar, and M. Hayashi, Tropospheric ozone climatology over peninsular Malaysia from 1992 to 1999, *J. Geophys. Res.*, submitted, 2001.
- Zawodny J. and M. P. McCormick, Stratospheric aerosol and gas experiment-II measurements of the quasi-biennial oscillations in ozone and nitrogen-dioxide, *J. Geophys. Res.*, **96**, 9371-9377, 1991.
- Ziemke, J. R., S. Chandra, A. M. Thompson and D. P. McNamara, Zonal asymmetries in southern hemisphere column ozone: Implications of biomass burning, *J. Geophys. Res.*, **101**, 14421-14427, 1996.

Table 1. Campaigns with tropical ozone data. (Still rough!)

Region	Acronym, Publication
South America- Atlantic-Africa	TROPOZ (xx & yy) ABLE-2A (Amazon Boundary-Layer Experiments, <i>J. Geophys. Res.</i> , DECAFE (Dynamique et Chimie en Afrique Experiment;) SAFARI-92/TRACE-A (Southern African Fire Atmospheric Research Initiative/Transport and Atmospheric Chemistry near the Equator- Atlantic; <i>J. Geophys. Res.</i> , 101, 30 Oct 1996) SCAR-B (Smoke, Clouds and Radiation-Brazil; <i>J. Geophys. Res.</i> , 103, December 1998) LBA-CLAIRE SAFARI-2000 Polarstern cruises (1987, 1988; Smit et al., 1989; 1993, 1994, Weller et al., 1996) Aerosols99 cruise [Thompson et al., 2000]
Pacific	ASHOE/MAESA (Airborne Southern Hemisphere Ozone Expt./ Mission for Atmospheric Effects of Stratospheric;) TOTE/VOTE STRAT PEM-Tropics Cruises - RITS, SAGA-3; CEPEX
Indian Ocean, Maritime Continent	STEP (Stratospheric-Tropospheric Expt - 1987; <i>J. Geophys. Res.</i> , 1993) INDOEX-1999 [Lelieveld et al., 2001] BIBLE-A/B (1998-99)

Table 2. Sites, period of measurements covered, references. Some stations pre-date SHADOZ, but this paper is based on their 1998-2000 data.

SHADOZ Sites	Lat./Long. (deg)		Sampling; Reference
Pago Pago, Am. Samoa	-14.23	-170.56	1995-2000 [Oltmans et al., 2001]
Papeete, Tahiti	-18.00	-149.00	1995-1999 [Oltmans et al., 2001]
San Cristóbal, Galapagos	-0.92	-89.60	1995-2000 [Oltmans et al., 2001]
Natal, Brazil	-5.42	-35.38	1978-2000 [Kirchhoff et al., 1988]
Ascension Island	-7.98	-14.42	1990-1992; 8/97-2000
Irene, South Africa	-25.25	28.22	1990-1993; 10/98-2000
Nairobi, Kenya	-1.27	36.80	1996-2000

La Réunion	-21.06	55.48	10/92-2000 [Baldy et al., 1996]
WatuKosek, Indonesia	-7.57	112.65	1993-2000 [Komala et al., 1996]
Suva, Fiji	-18.13	178.40	1996-2000 [Oltmans et al., 2001]
Kaashidhoo, Maldives	5.0	73.5	1-3/99 [Lelieveld et al., 2001]
Aerosols99 Cruise	--	--	1-2/99 [Thompson et al., 2000]

Table 3. Summary of integrated column amounts from 1998-2000 SHADOZ data and associated campaigns. SN = number of samples, 1-sigma is standard deviation from mean. Total and stratospheric ozone obtained with SBUV climatological extrapolation [THOM1]. Tropospheric ozone from integration of sonde. All in Dobson Units. From March-April-May (MAM) and September-October-November (SON) sets.

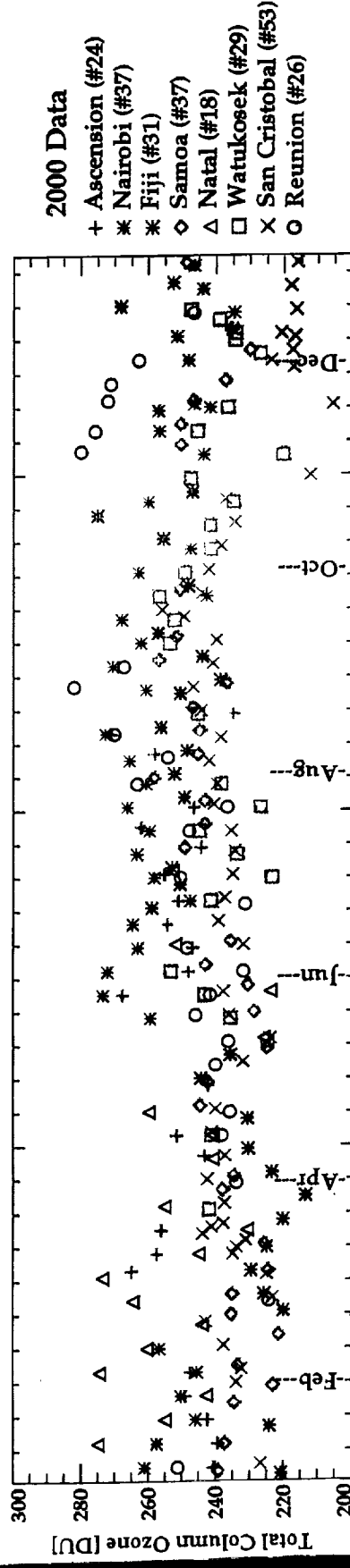
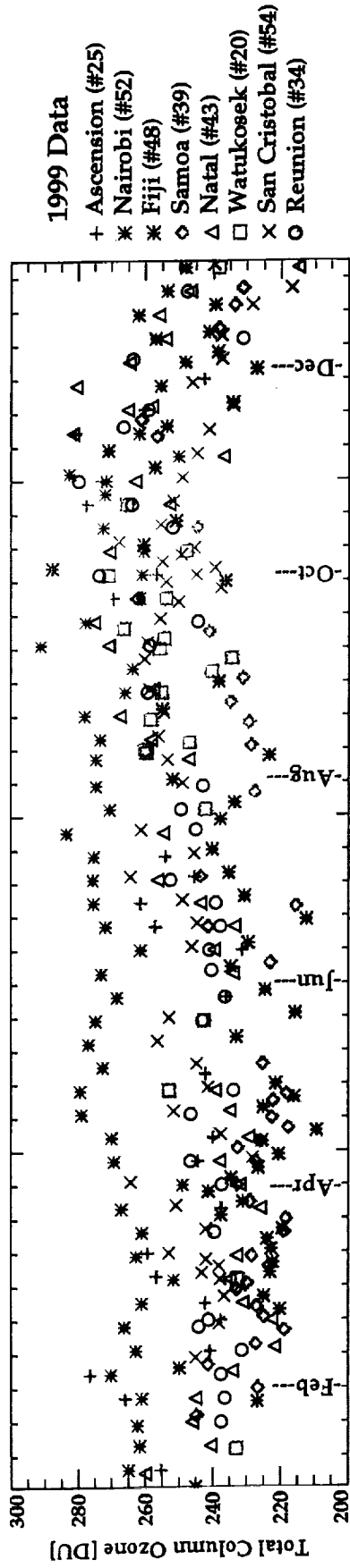
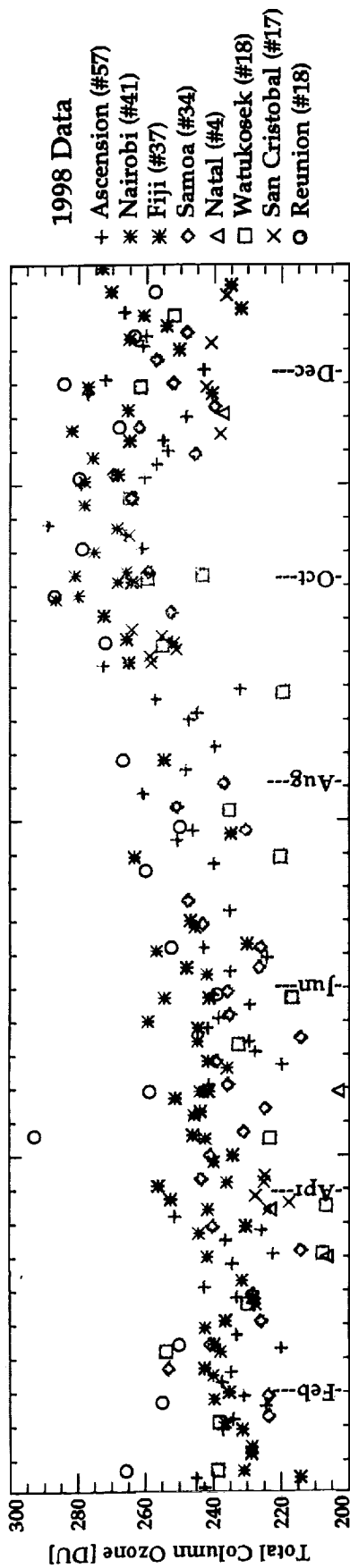
SITE	TOTAL Mean (1 σ)			STRAT Mean (1 σ)		TROP Mean (1 σ)		
	SN	MAM	SON	MAM	SON	SN	MAM	SON
Samoa	35/19	229 (8)	252 (9)	212 (6)	229 (6)	41/24	16 (5)	23 (5)
Tahiti	24/17	226 (7)	257 (6)	208 (7)	230 (8)	26/17	17 (4)	27 (4)
San Crist.	38/41	237 (14)	246 (14)	216 (13)	219 (11)	38/41	21 (3)	27 (4)
Natal	20/22	235 (16)	269 (14)	209 (14)	227 (13)	20/22	26 (5)	41 (6)
Ascension	29/29	242 (12)	263 (16)	210 (7)	220 (12)	29/30	33 (7)	43 (7)
Nairobi	29/38	257 (15)	266 (13)	228 (12)	235 (10)	29/40	29 (6)	31 (6)
Irene	13/22	254 (11)	284 (9)	224 (11)	248 (9)	13/23	30 (6)	38 (7)
Reunion	18/20	243 (14)	270 (11)	213 (9)	229 (8)	21/22	29 (7)	41 (5)
WatuKosek	14/23	233 (15)	247 (11)	211 (15)	222 (10)	19/25	20 (5)	25 (6)
Fiji	35/24	233 (11)	260 (18)	215 (8)	231 (15)	35/25	18 (6)	28 (8)
CAMPAIGNS								
Aerosol99	12	252 (14)		214 (12)		37 (3)		
INDOEX	48	246 (9)		218 (8)		29 (5)		

CAPTIONS

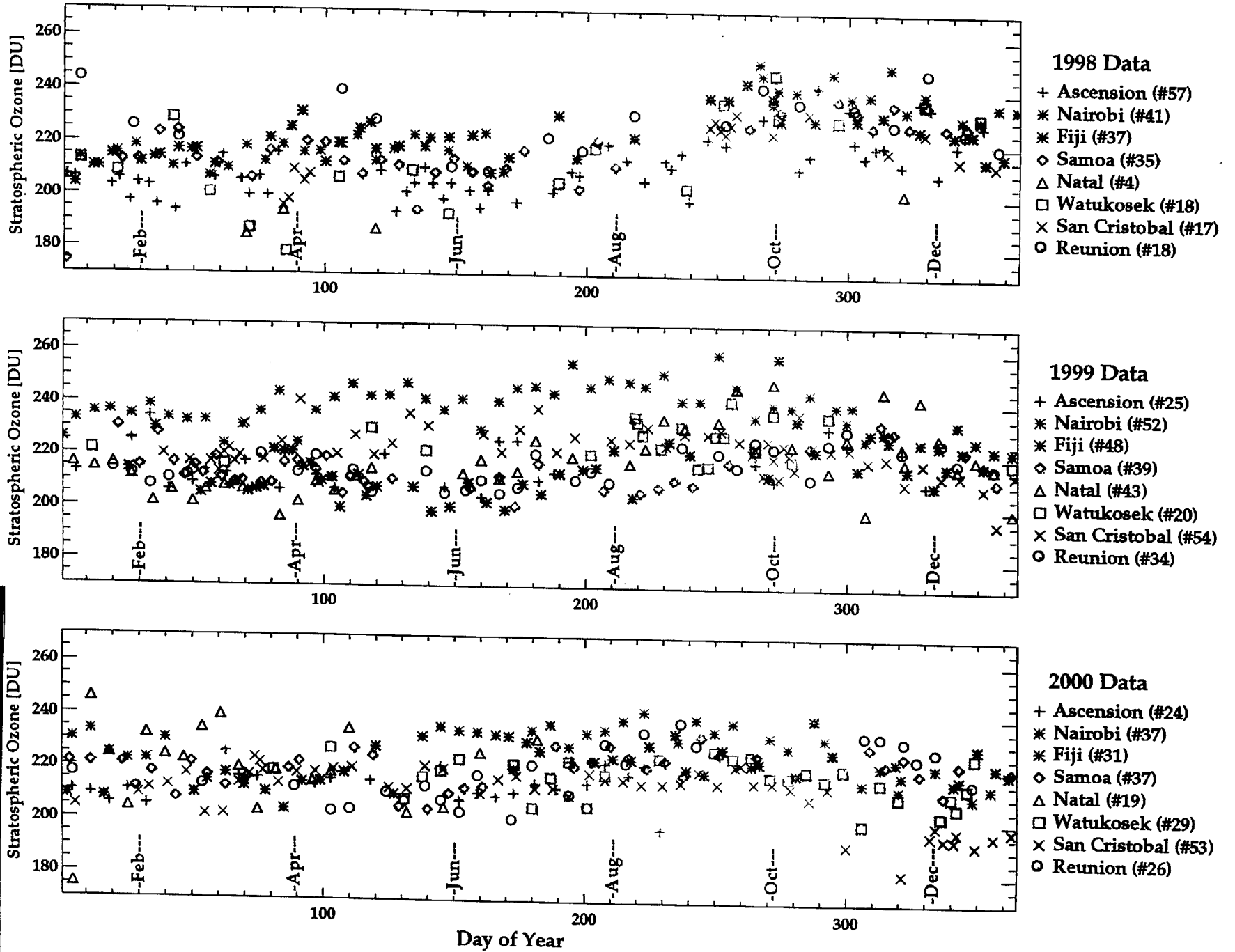
- Fig 1 Time series of total column ozone [DU] for eight SHADOZ stations for 1998 (upper), 1999 (middle) and 2000 (lower). Station and sample number are indicated to the right. Total ozone calculations use the SBUV extrapolation from 7hPa or balloon burst to the top of the atmosphere.
- Fig 2 As Figure 1, except for stratospheric column ozone [DU]. Values are determined by integration from the tropopause (determined by ozone gradient, see text) to 7 hPa or burst with SBUV extrapolation.
- Fig 3 Tropopause heights in 1998-2000. Top panel - Pacific sites (Samoa, San Cristóbal, Tahiti and Fiji). Middle panel - Atlantic stations (Natal, Ascension) and Irene. Bottom panel - Indian

- Ocean stations (Réunion, Watukosek) and Nairobi. Ozone gradient technique is used to calculate the height.
- Fig 4 Time-vs-altitude stratospheric ozone mixing ratio (in ppmv) is based on 0.25 km averages for (A) Nairobi; (B) San Cristóbal.
- Fig 5 Seasonal profiles using 1998-2000 data for six stations: San Cristóbal (A), Ascension (B), Nairobi (C), Reunion (D), Fiji (E), and Samoa (F). Solid line represents March-April-May (MAM) 0.25 mean profiles. Dashed lines represents September-October-November (SON) means. Grey shading is the 1-sigma deviation around the mean.
- Fig 6 Contoured ozone mixing ratio (ppbv) for (A) MAM 1998-2000 months. Station locations (latitude in brackets) are indicated below. Calculations are based on 0.25 mean profiles at each station for those months. (B) Same as (A) except analyses for SON months.
- Fig 7 Same as Fig 6B, except analyses for relative humidity with respect to liquid water (%).
- Fig 8. Schematic of large-scale dynamical features affecting tropical ozone: Walker circulation (arrows) and resulting convection (clouds) and subsidence (downward arrows) under normal conditions.
- Fig 9 Same as Figure 3 except integrated tropospheric ozone (DU) from sondes.
- Fig 10 Time-vs-altitude curtain of ozone mixing ratio below 20 km (in ppbv) based on 0.25 km averages. (A) Ascension; (B) Natal; (C) Nairobi; (D) Réunion; (E) Fiji; (F) Samoa.
- Fig 11 Ozone mixing ratio, in 1-km averages (35, 50, 80 ppbv contours) from Aerosols99 cruise launches between 20N-20S (23 Jan.- 4 Feb. 1999). ITCZ range indicated above.
- Fig 12 Time series of ozone mixing ratio (ppbv) during INDOEX campaign launches at Kaashidhoo (5N,75E). 50 ppbv contour shown.
- Fig 13 Statistically determined annual cycle of TOMS tropospheric ozone (TTO) (solid) and absorbing aerosol (dashed) using eleven years of Nimbus7/TOMS satellite measurements (see *Thompson et al.*, 2001 for description of calculation). Within each region, tropospheric ozone from sondes at a representative station are shown (stars, gray shading indicating range of maximum and minimum values). Regional averages as follows: (A) South Tropical Atlantic; mean region= [0-10S, 0-20W], Ascension station; (B) central Pacific [5-15S, 160-180W] with Samoa sondes; (C) Indonesian Maritime continent [0-10S, 100-120E] with Watukosek sondes; (D) eastern Pacific [5S:5N, 100W:80W] with San Cristóbal sondes.
- Fig 14 Origins (diamonds) of air parcel back-trajectories initialized at 500 hPa from eight station locations for all 1998-2000 launches and run for 5 days. NASA/Goddard kinematic trajectory model used with NCEP 2.5x2.5 gridded wind fields. Station location (filled triangle) and number of sondes used are indicated. (A) Ascension; (B) Natal; (C) Nairobi; (D) Reunion; (E) Fiji; (F) Watukosek; (G) San Cristóbal.
- Fig 15 For each station, 9-day running means at five SHADOZ stations of (A) EP/TOMS absorbing smoke aerosol (AI) and (B) TRMM (Tropical Rainfall Measuring Mission) precipitation. Data are averaged over +/- 10 degrees longitude and latitude around each station. Aerosol data from <<http://toms.gsfc.nasa.gov>>. TRMM data is provided by TRMM group at NASA/GSFC/ Mesoscale Atmospheric Process Group. Instrument degradation in EP/TOMS may affect TOMS aerosol data for second half of 2000.
- Fig 16 Three year seasonal profiles of ozone mixing ratio (ppbv). Individual profiles (black) are plotted for MAM and SON. Thick solid lines are 0.25 km seasonal means: MAM=blue, SON=red. Ascension (A), Natal (B), Reunion (C), Fiji (D), Nairobi (E) and Irene (F).
- Fig 17 Histograms of mean ozone mixing ratio (ppbv) within 5-km layers during MAM. Designations 0-5 km (purple), 5-10 km (blue), 10-15 km (yellow). (A) Ascension; (B) Natal; (C) Réunion; (D) Fiji; (E) Samoa.
- Fig 18 Same as Fig. 17 except for SON.
- Fig 19 TOMS 250 DU climatological profile (black) with seasonally averaged profiles for MAM (blue) and SON (red) based on 1998-2000 SHADOZ data. (A) Ascension; (B) Natal; (C) Réunion; (D) Fiji; (E) Samoa.

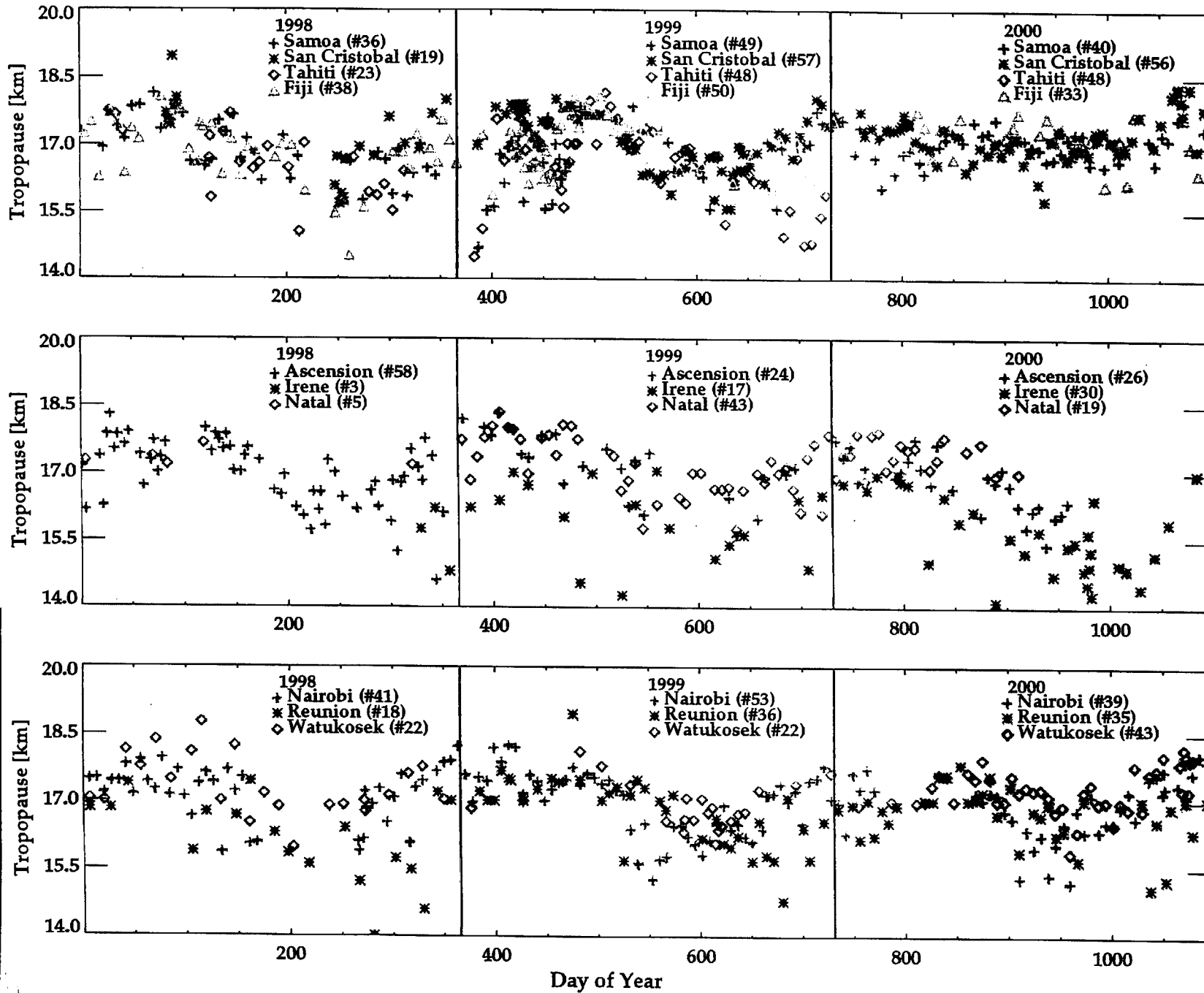
SHADOZ Sites 1998-2000



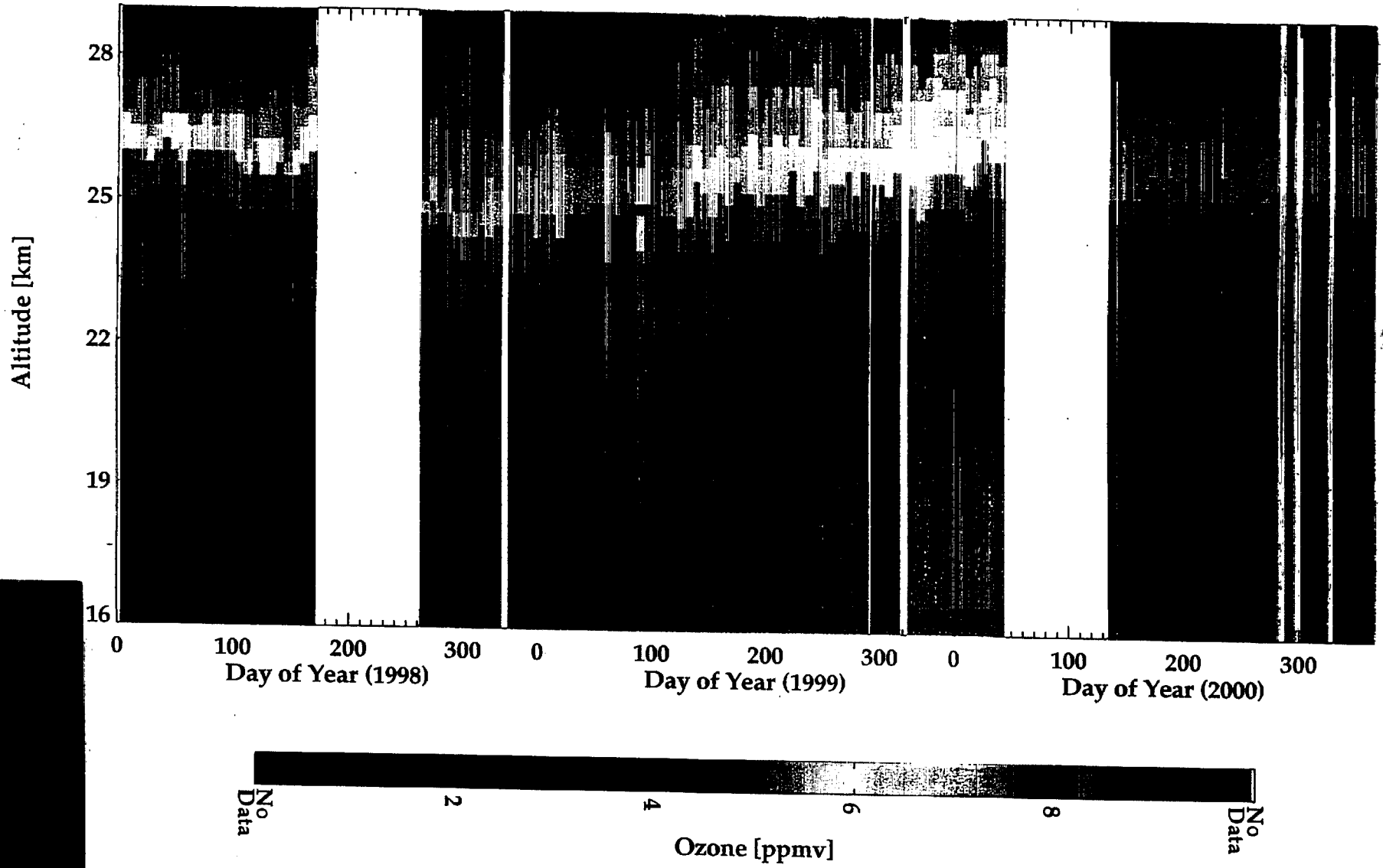
SHADOZ Site 1998-2000



SHADOZ Stations: 1998-2000

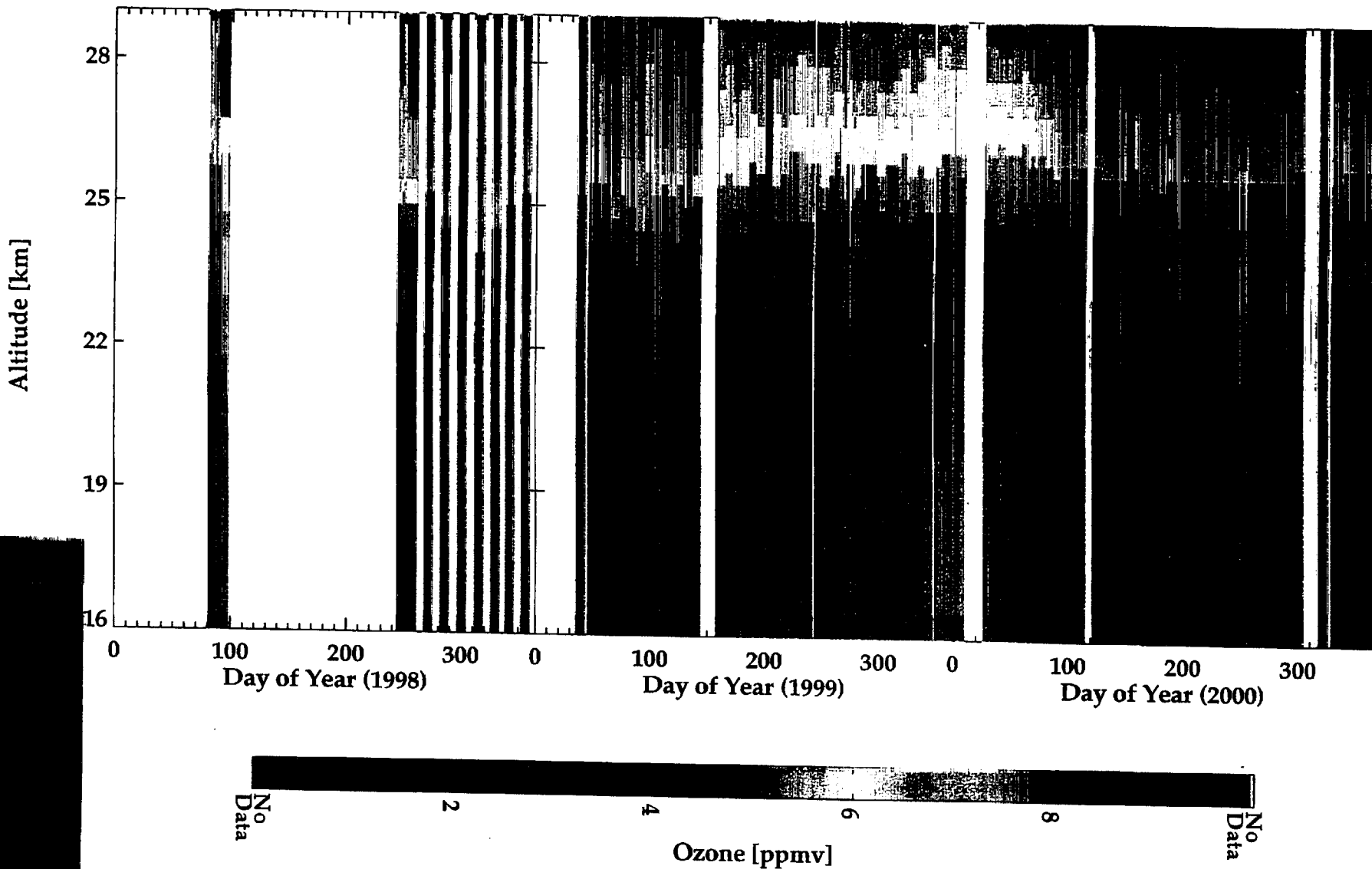


Nairobi, Kenya 1998-2000 Data - 0.25km Bins



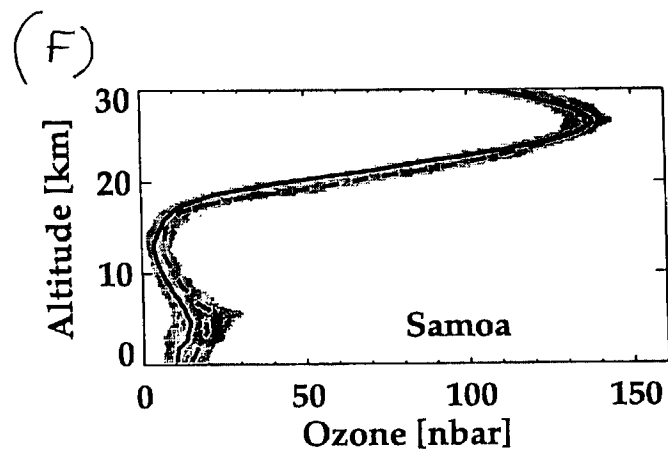
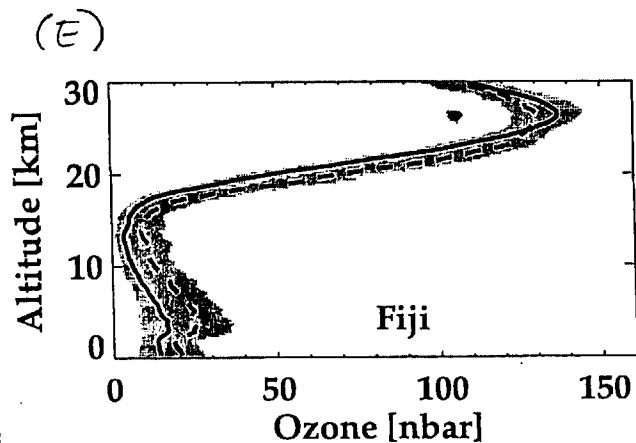
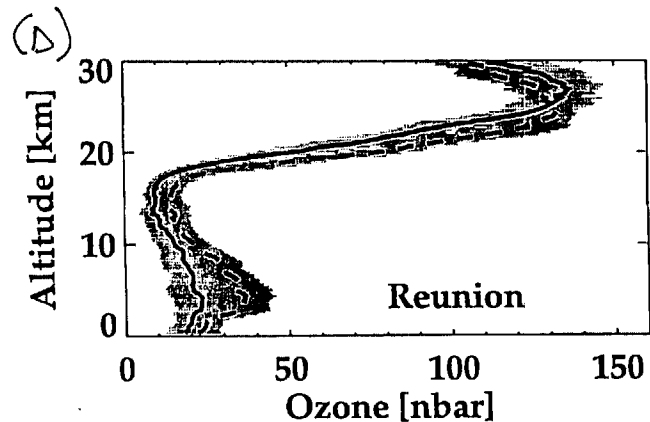
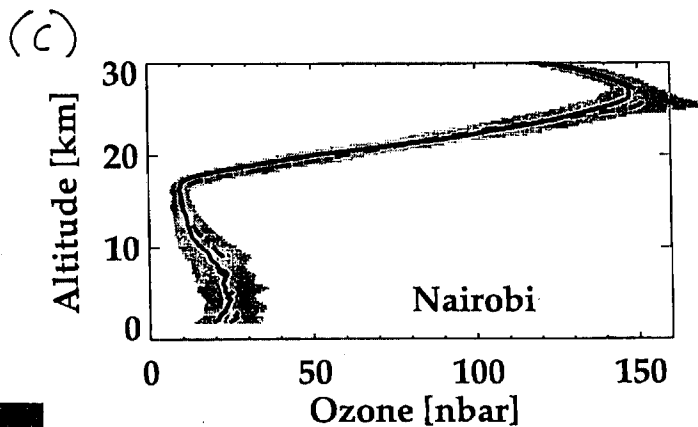
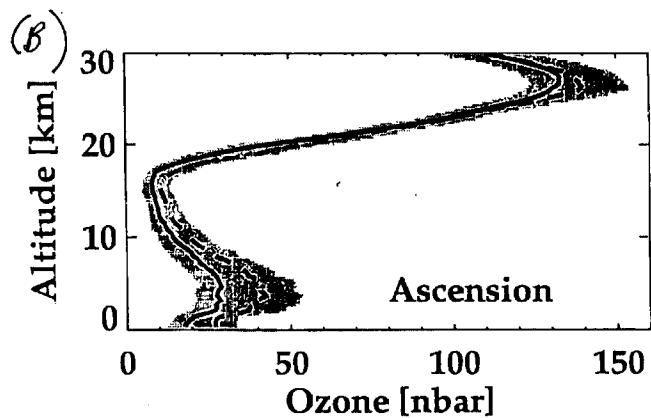
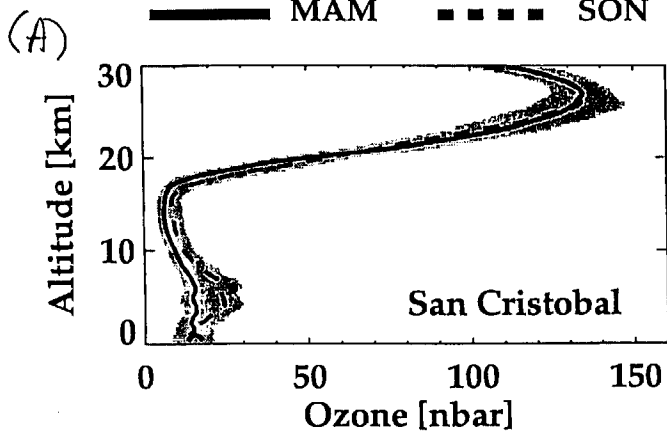
/writte/shadoz/paper2/CONT_IMAGES/curtain98-00_colr_strat_pap2.pro/010910

San Cristobal Is. 1998-2000 Data - 0.25km Bins

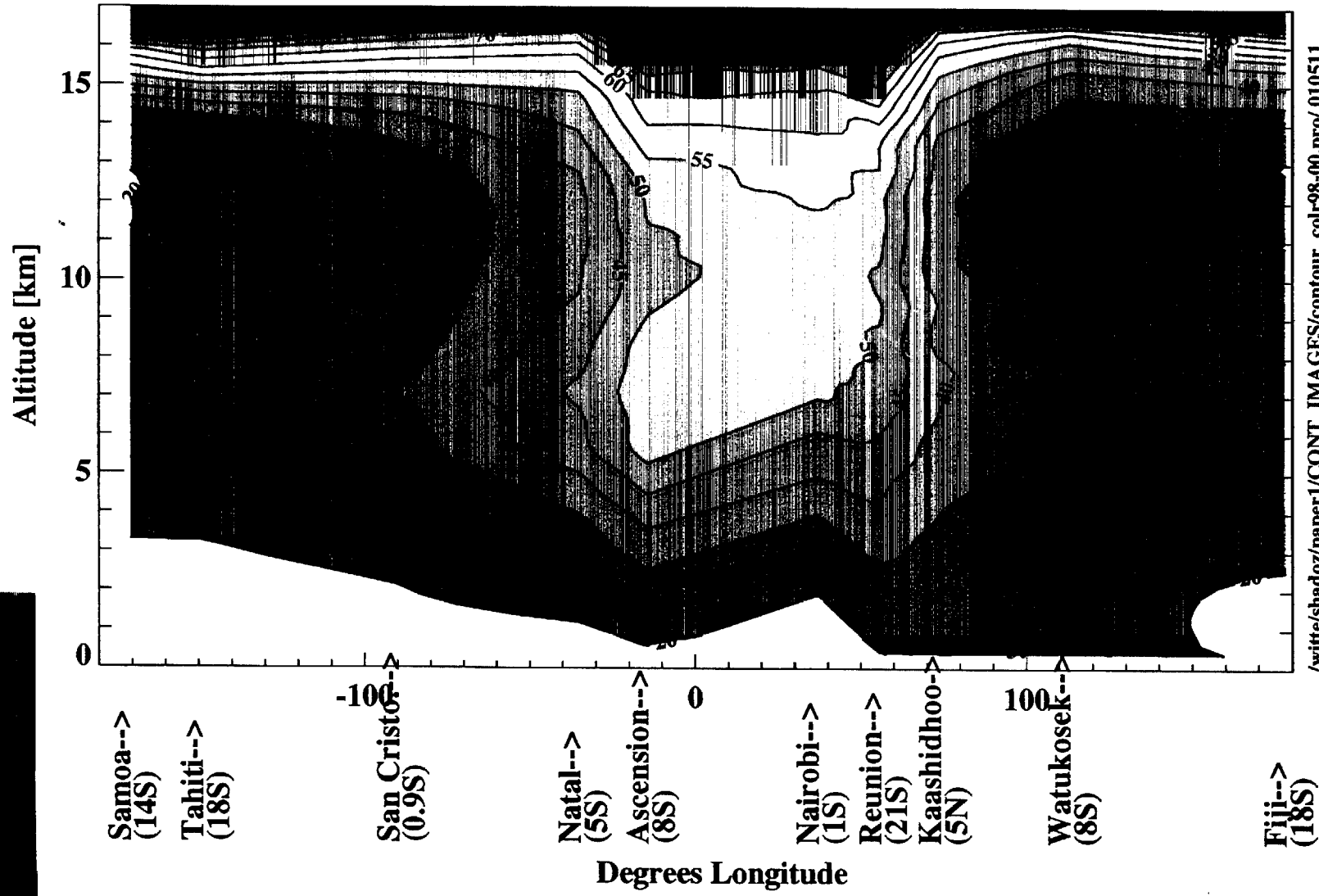


SHADOZ 1998-2000 Dataset - 0.25km mean profiles

— MAM - - - - SON

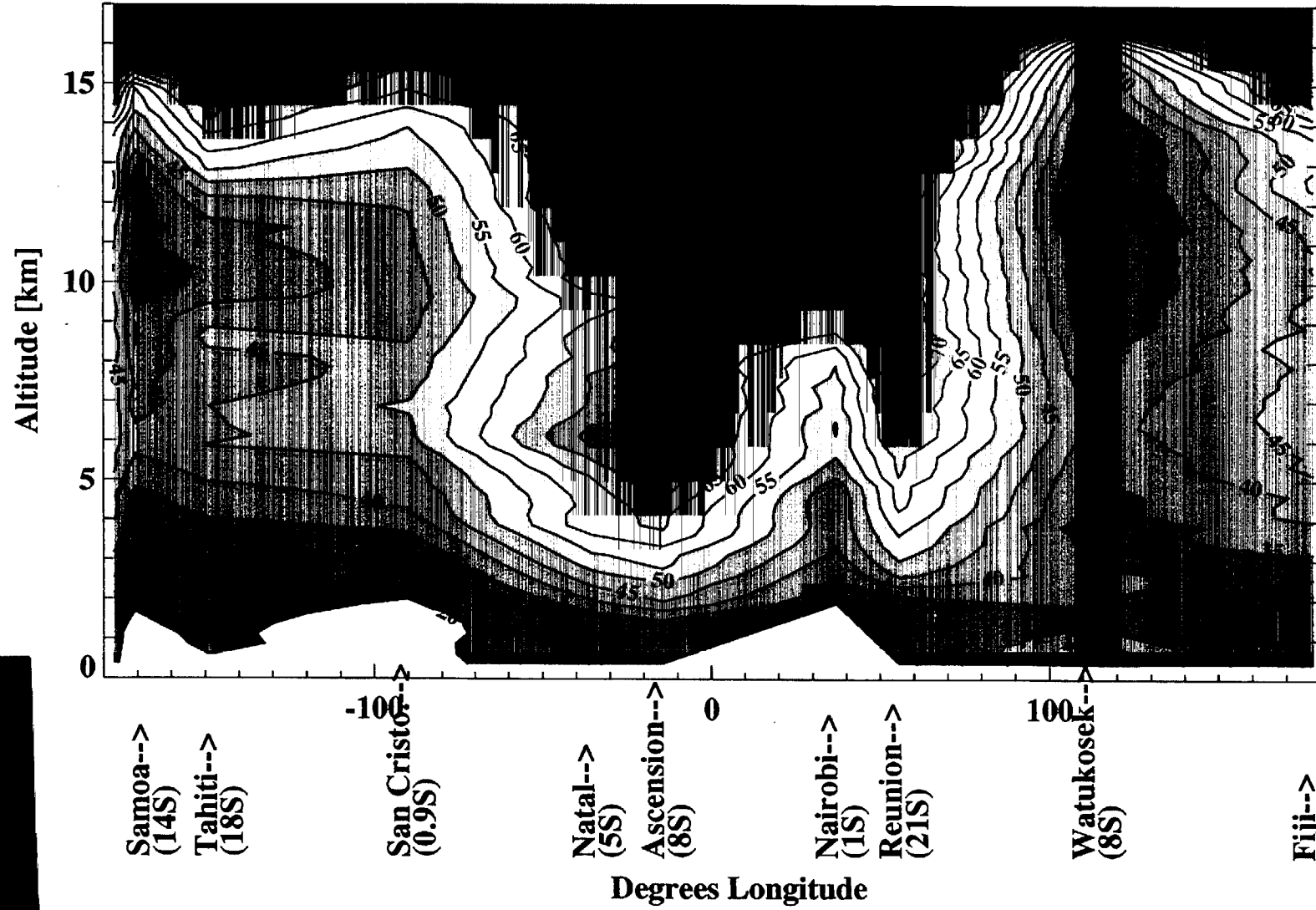


Contoured Mixing Ratio [ppbv]
March/April/May 1998-2000 0.25km Means



Contoured Mixing Ratio [ppbv]

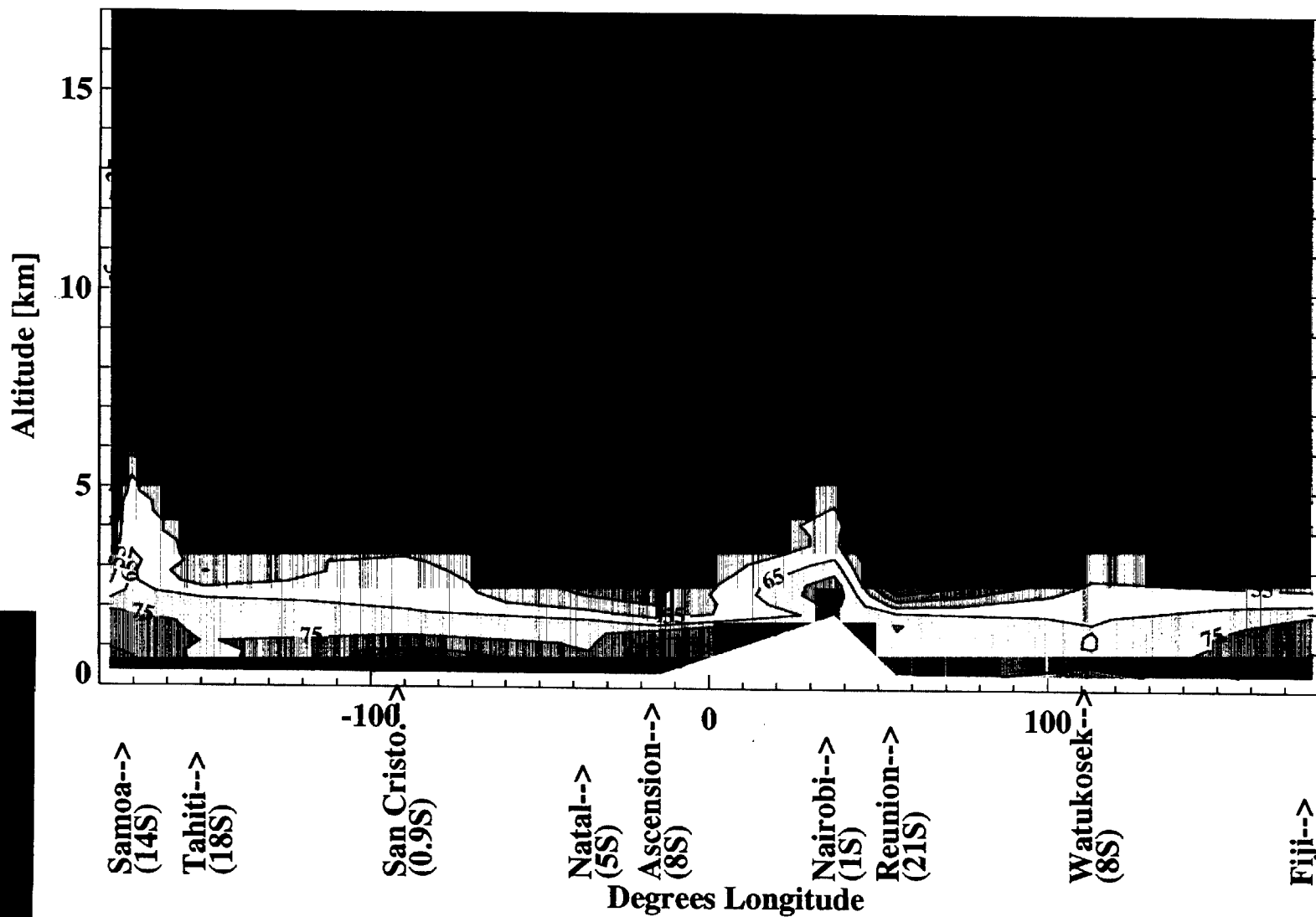
September/October/November 1998-2000 0.25km Means



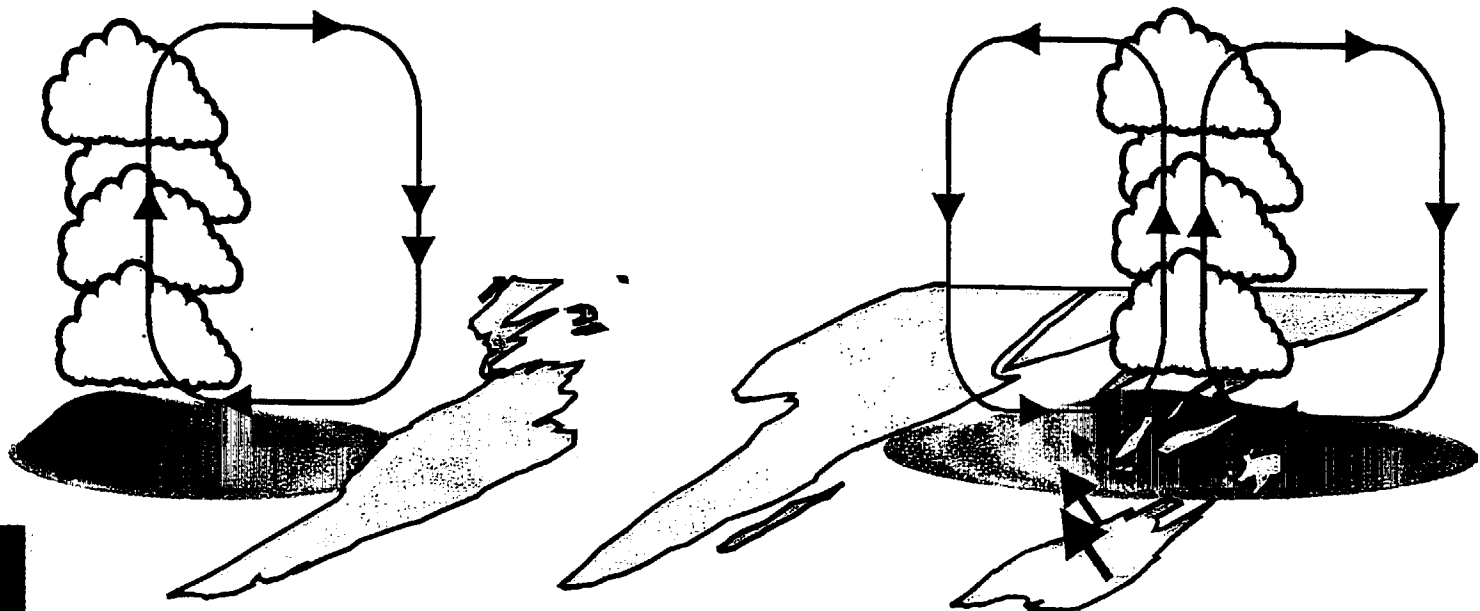
/witten/shadoz/paper2/CONT_IMAGES/hov98-00_col_allsites_ppb_v2/010823

Contoured Relative Humidity [%]

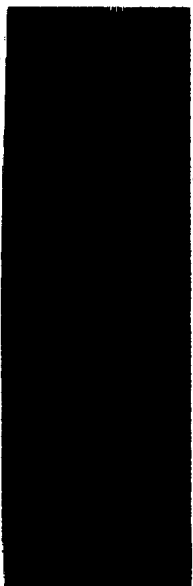
September/October/November 1998-2000 0.25km Means



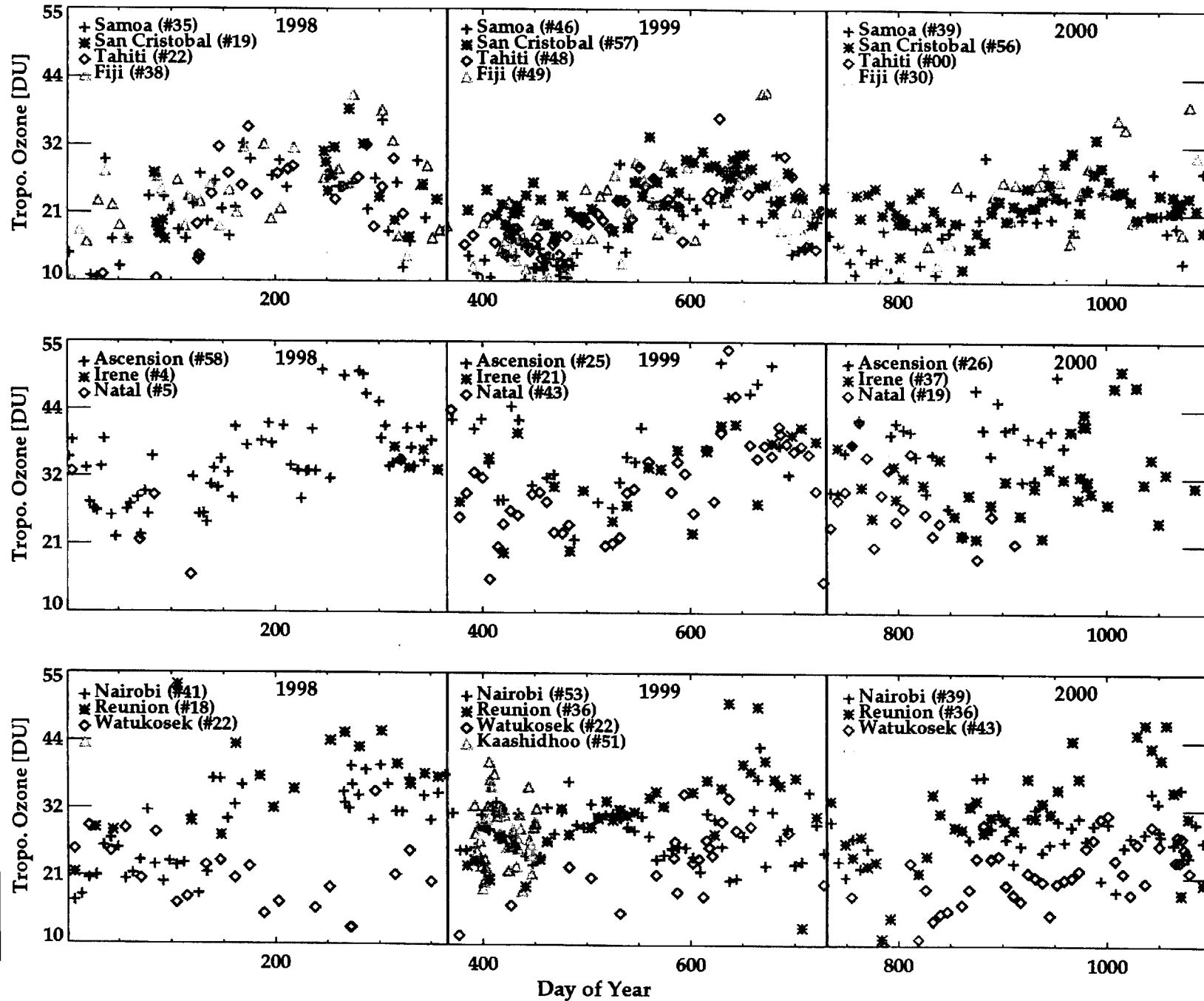
/wite/shadoz/paper1/CONT_IMAGES/hov98-00_col_allsites_rh.pro/020204



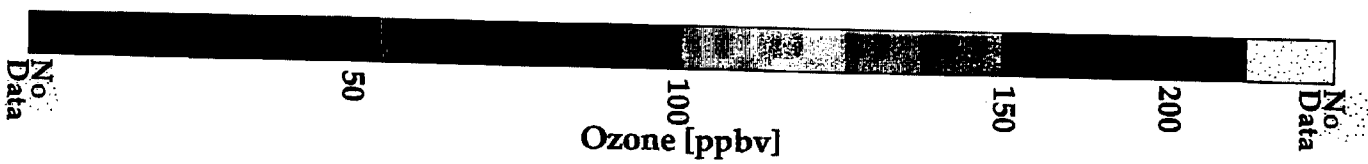
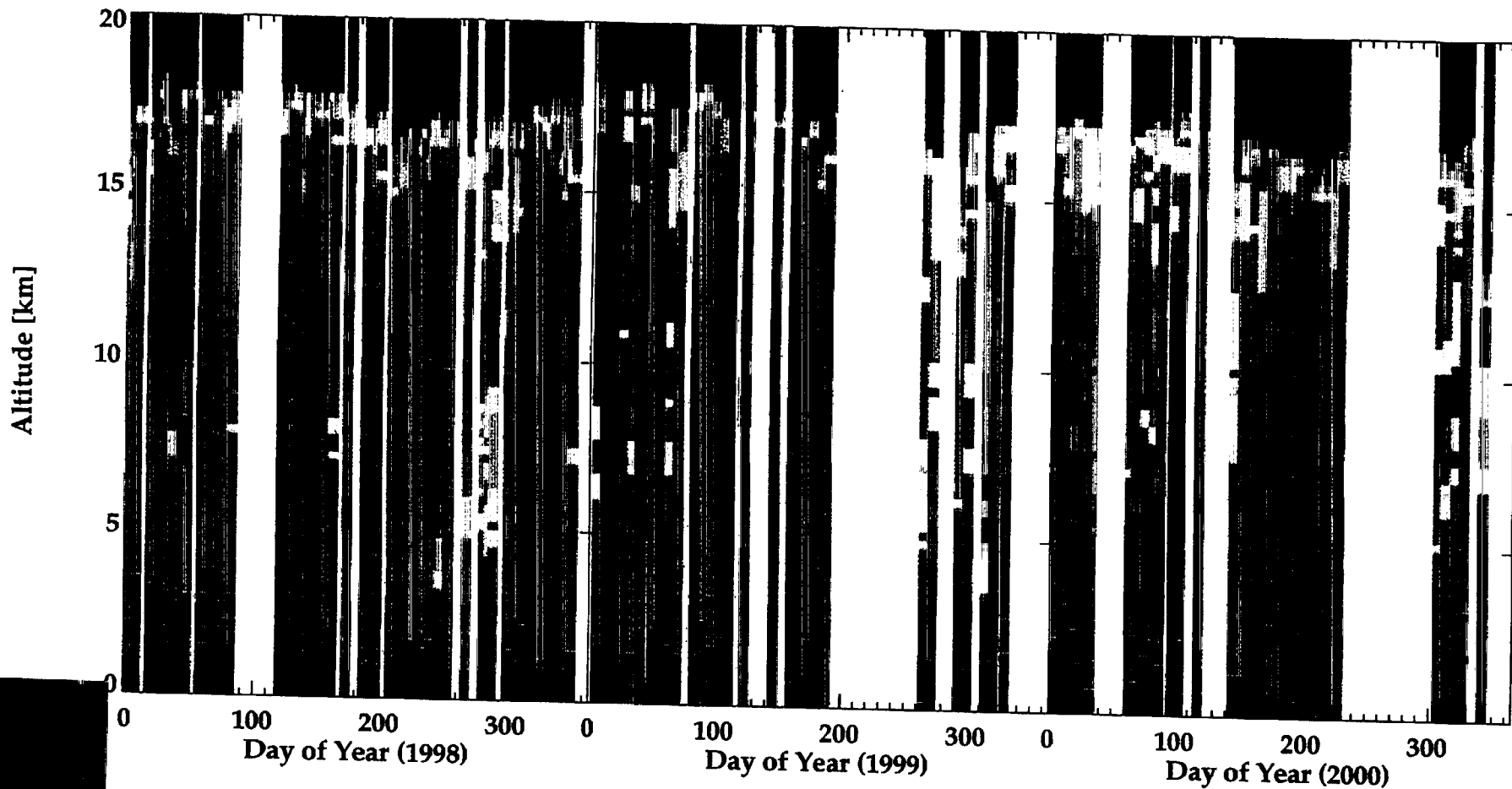
Normal Conditions



SHADOZ Stations: 1998-2000



Ascension Is. 1998-2000 Data - 0.25km Bins



/witt/shadoz/paper2/CONT_IMAGES/nov_3pan_colr_pap2.pro/010821

Natal, Brazil 1998-2000 Data - 0.25km Bins

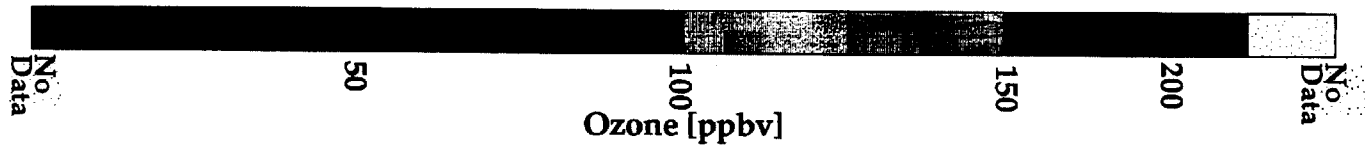
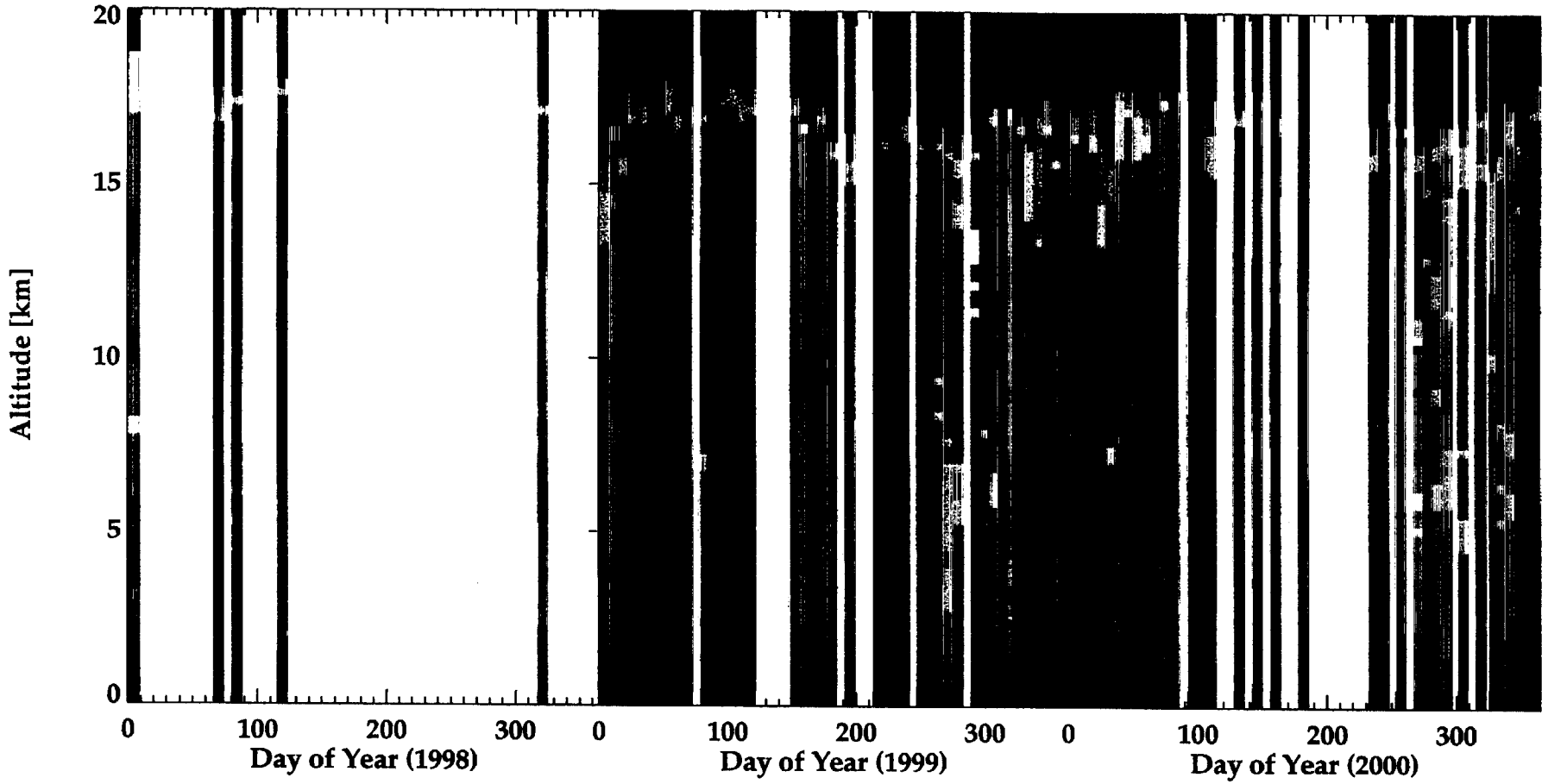


FIG 16B

Nairobi, Kenya 1998-2000 Data - 0.25km Bins

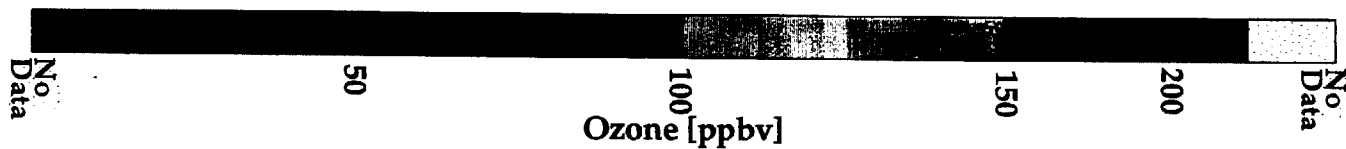
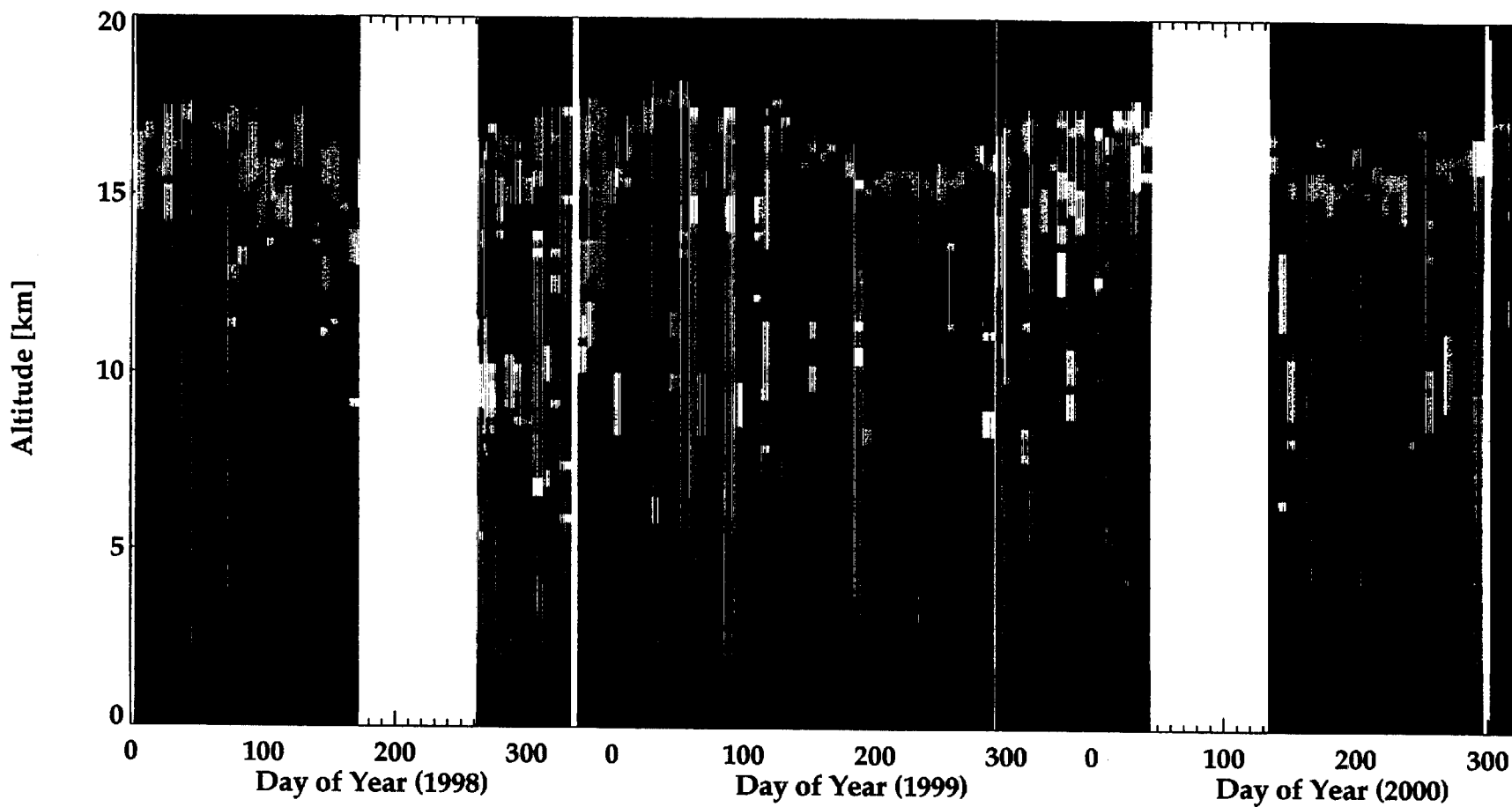


FIG 10C

/writte/shadoz/paper2/CONT_IMAGES/hov_3pan_colr_pap2.pro/010821

La Reunion 1998-2000 Data - 0.25km Bins

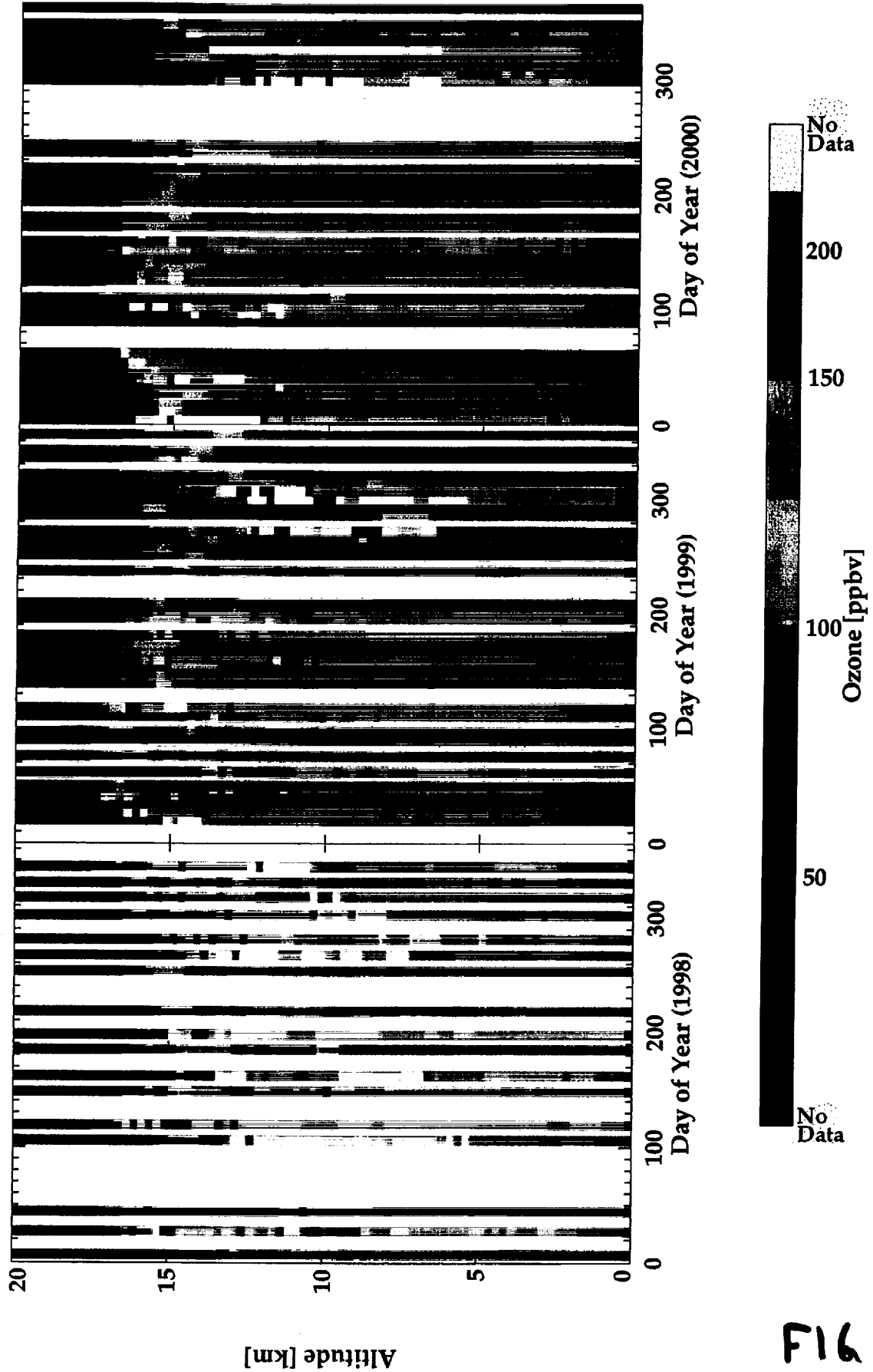


FIG 10D

Suva, Fiji 1998-2000 Data - 0.25km Bins

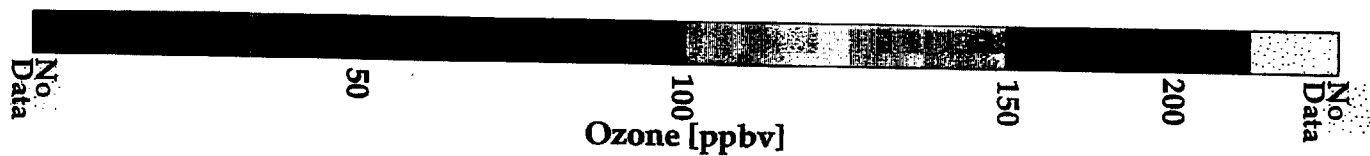
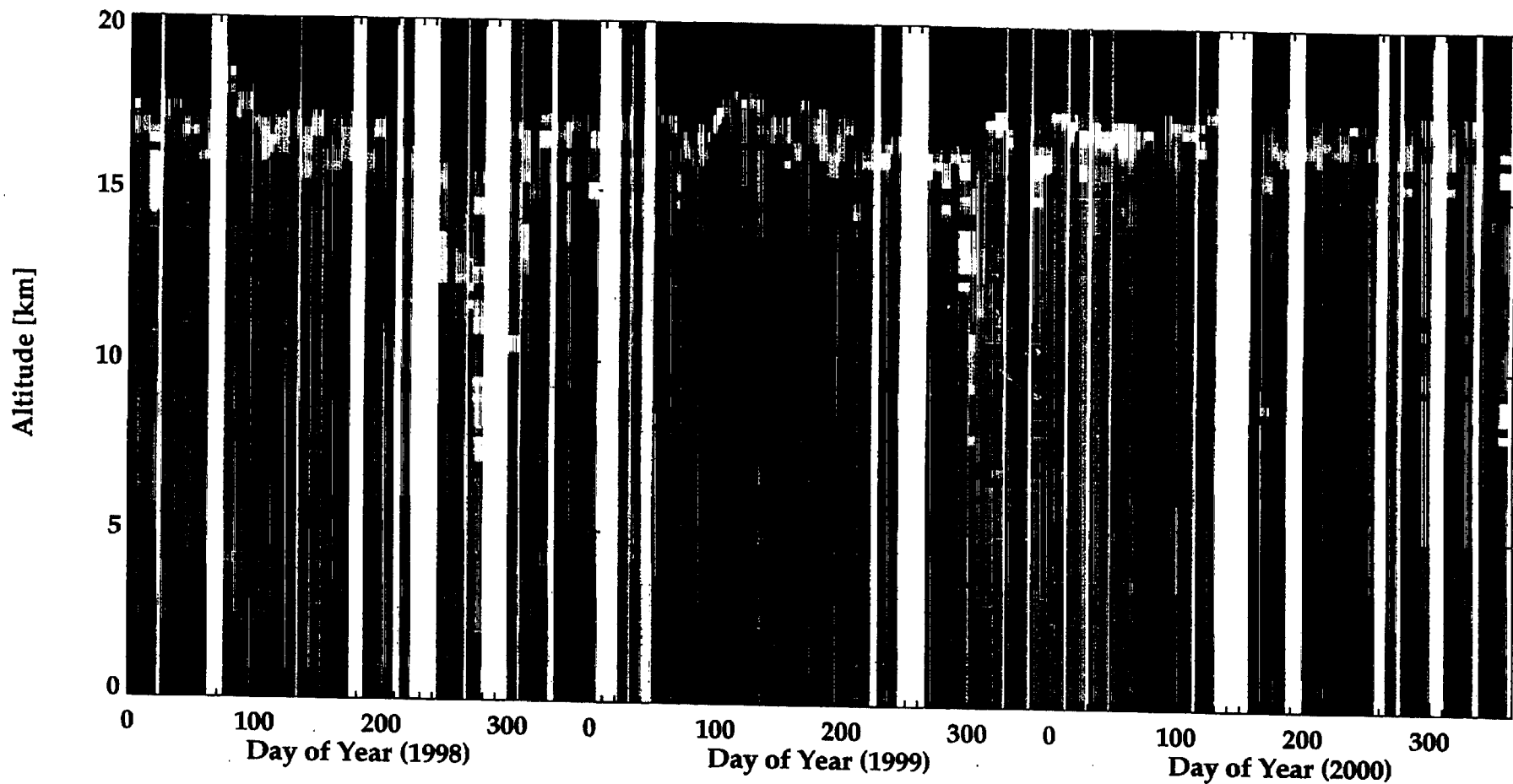
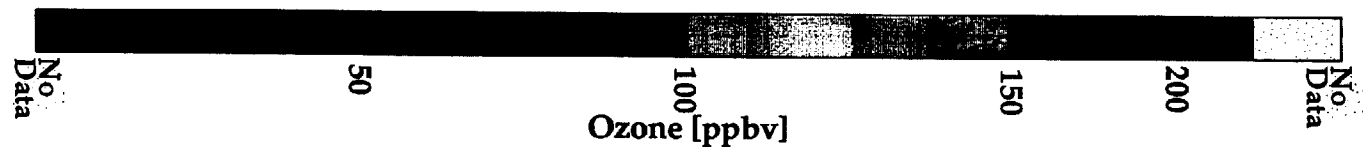
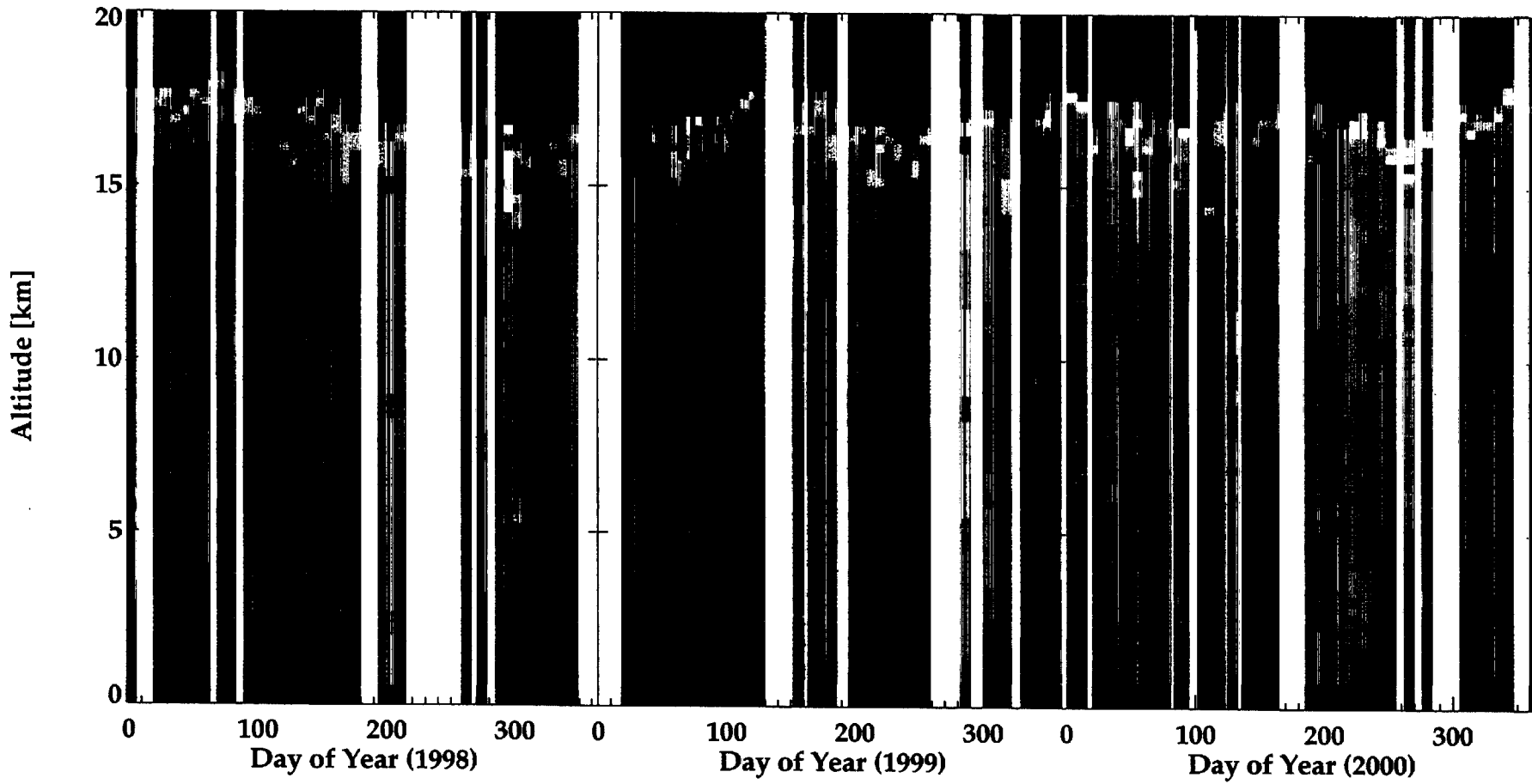


FIG 10E

Am. Samoa 1998-2000 Data - 0.25km Bins



F1610F

/withe/shadoz/paper2/CONT_IMAGES/curtain98-00_colr_pap2.pro/020212

Aerosols99 Ozone Mixing Ratio (ppbv)

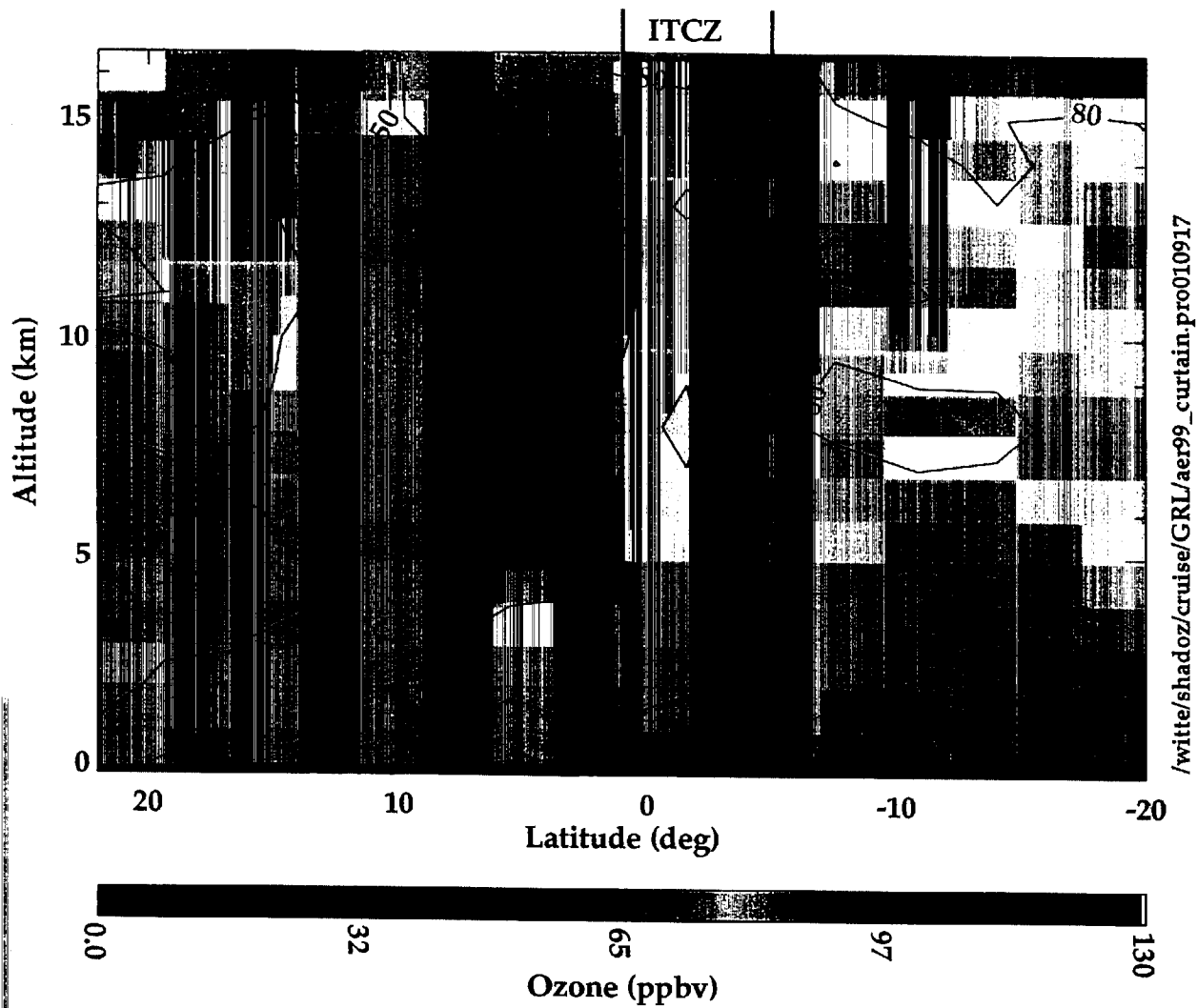
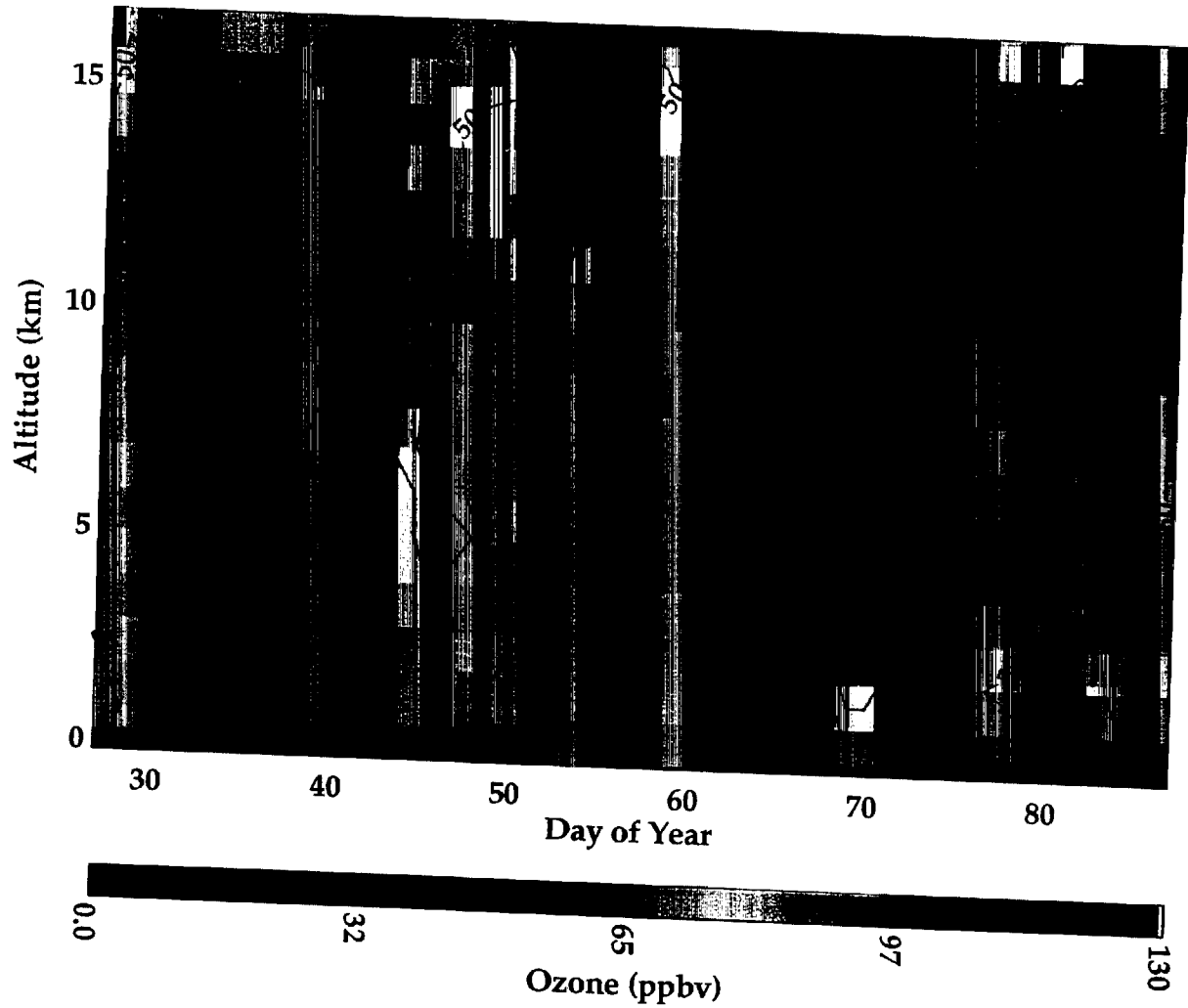


FIG 11

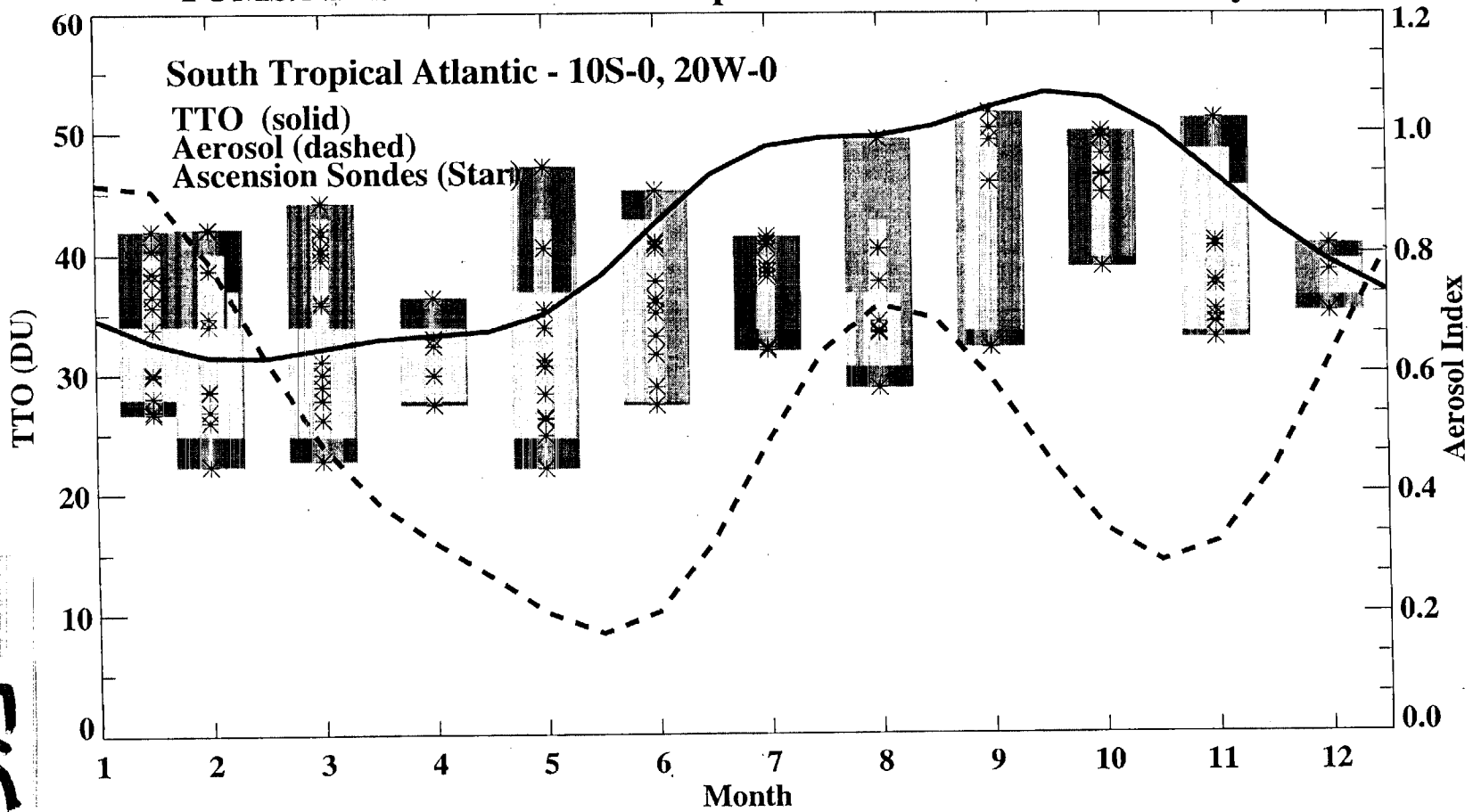
Kaashidhoo-Maldives INDOEX Ozone Mixing Ratio (ppbv)



/witte/shadoz/paper2/kaash_curtain_pap2.pro010917

FIG 12

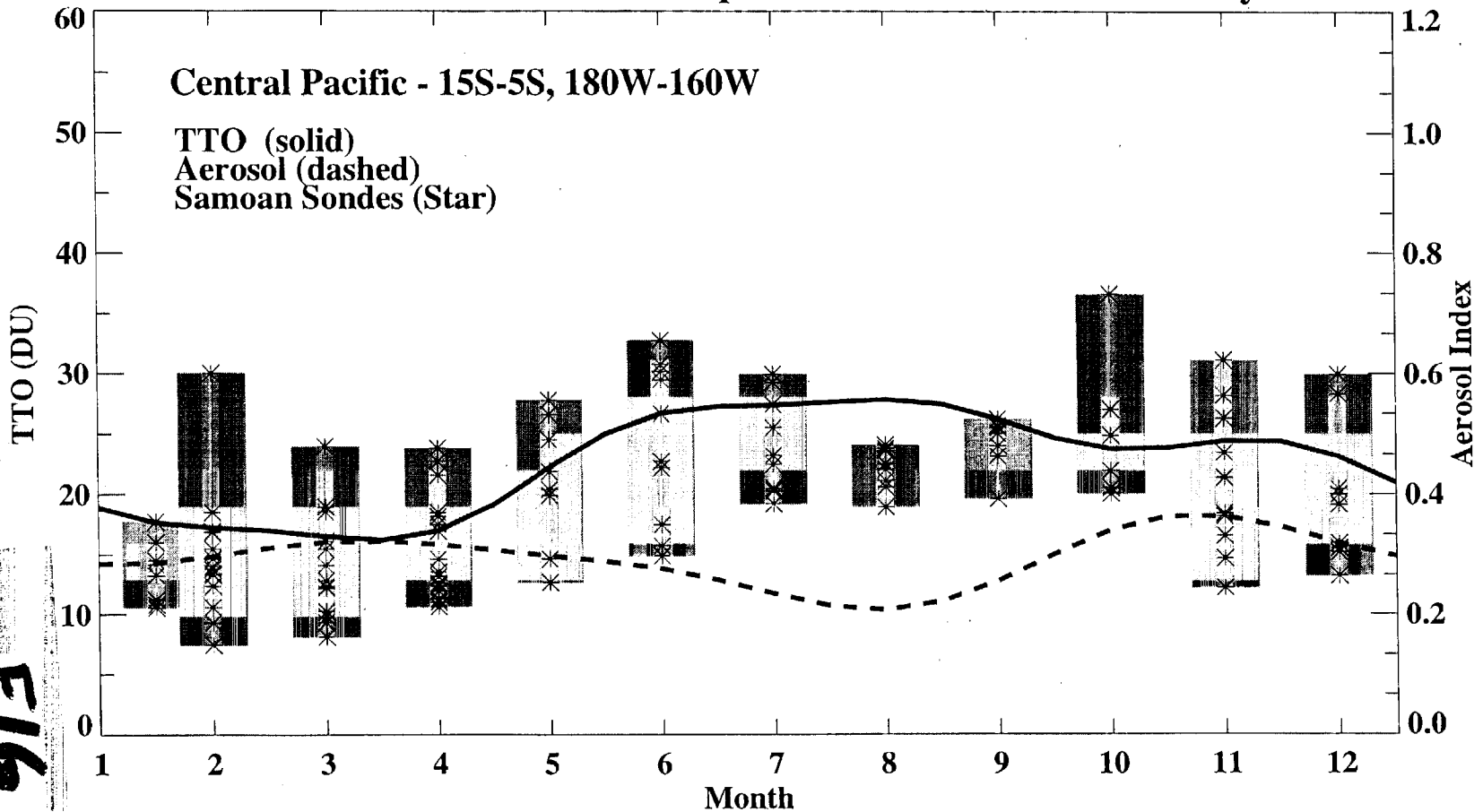
TOMS/Nimbus-7 1980-1990 Trop. Ozone & Aerosol Seasonal Cycle



/witte/TRENDS/seas_plt_1pan.pro/010516

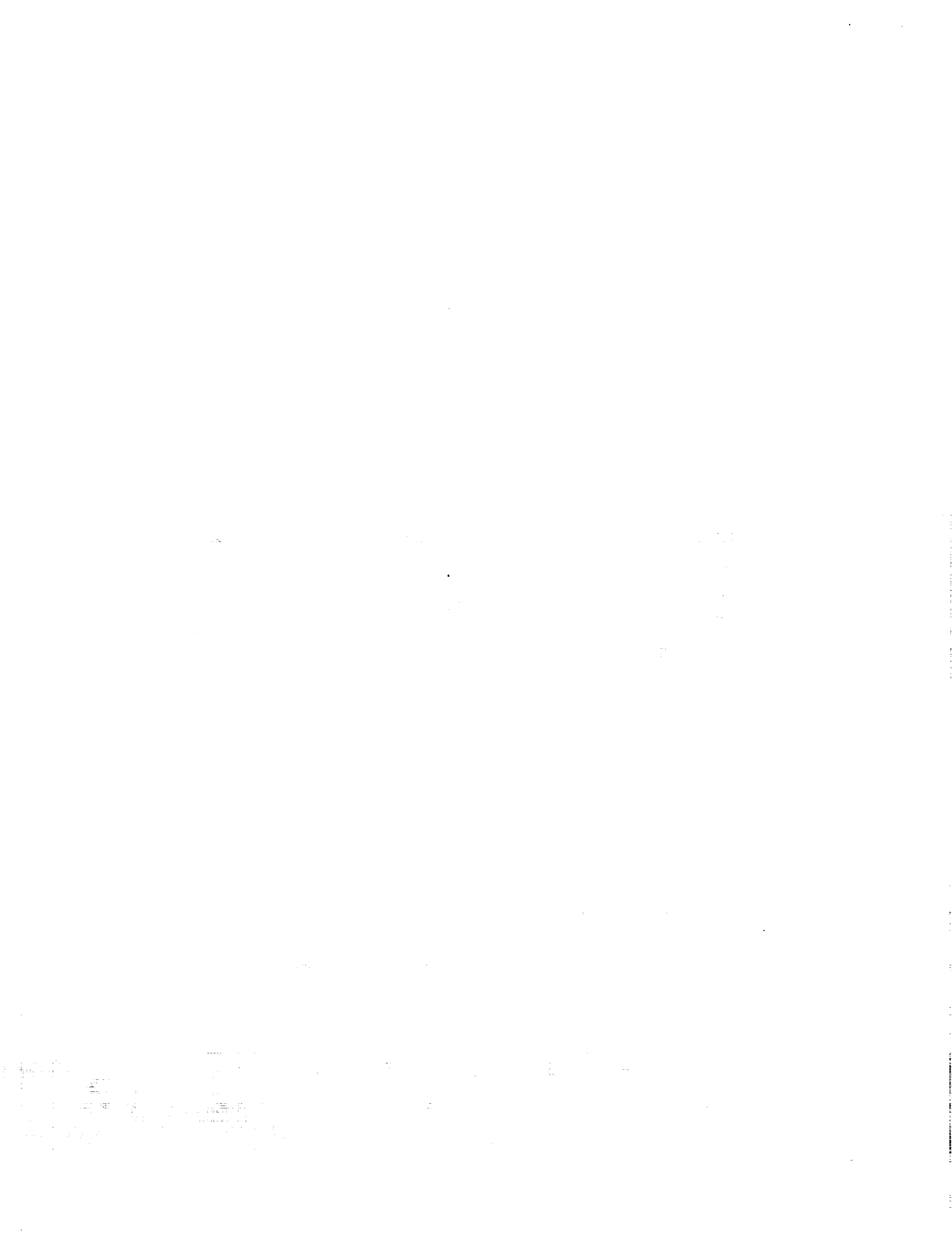
FIG 13A

TOMS/Nimbus-7 1980-1990 Trop. Ozone & Aerosol Seasonal Cycle

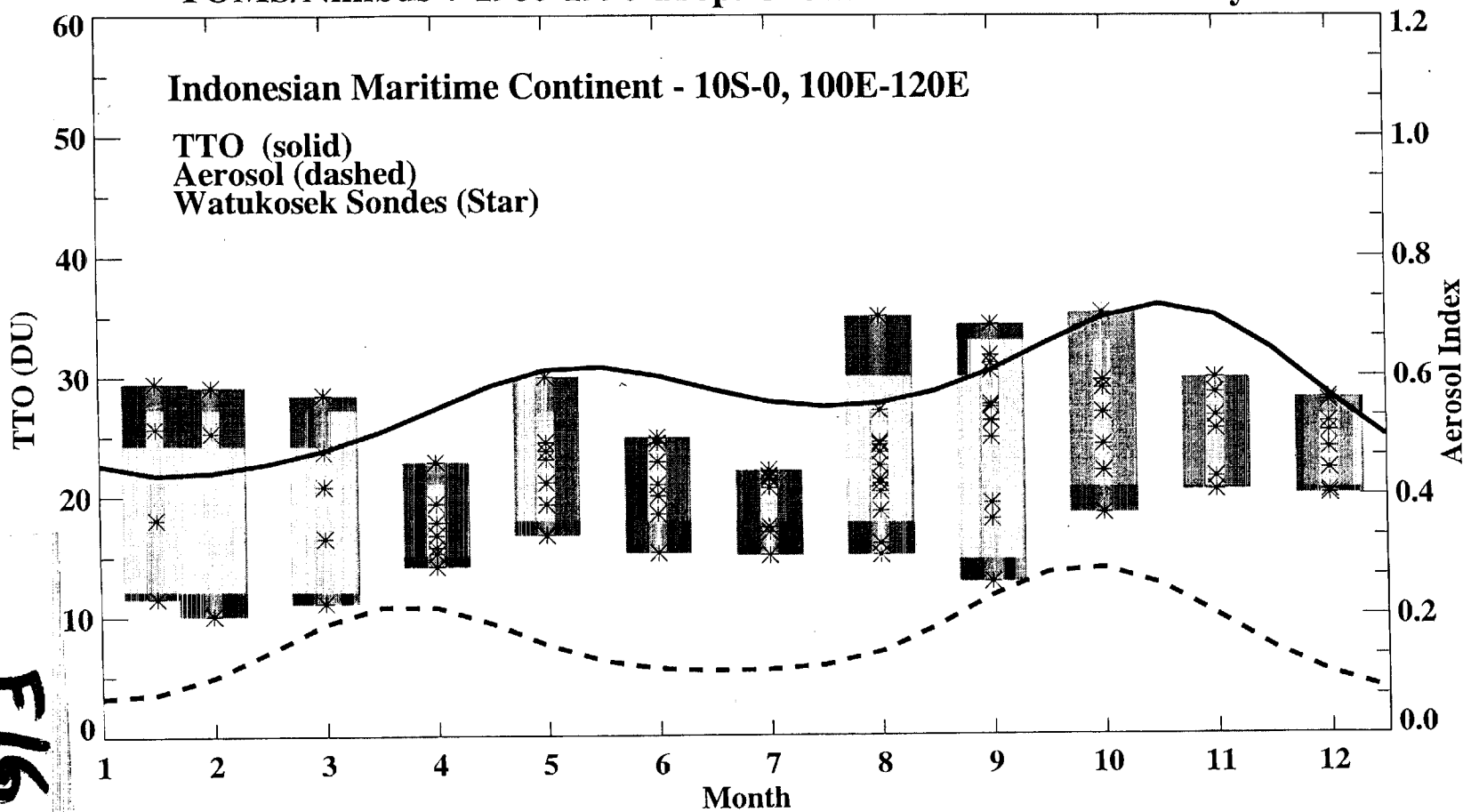


/witte/TRENDS/seas_plt_1pan.pro/010516

FIG 13B



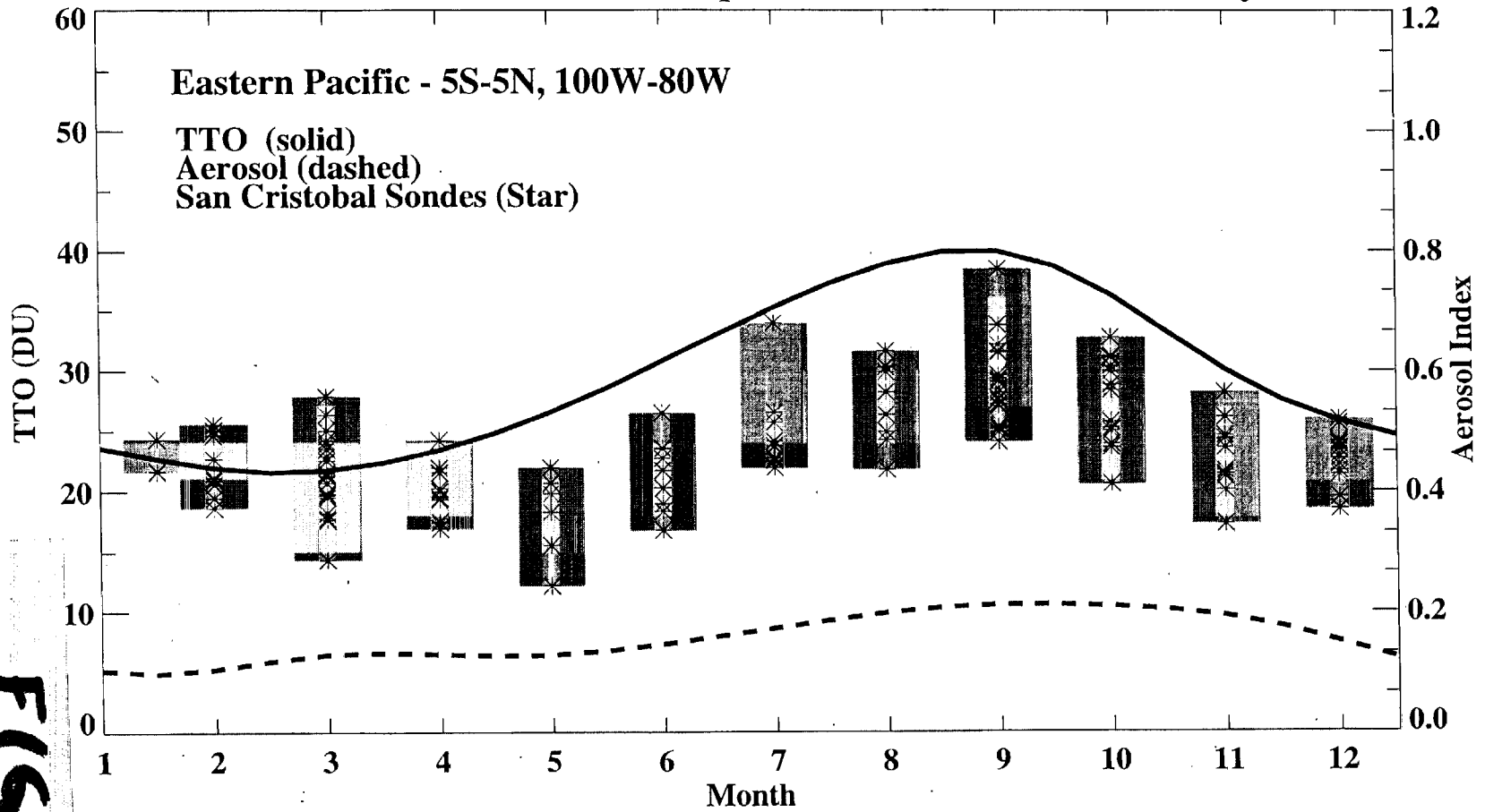
TOMS/Nimbus-7 1980-1990 Trop. Ozone & Aerosol Seasonal Cycle



/witte/TRENDS/seas_plt_1pan.pro/010516

FIG 13C

TOMS/Nimbus-7 1980-1990 Trop. Ozone & Aerosol Seasonal Cycle

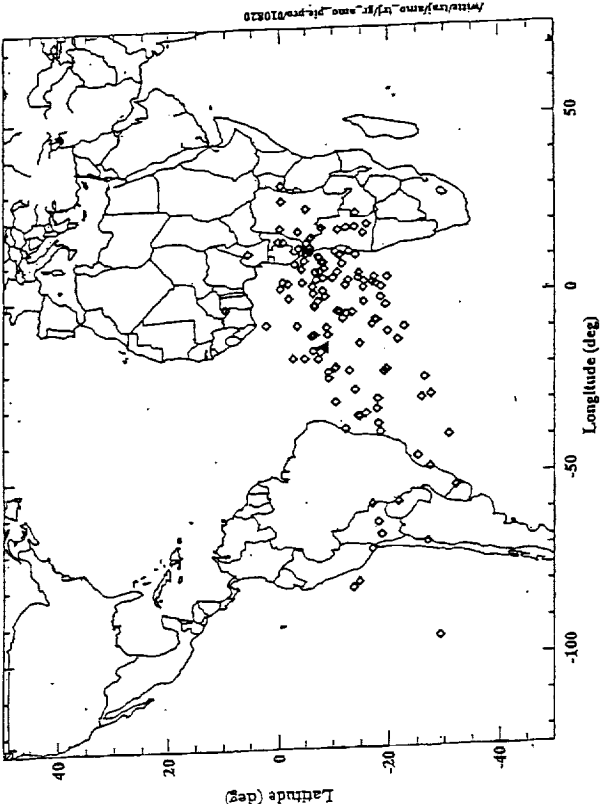


/witte/TRENDS/seas_plt_1pan.pro/010516

F1513D

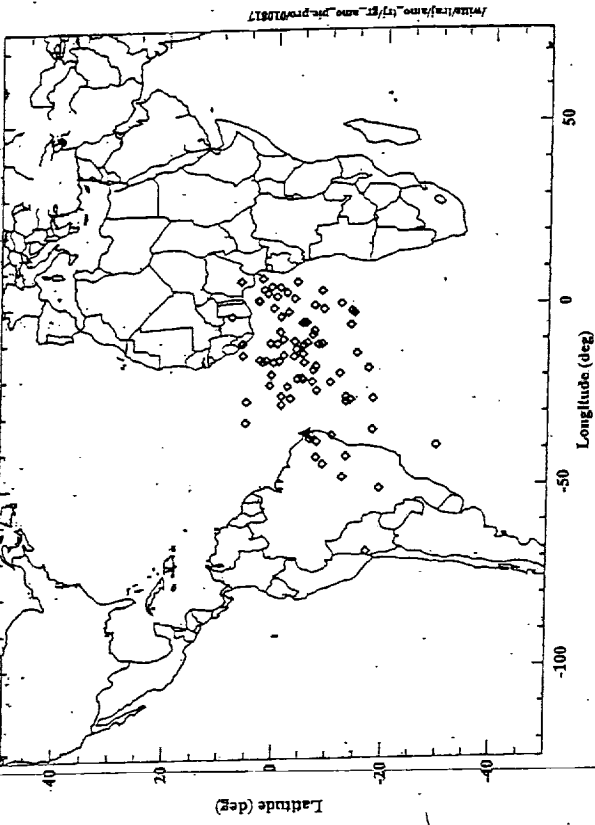
(a)

Ascension Is. 1998-2000 data
Air Parcel End Locations after 5 Days SN=126



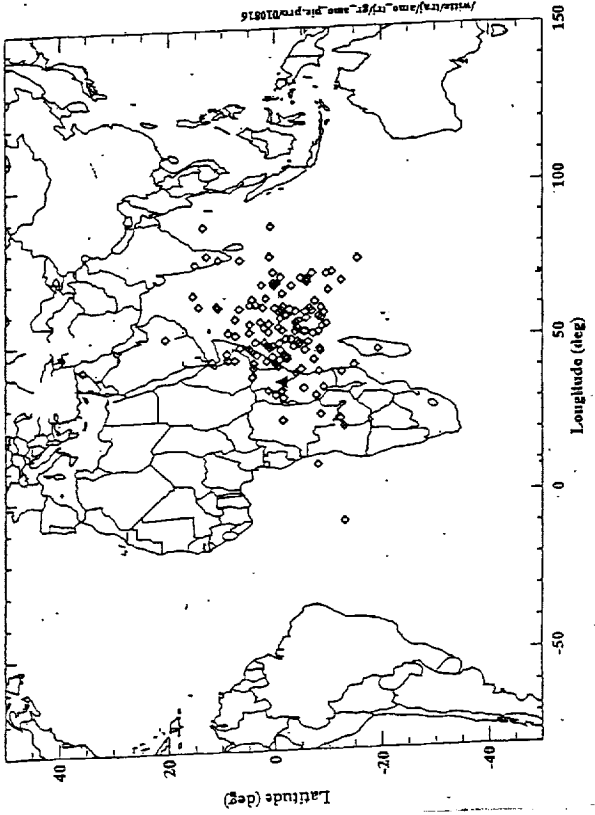
(b)

Natal, Brazil 1998-2000 data
Air Parcel End Locations after 5 Days SN=83



(c)

Nairobi, Kenya 1998-2000 data
Air Parcel End Locations after 5 Days



(d)

La Reunion 1998-2000 data
Air Parcel End Locations after 5 Days

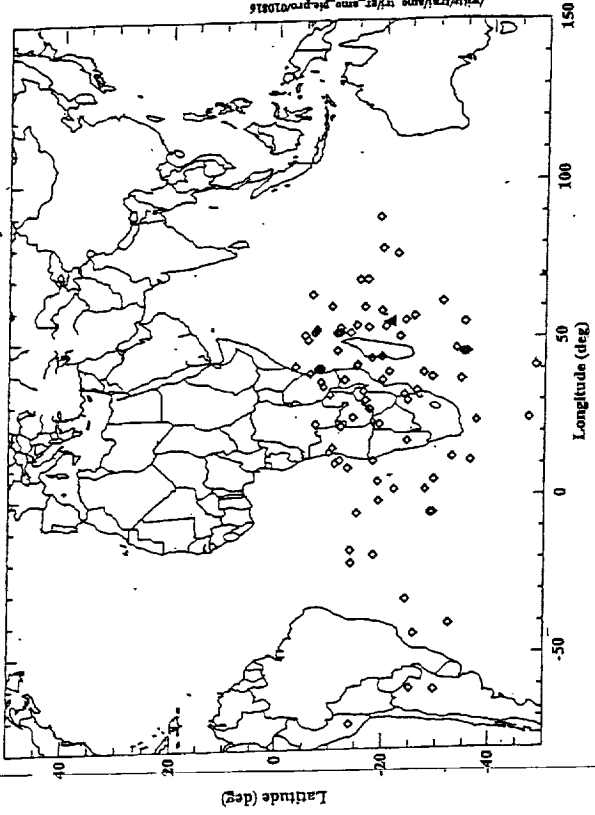
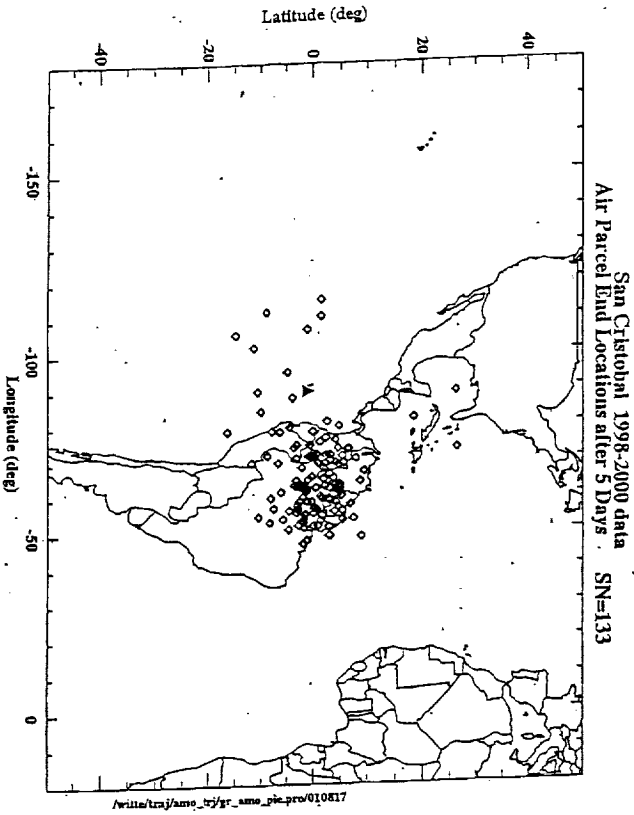
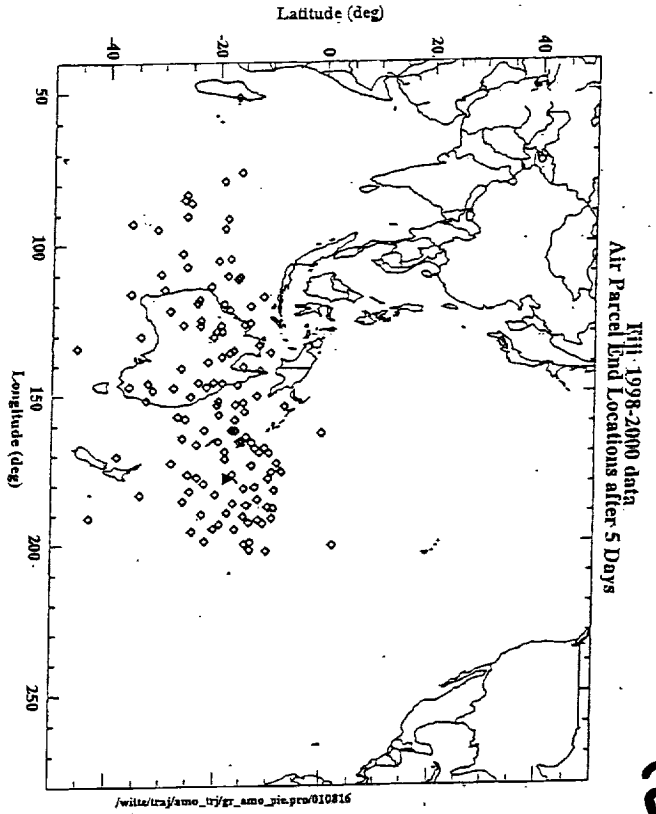


FIG 1A

Fig 19, cont'd.

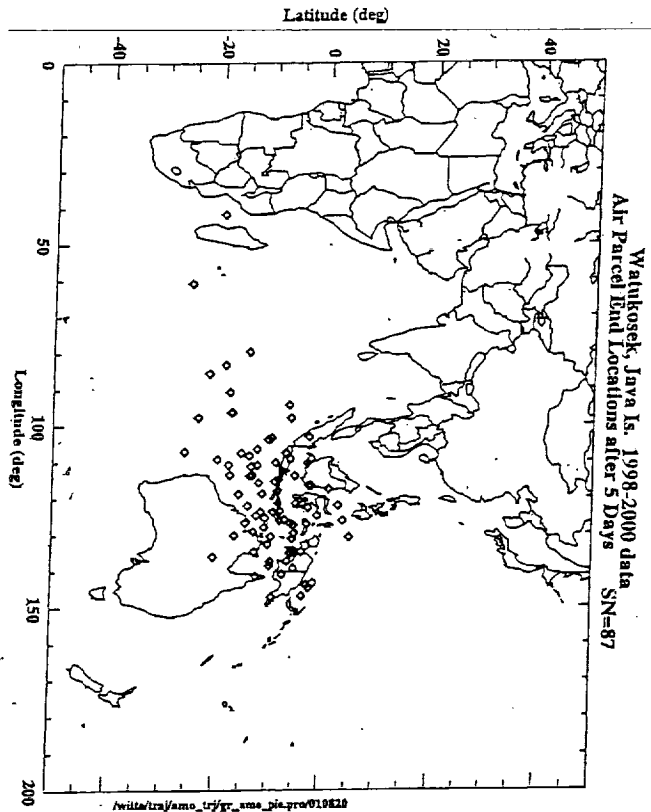


(g)

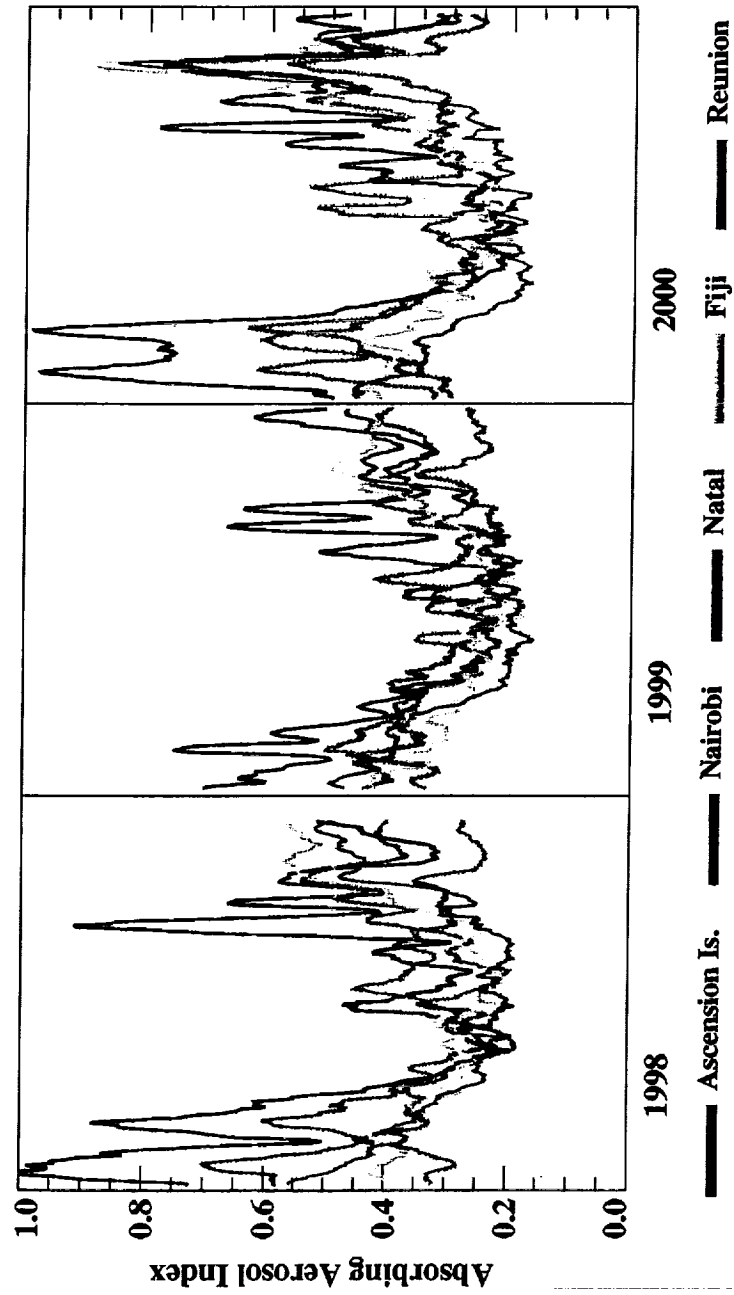


(e)

(f)







F16 15A

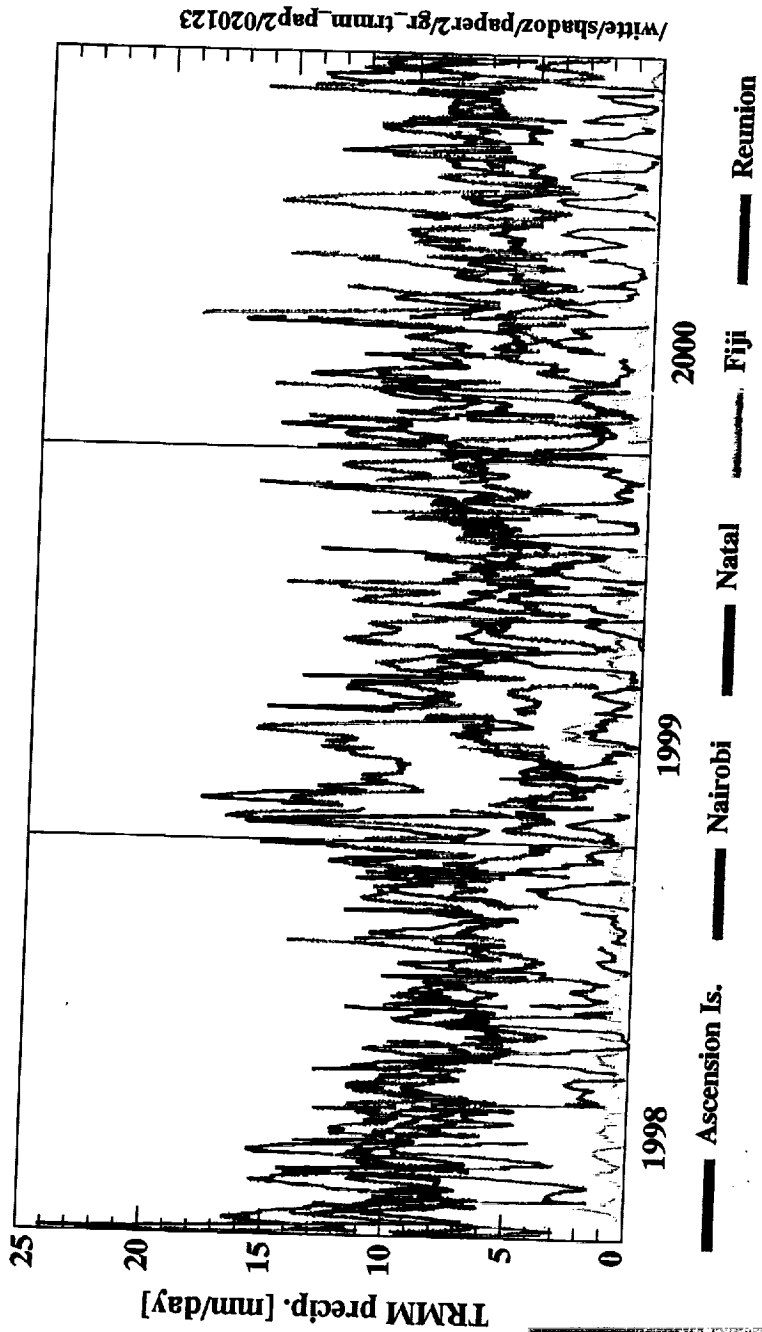
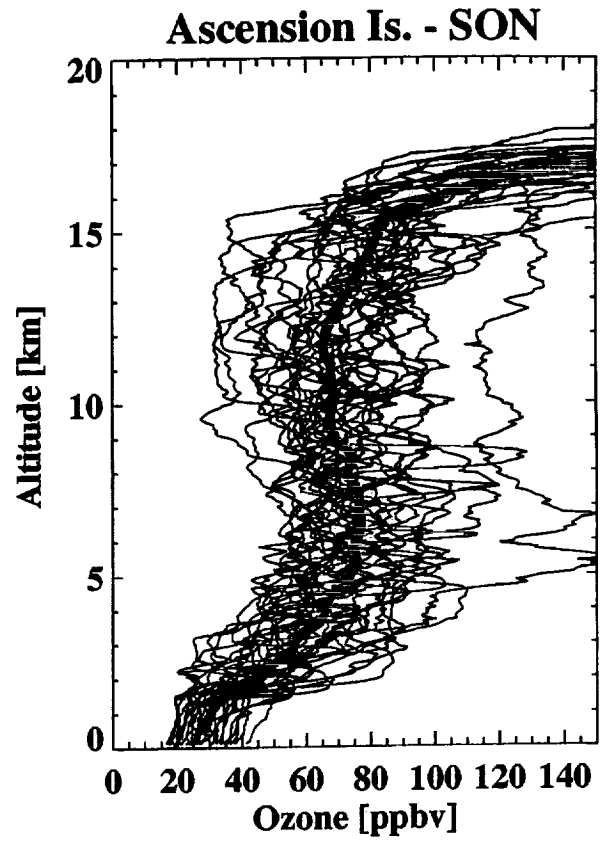
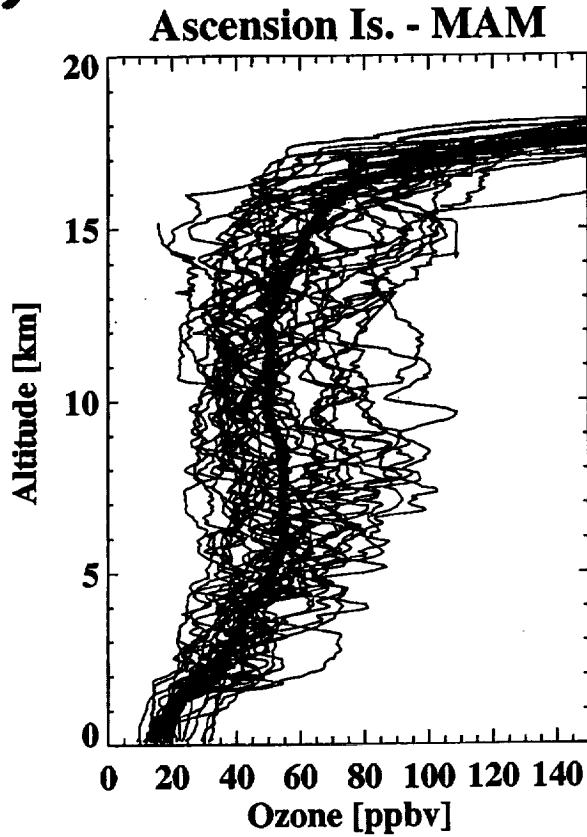


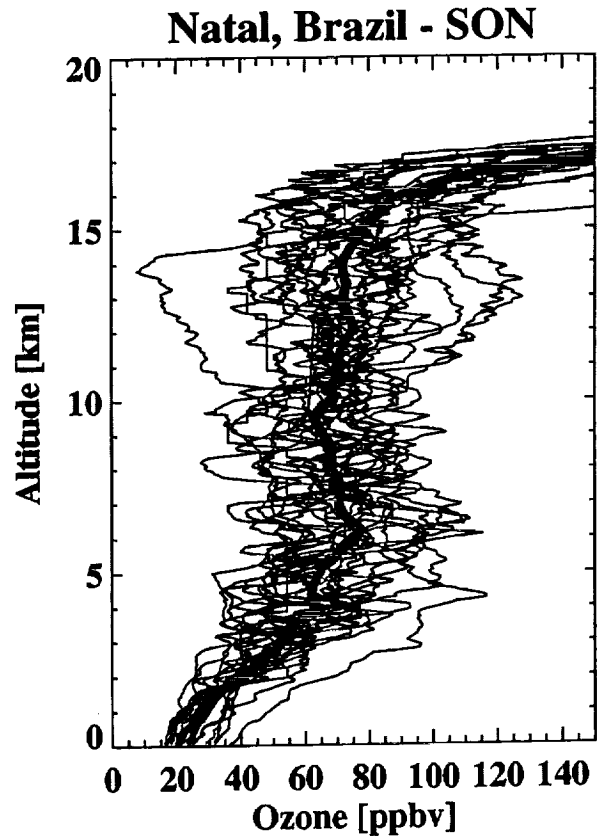
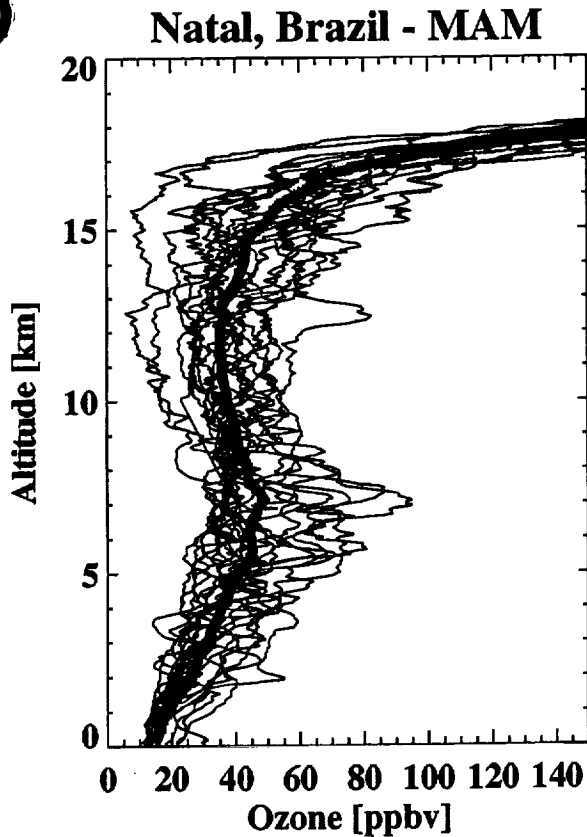
FIG 15B

(A)

1998-2000 Seasonal Profiles



(B)



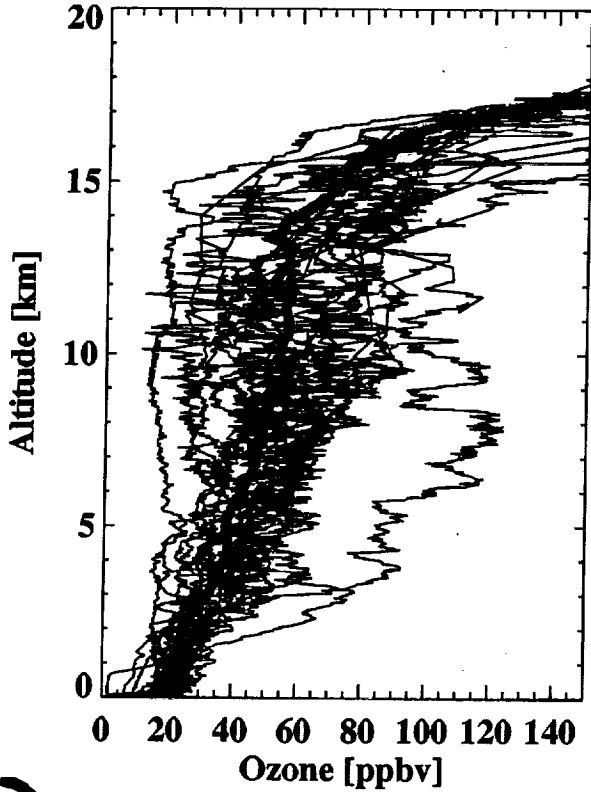
/writte/shadoz/paper2/gr_MAMSON_2pan_pap2-pro/010830

FIG 16 A,B

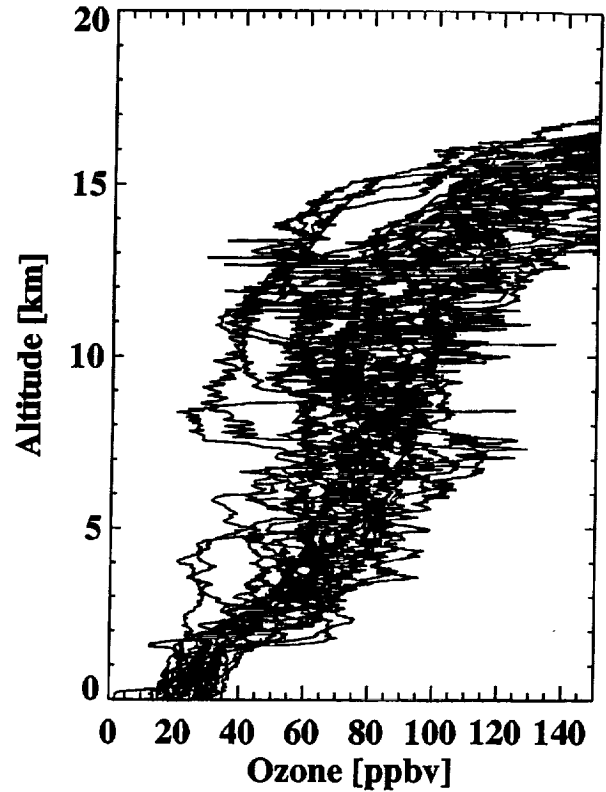
1998-2000 Seasonal Profiles

(C)

La Reunion - MAM

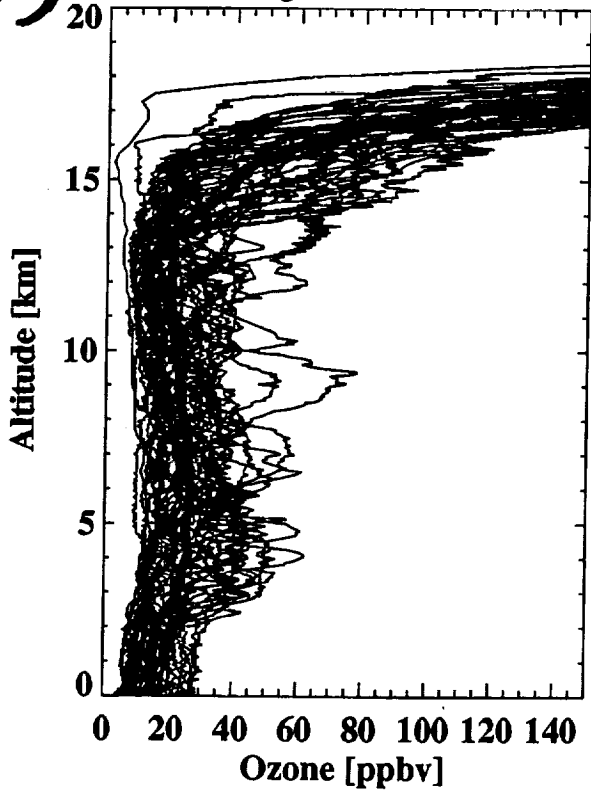


La Reunion - SON

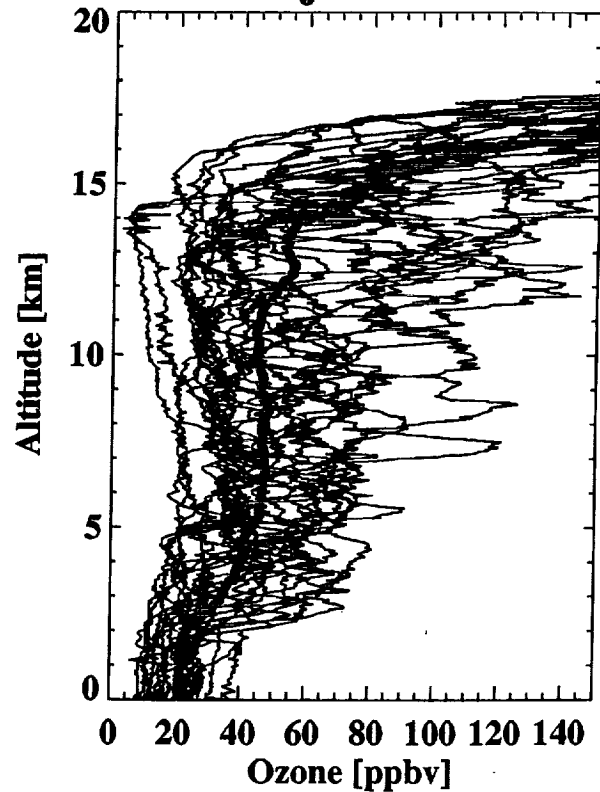


(D)

Fiji - MAM



Fiji - SON



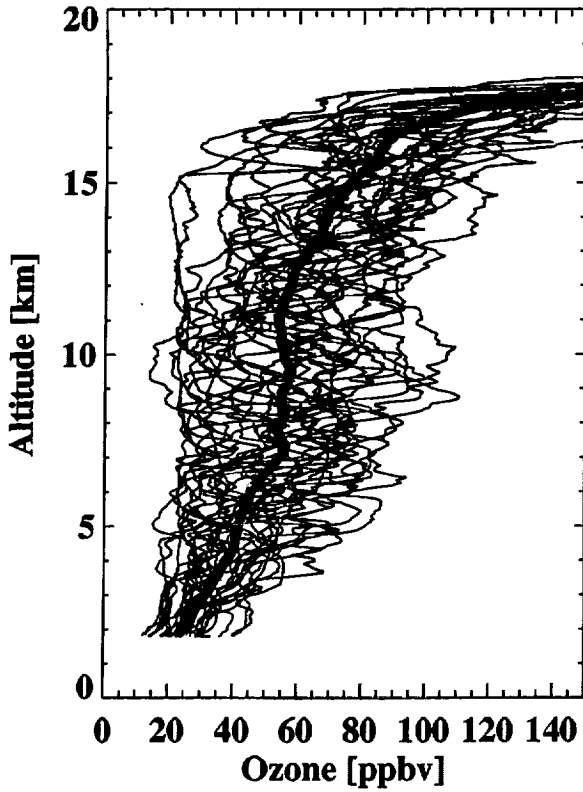
/witten/shadoz/paper2/gr_MAMSON_2pan_pap2.pro/010820

FIG 16C,D

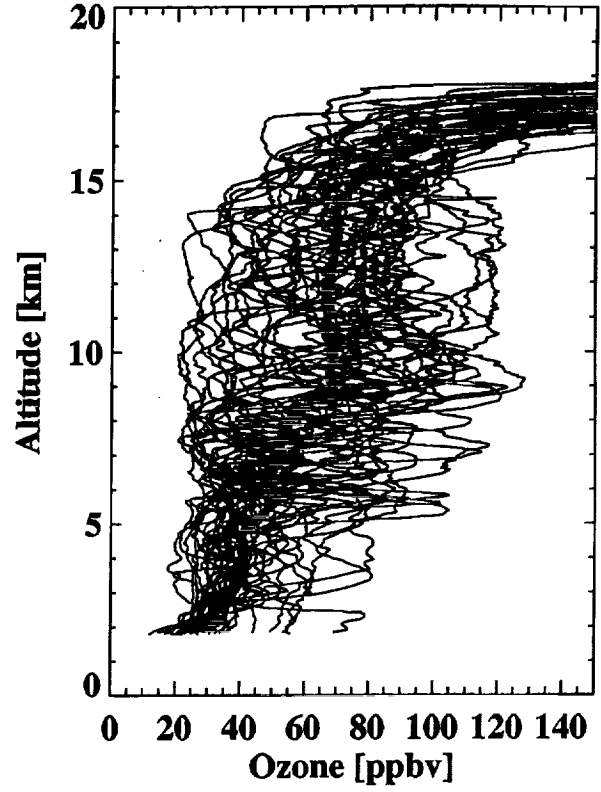
(E)

1998-2000 Seasonal Profiles

Nairobi - MAM

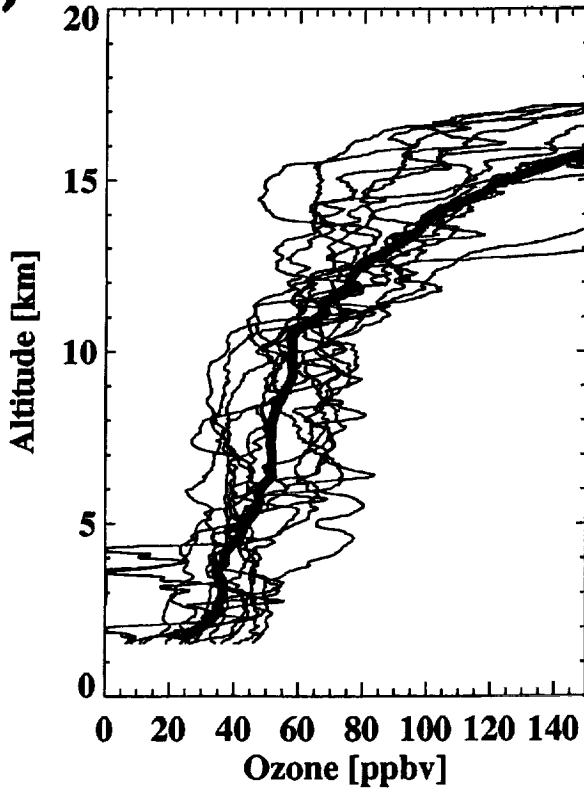


Nairobi - SON

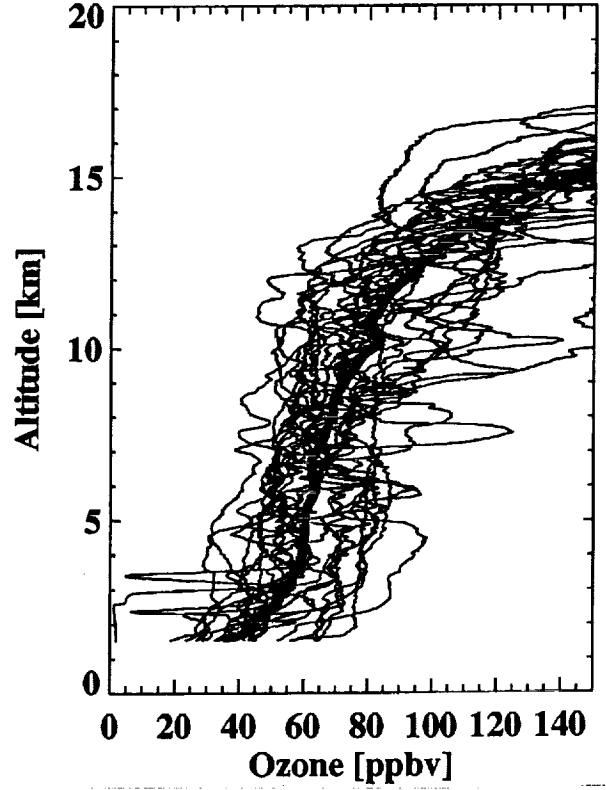


(F)

Irene - MAM



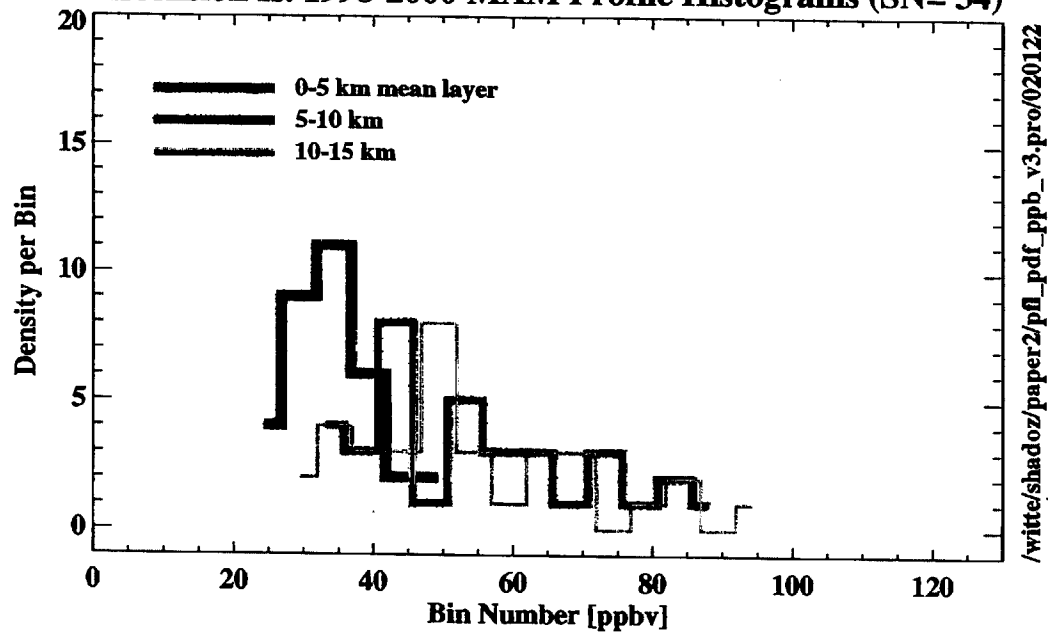
Irene - SON



/witteshadoz/paper2/gr_MAMSON_2pan_pap2.pro/010918

FIG 16E,F

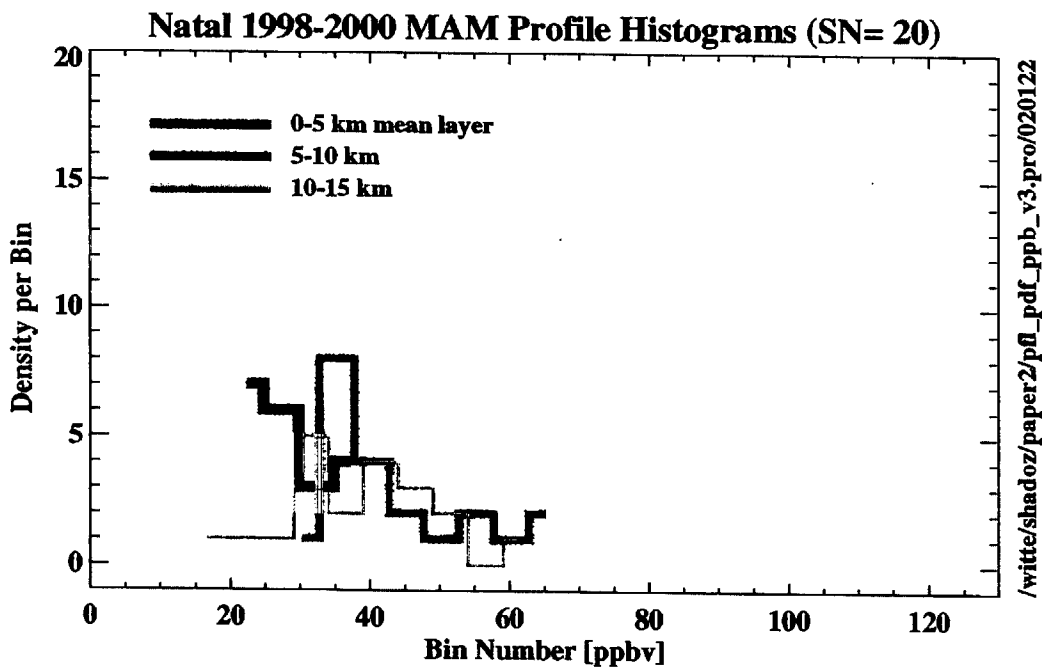
Ascension Is. 1998-2000 MAM Profile Histograms (SN= 34)



/writte/shadoz/paper2/pfl_ppb_v3.pro/020122

FIG 17A

FK 17 B



/writte/shadoz/paper2/pfl_ppb_v3.pro/020122

FIG 17c

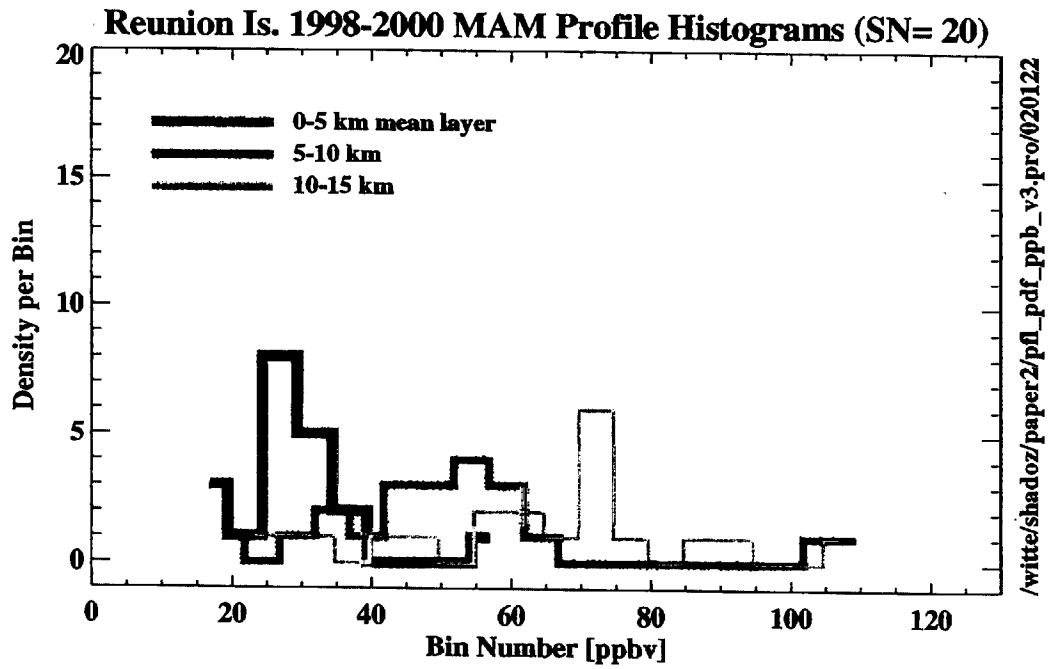
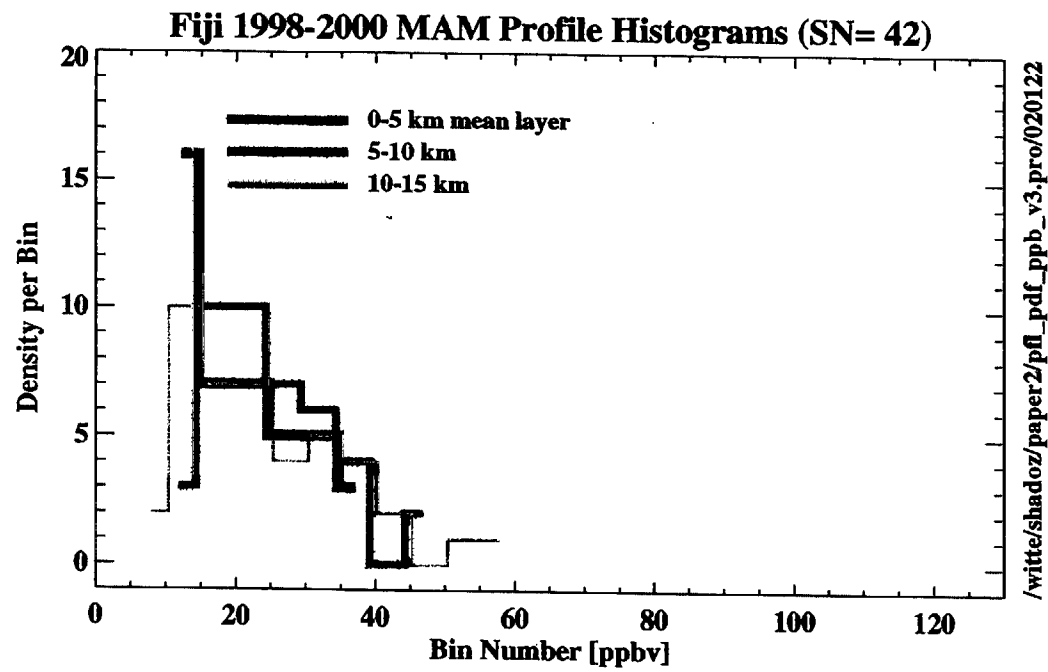


FIG 17D



/writte/shadoz/paper2/pfl_ppb_v3.pro/020122

Am. Samoa 1998-2000 MAM Profile Histograms (SN= 43)

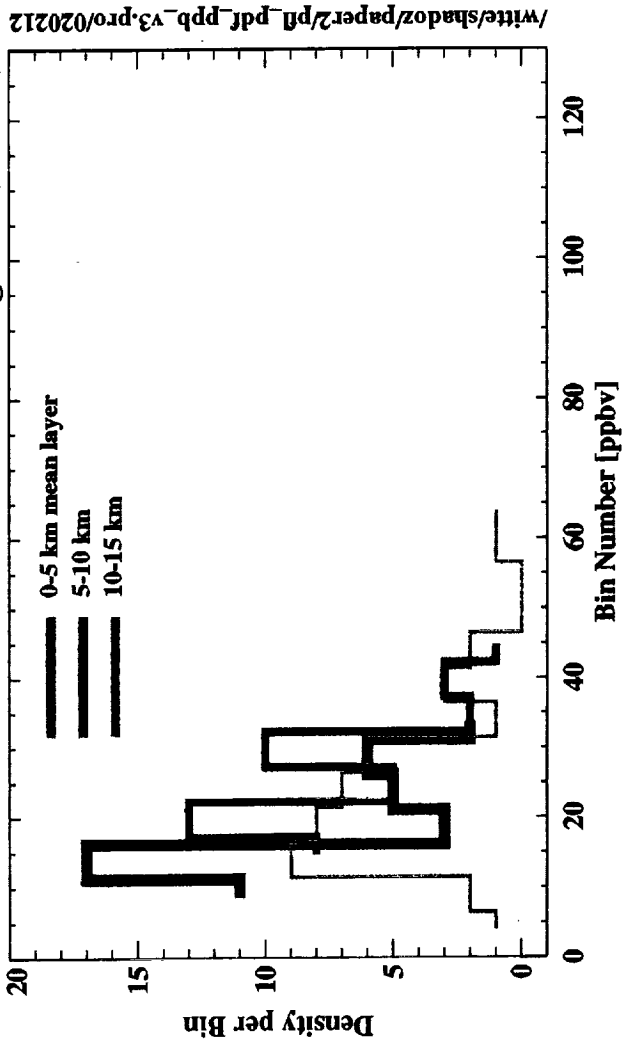


FIG 17E

FIG 18A

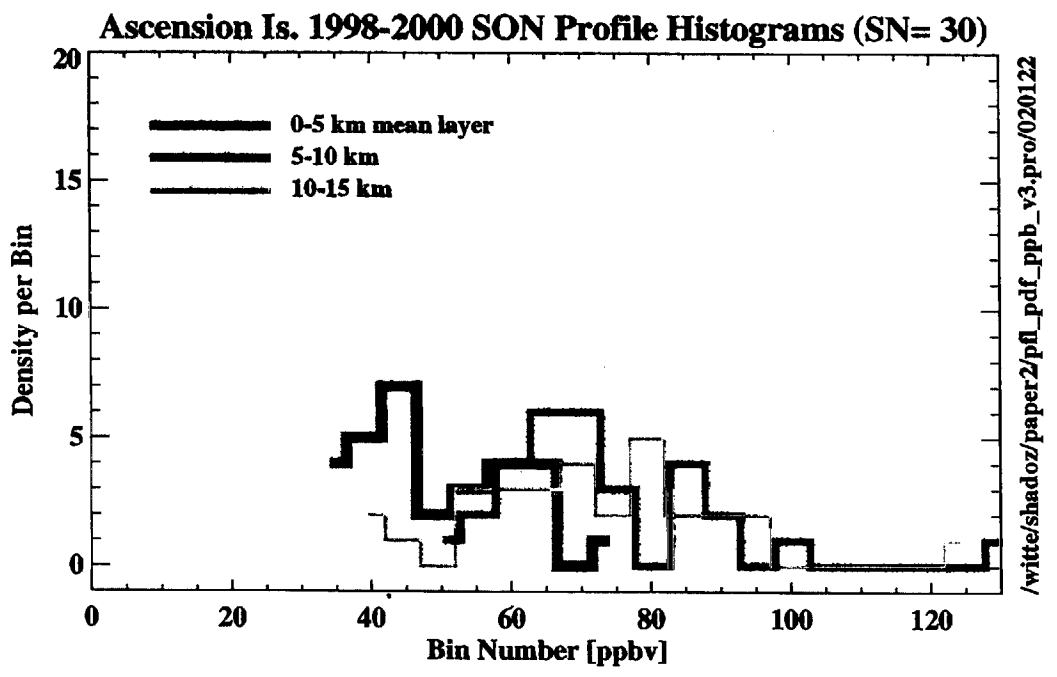
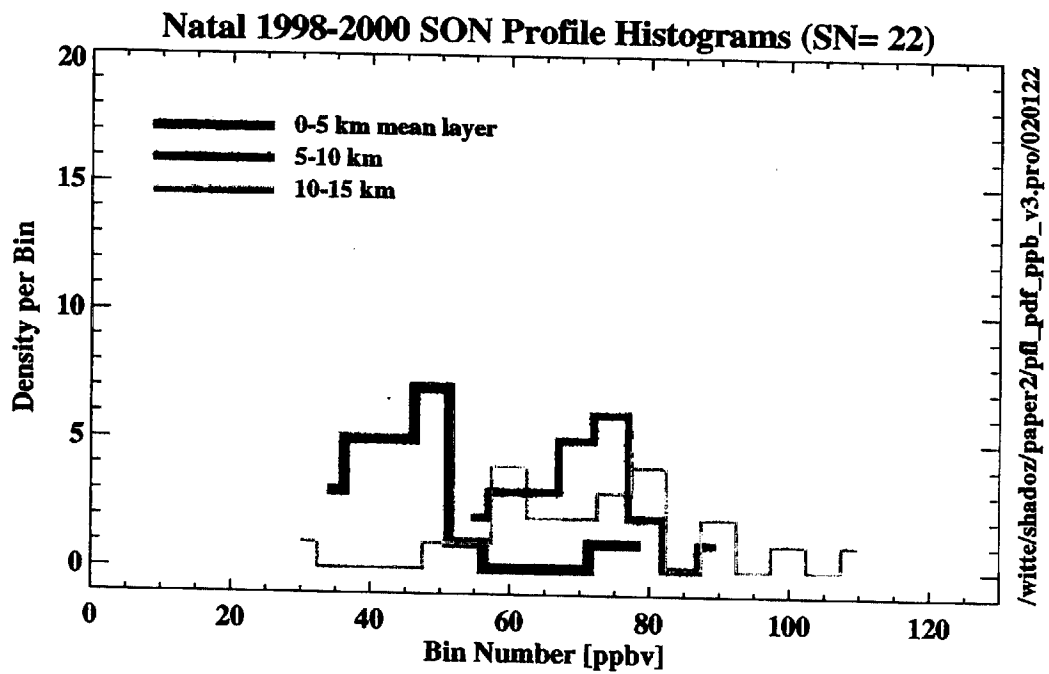
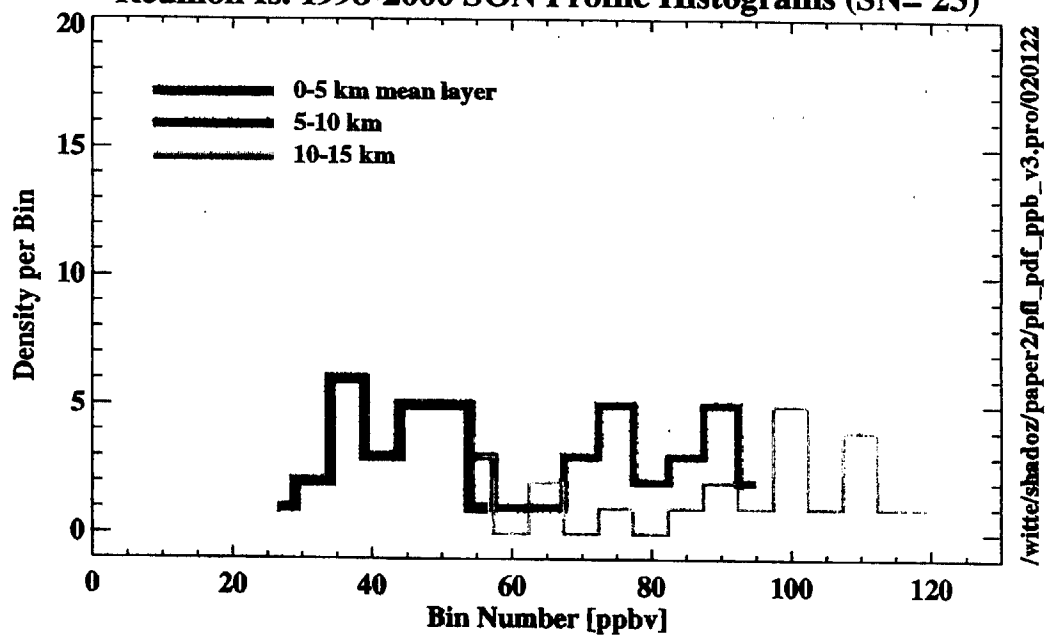


FIG 18B





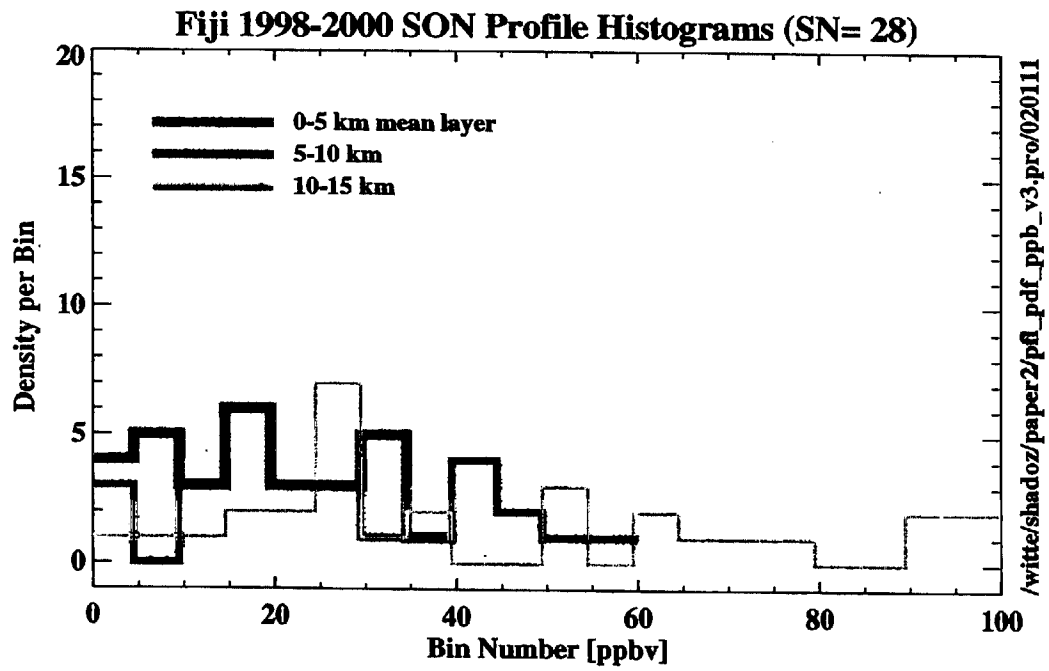
Reunion Is. 1998-2000 SON Profile Histograms (SN= 23)



/writte/shadoz/paper2/pfl_pdf_ppb_v3.pro/020122

F16 18C

F16 18D



/witt/shadoz/paper2/pfl_pdf_ppb_v3.pro/020111

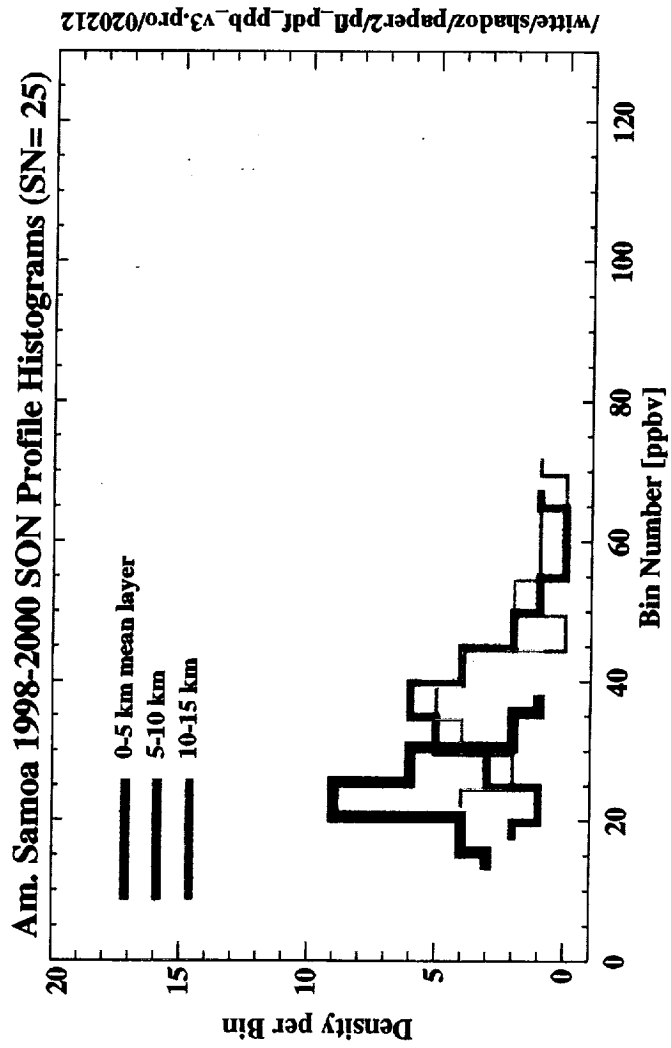


FIG 18E

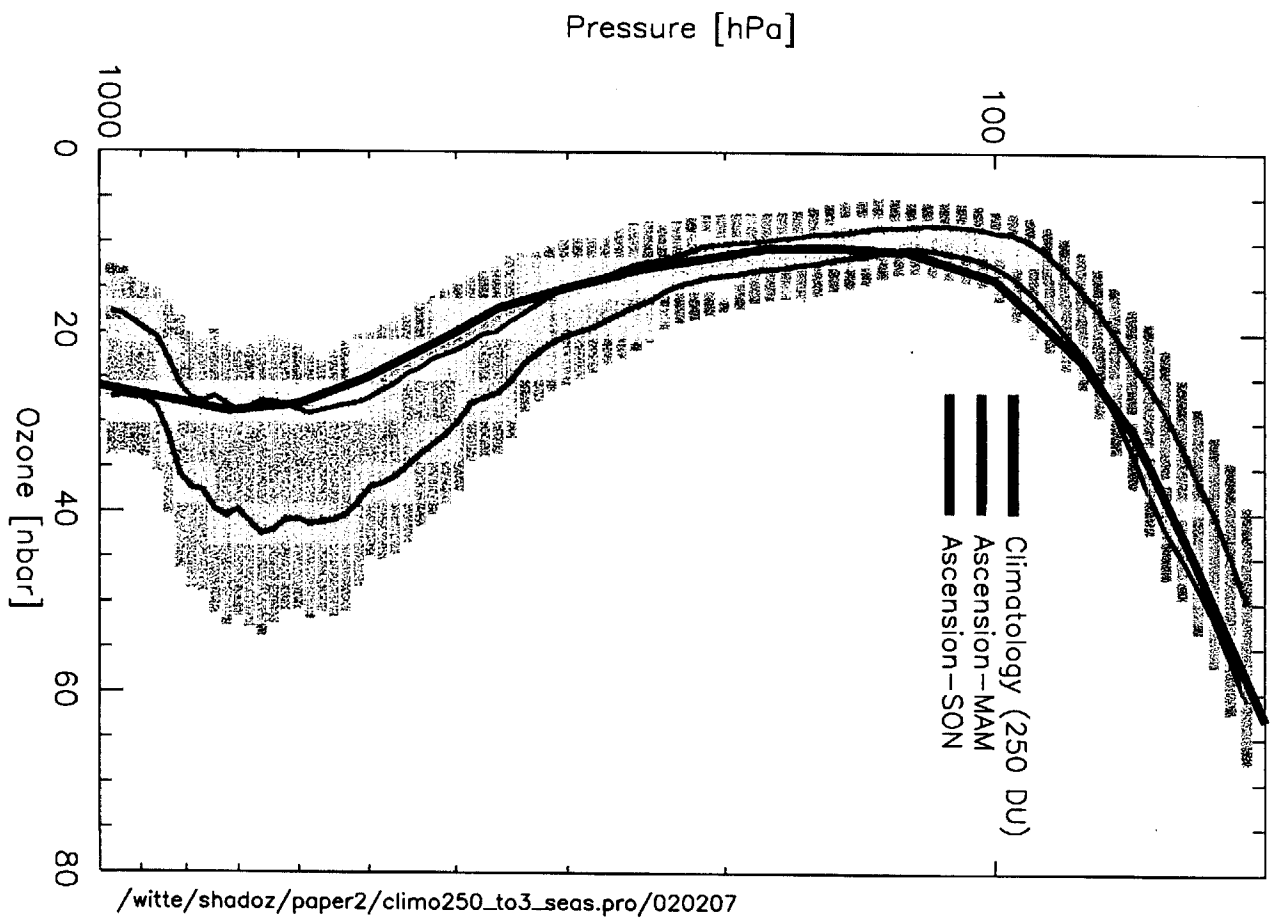
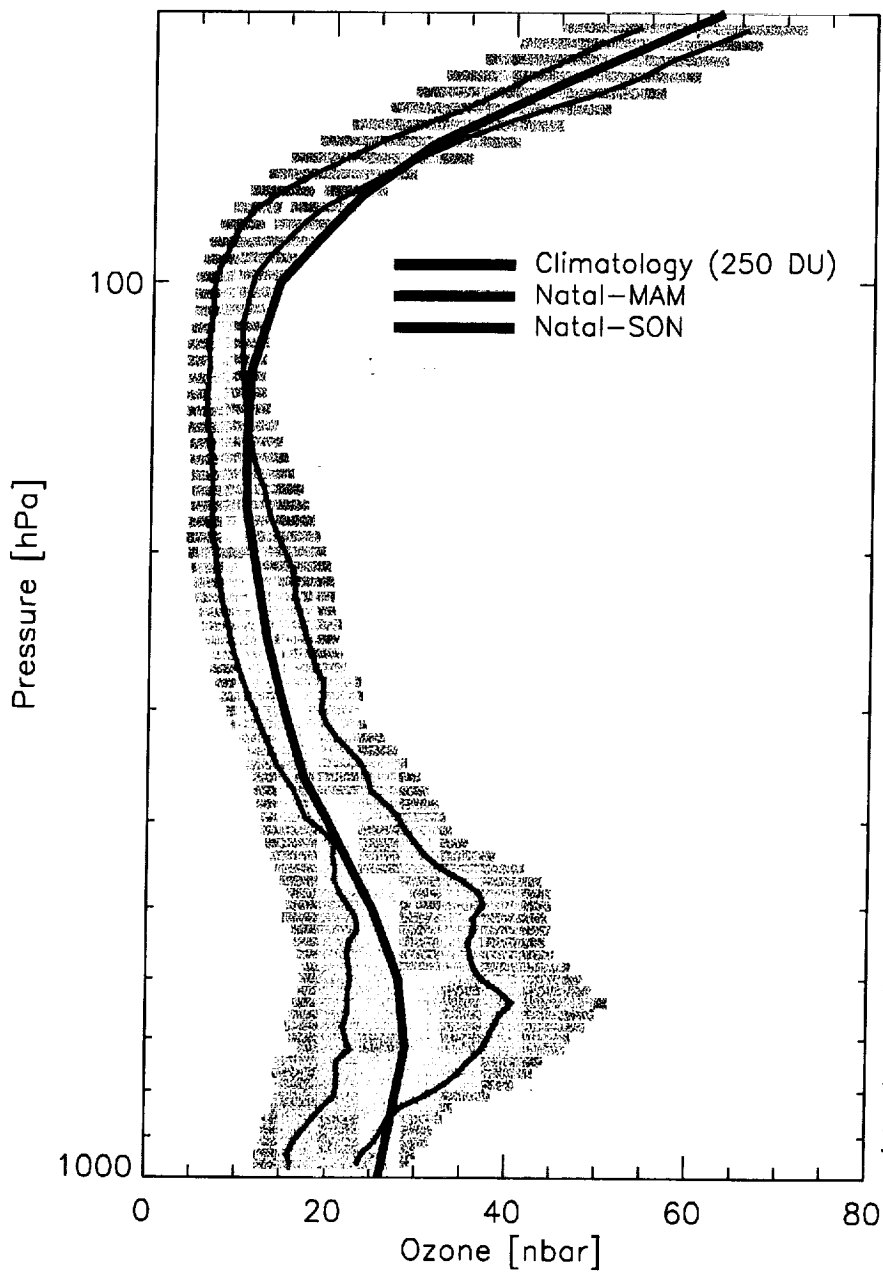
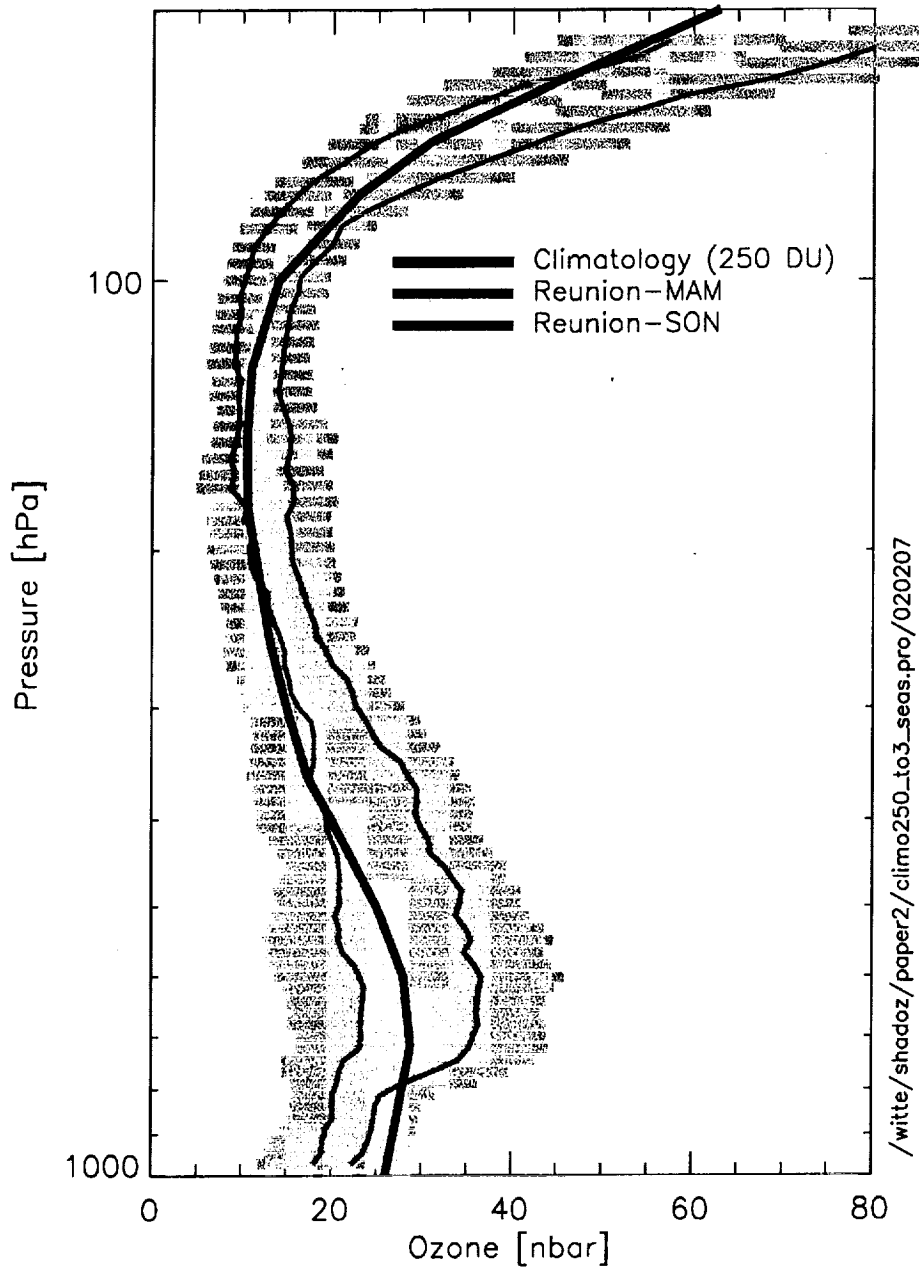


FIG 19A



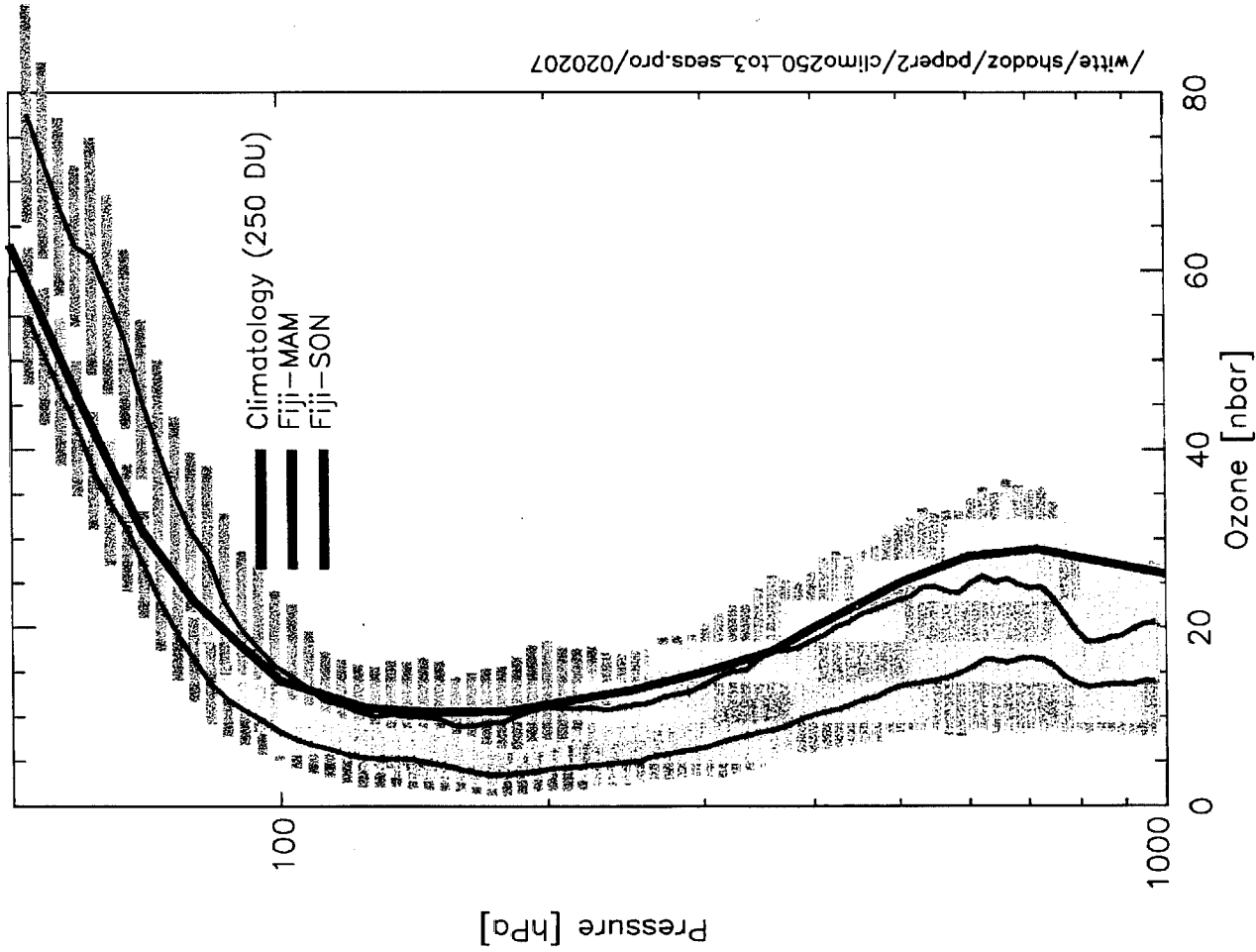
/witte/shadoz/paper2/climo250_to3_seas.pro/020207

FIG 19 B



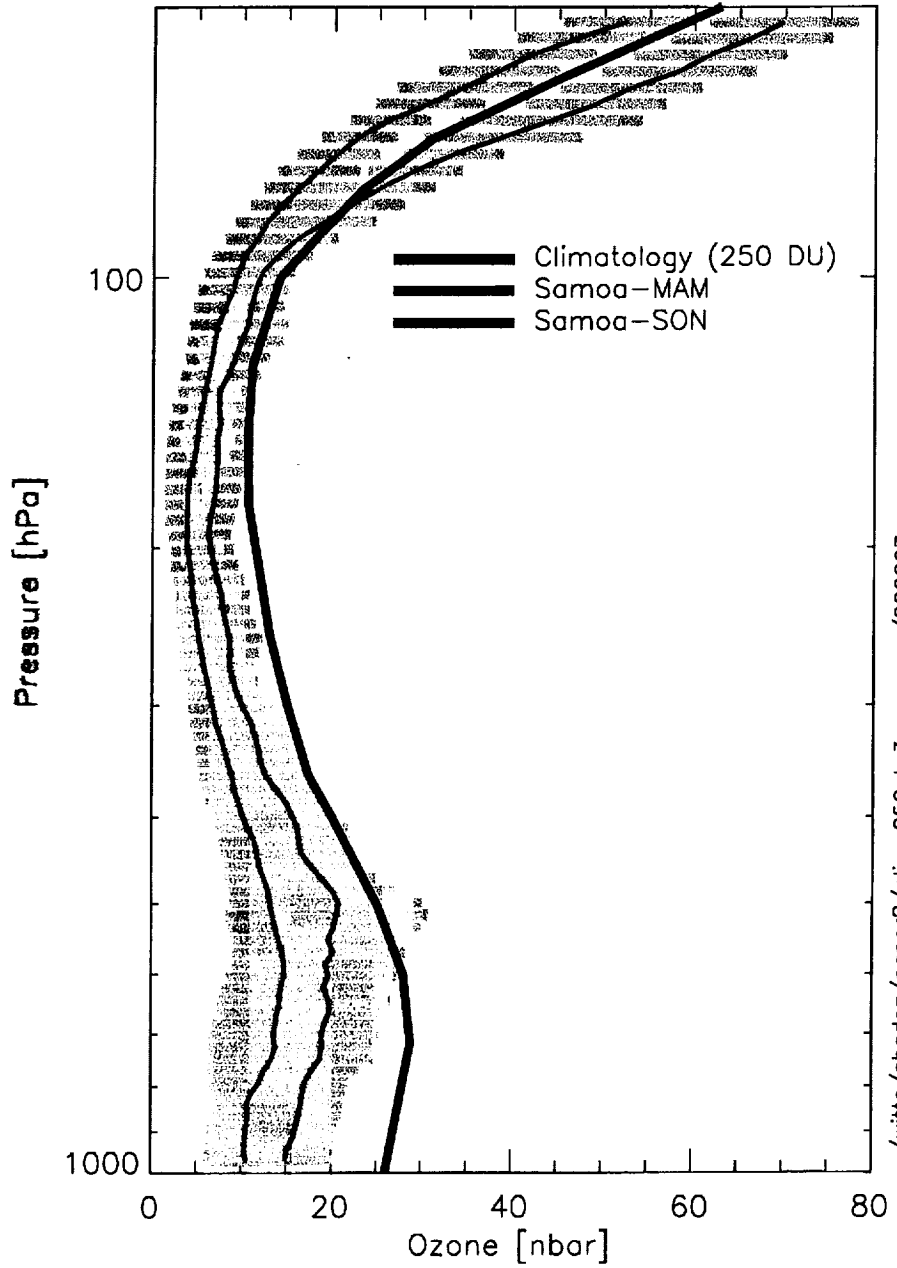
/witte/shadoz/paper2/climo250_to3_seas.pro/020207

FIG 19C



/write/shadoz/paper2/climo250_to3_seas.pro/020207

F16 19D



/witte/shadoz/paper2/climo250_to3_seas.pro/020207

FIG 19 E

